5-2017

Petrology of the hastingsite-riebeckite Granite of Mt. Cabot, NH

Colin Robert Kraft
Bates College, ckraft@bates.edu

Petrology of the Hastingsite-Riebeckite Granite of Mt. Cabot, New Hampshire

A Senior Thesis

Presented to

The Faculty of the Department of Geology

Bates College

In partial fulfillment of the requirements for the

Degree of Bachelor of Science

By

Colin Kraft

Lewiston, Maine

April 7, 2017

Acknowledgements

I would like to thank my advisor Professor Geneviève Robert for her guidance and feedback during the whole thesis project. Her knowledge, expertise, and consistent push allowed me to deeply understand my topic and foster a love for igneous petrology.

This summer could not have been possible without the help from Professor Dyk Eusden and fellow classmate Ian Hillenbrand. I would like to thank Professor Dyk Eusden for the opportunity to work on this project and the help he gave during the data collection and field season period. I would also like to thank you my other field partner, Ian Hillenbrand, for showing me how to navigate GIS and helping me create the mineralogical and textural maps.

I am incredibly grateful for the time the Greg Anderson spent helping me learn the correct way to use the SEM-EDS for my thin sections. Unfortunately, I did not get far enough in the process to include the results in my thesis but I will treasure the information.

Special thanks to David Gibson and his lab assistants for analyzing my rock sample for XRF data at their laboratory at the University of Maine- Farmington.

To the rest of the geology department: Mike Retelle, Beverly Johnson, Marita Bryant, Raj Saha, Phil Dostie, and the visiting professors, thank you for inspiring me throughout my studies in geology.

Thank you to all my friends and fellow geology students who have made these four years a blast every step of the way

A special thanks to my family for supporting me every step of the way and for allowing me the opportunity to be where I am today.

Table of Contents

Table of Figures

Table of Tables

Abstract

The purpose of this study was to produce a model of the petrogenesis of the Mt. Cabot hastingsite-riebeckite granite located in the northern half of the Northern Jefferson 7.5' quadrangle. This study aims to build on the structural information and the map produced by Hillenbrand (2017) as part of the USGS/NHGS StateMap program.

The Mt. Cabot area contains older surrounding bed rock of the Middle-Upper Ordovician Ammonoosuc Volcanics, the Lost Nation group, Jurassic igneous intrusives of the Pliny ring dike complex, and xenoliths of Conway Granite. The hastingsite-riebeckite granite is the largest pluton in the area. The pluton is part of the White Mountain Magma series and was formed after the tectonic events involving the Early-Mid Mesozoic opening of the Atlantic Ocean and part of the magmatic melting associated with ring dike formation and caldera collapses.

I analyzed samples of the hastingsite-riebeckite granite pluton of Mt. Cabot, NH, for their mineralogy, textures, and geochemistry. Discrete zones of hastingsite and riebeckite bearing granites suggest varying oxygen fugacity conditions across the magma body during crystallization or that distinct Na-rich or Ca-rich magmas makeup the pluton. Modal analysis shows two different rock types within the pluton, syenogranite, and quartz syenite. Exsolved alkali feldspar indicates crystallization at low pressure and depth, around 1.5- 2.1 kbar and 5.3-7.6 km. Intergranular albite and albite rims on alkali feldspars indicate late stage albitization and replacement and unmixing of alkali feldspar at 410 ºC and 370ºC during crystallization. Sericitization of alkali feldspar and hydration of amphiboles suggest post magmatic hydrothermal alteration. XRF bulk-rock geochemistry and trace element data suggest that the Mt. Cabot granite is chemically similar to other riebeckite granites of the New Hampshire region.

The discrete mineralogical zones were most likely caused by the influx and movement of melt that are controlled by the structural nature and instability of ring dike complexes.

Introduction

1.1 Field Location

The study area and field area is the northern portion of the northern half of the Jefferson 7.5' New Hampshire (Figure 1.1). Mount Cabot is part of the Pliny Range and is the fifth highest mountain in New Hampshire with an elevation of 4170 ft (1271 m). Around 90% of the area is wooded and within the northern portion of the White Mountain National forest or the land of private landowners. The Mt. Cabot region in the Jefferson 7.5' quadrangle is densely wooded with two main entrance points. Previous access to the area was through the western side using the Mt. Cabot Trail. The study area is primarily accessible through a trail system on the eastern side from the Berlin Hatchery through Bunnell Brook and York Pond Trail. The area is underlain by intrusive igneous rocks into the surrounding metasedimentary bedrock. The greatest amount of outcrop is located on the trails and ledges of Mt. Cabot. Bedrock also outcrops on the ledges of Mt. Terrace, Mt. Weekes, and in the streams running down from each mountain. Previous mapping of Jefferson quadrangle and the Mt. Cabot region was performed by Chapman (1942).

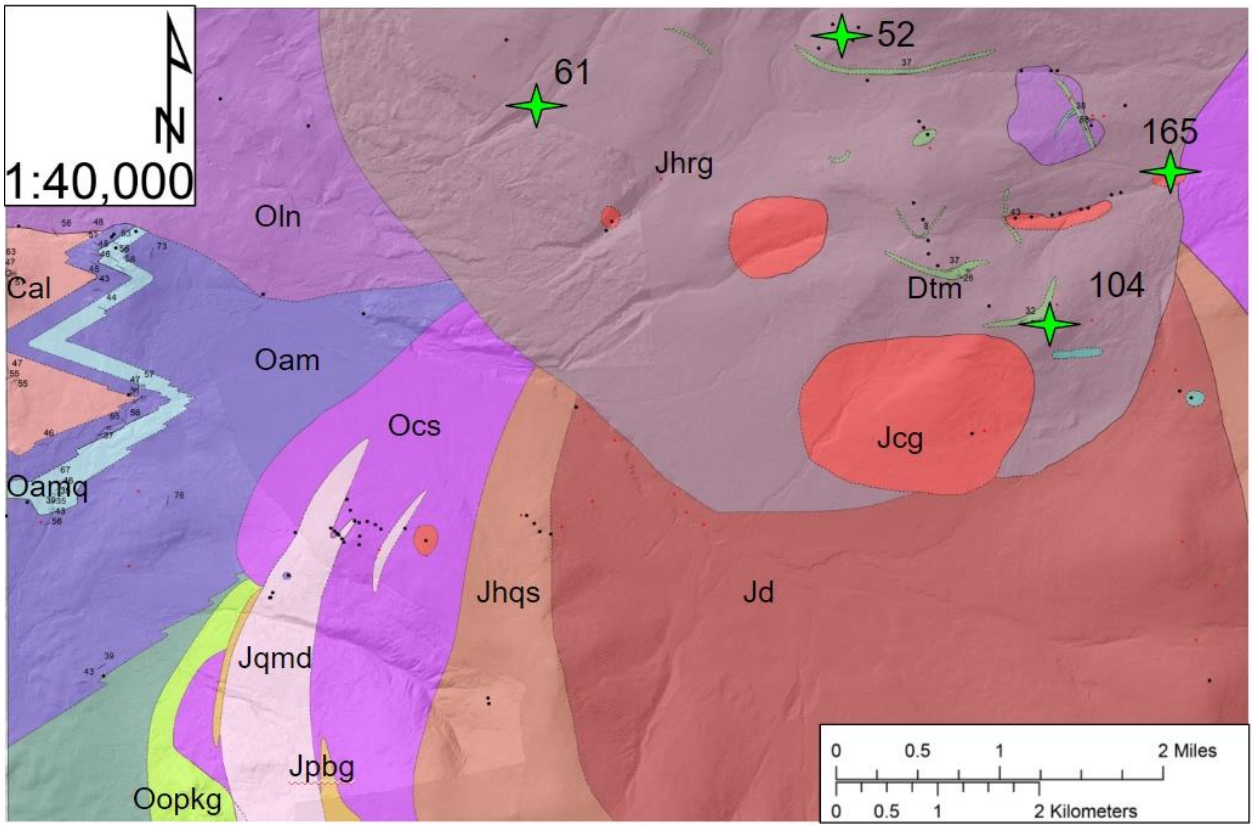

Figure 1.1: Geologic map of the Northern Jefferson quadrangle's Pliny region and Mt. Cabot pluton region. Modified from Hillenbrand (2017). For a more detailed description of the structural geology and a large map of the whole Jefferson 7.5" quadrangle refer to Hillenbrand (2017). Jhrg: Jurassic hastingsite-riebeckite granite, Dtm: Devonian Tarratine formation, Jcg; Jurassic Conway granite, Oln: Ordovician Lost Nation formation, Cal: Cambrian Albee Formation, Oam: Ordovician Ammonoosuc Volcanics, Oamq: Ordovician Ammonoosuc Volcanics quartzite, Oopkg: Ordovician Oliverian porphyritic K-feldpsar granite, Jqmd: Jurassic quartz monzodiorite, Jpbg: Jurassic plagioclase biotite granite, Ocs: Ordovician coarse syenite, Jhqs: Jurassic hastingsite quartz syenite, and Jd: Jurassic diorite. Rock samples and thin section sample locations are shown on the map with green stars.

1.2 Tectonic History of Area

The Mt. Cabot region is located within the Pliny Range and part of the Northern half of the Appalachian orogeny. The Appalachian mountain chain extends from Newfoundland to 300 km southwestward to Alabama. The northern half stretches from Connecticut to Newfoundland. The Appalachian orogen is a Paleozoic orogen and represents a full Wilson cycle of orogenic events. The Appalachian mountain chain was produced by three orogenies: the Taconic orogeny, Acadian-Neoacadian orogeny, and Alleghany orogeny (Hatcher, 2010). Much of the geology in Figure 1.1 was controlled by the events in the Taconic and subsequent Jurassic magmatism. The Mt. Cabot pluton itself was formed through Jurassic post orogenic melting during formation of the Pliny and Percy ring dike complexes (Chapman 1942; 1948; and Eichelberge, 1971).

1.2.1 Taconic

The Taconic orogeny occurred approximately 509 Mya in the Middle -Late Cambrian and subsided in the late Ordivicaian (445-435 Mya). The first phase of the Taconic orogeny was the development of a subduction zone along Dashwood and Lushes Bright plates. The second phase was a major mountain building event (Figure 1.2 and 1.3). A subduction zone formed along the Humber Seaway which resulted in the collision of the Notre Dame arc and Laurentia and a west dipping subduction zone. Later, the Annieopsquotch Ophiolite belt thrusted westward to create the Annieopsquotch oceanic tract. The third phase involved a collision of the Gander and Bronson Arc Hill to Laurentia (Van Staal et al., 2009) (Figure 1.3). During this phase of tectonics the Ammonoosuc volcanics group, Lost Nation group, Albee formation, and the Ordovician coarse syenite all were emplaced. The first three groups are all metasedimentary rocks and the syenite was formed through heating of the crust and the formation of magmatic

plutons from subduction zones. The syenites of the region from the Ordivician relate to the Oliverian Plutonic series (Eichelberger, 1971).

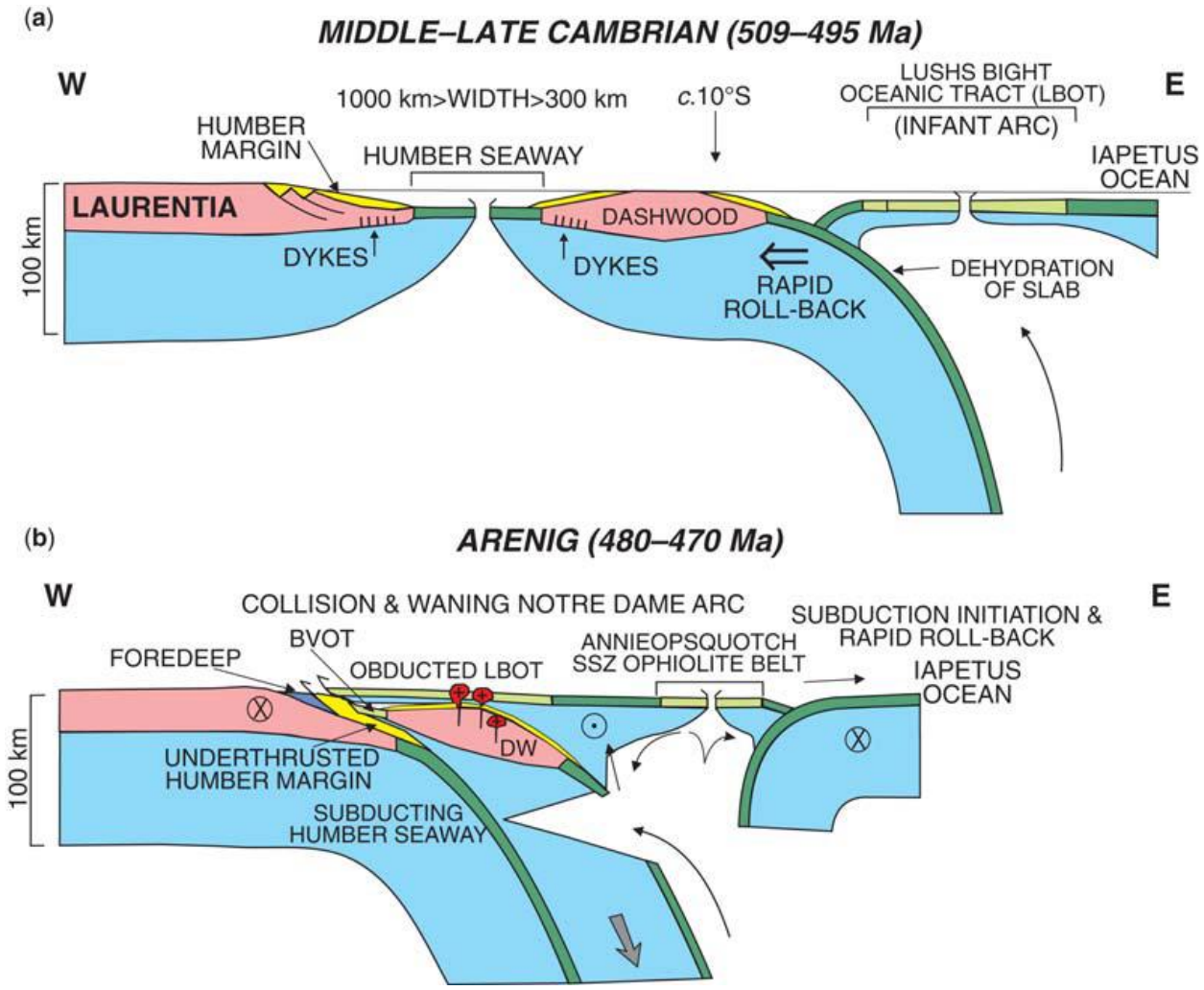

Figure 1.2: Cross sectional view of Taconic 1 and Taconic 2 (a) Taconic 1, (b) Taconic 2 (Van Staal et al., 2009).

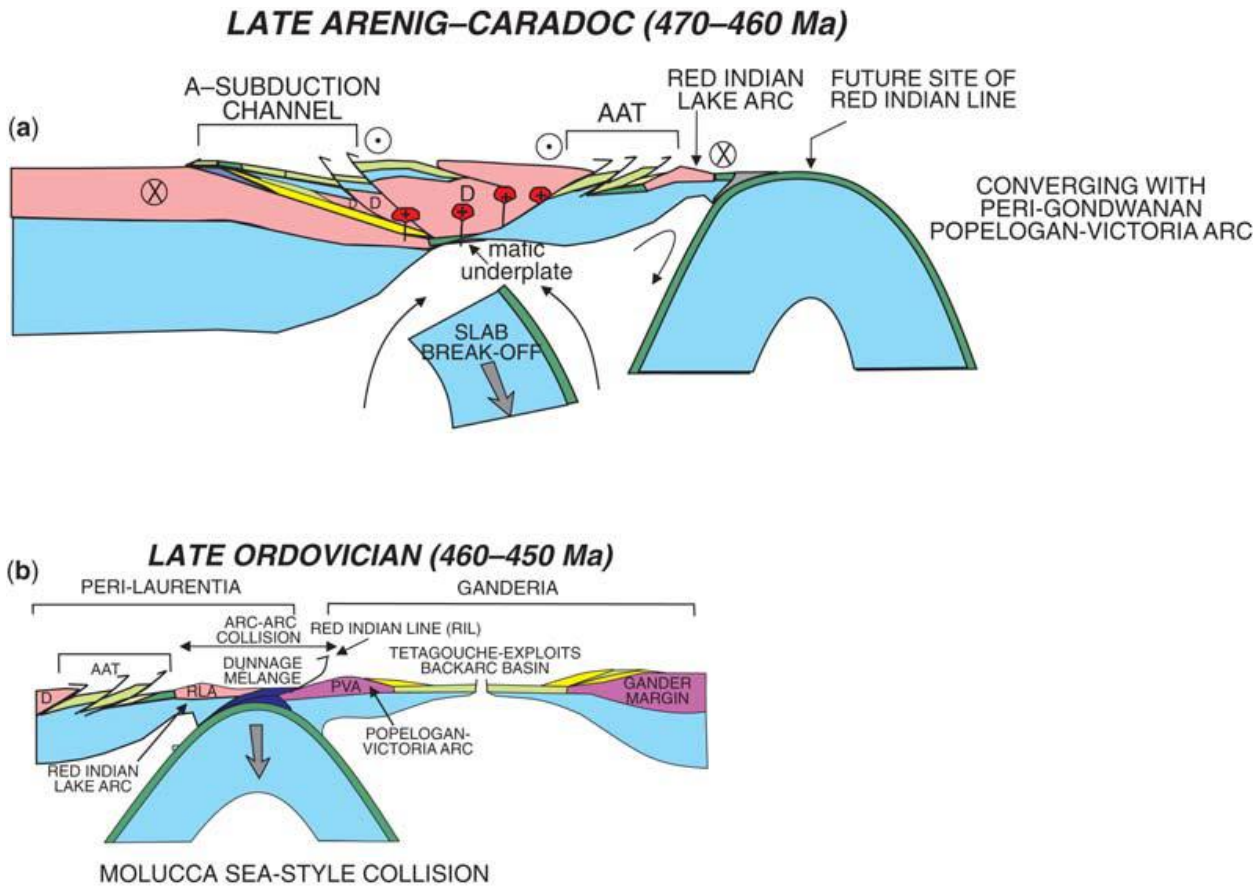

Figure 1.3: Figure 1.2: Cross sectional view of Taconic 2 and Taconic 3 (a) Taconic 2.5 (b) Taconic 3 (Van Staal et al., 2009).

1.2.2 Acadian-Neoacadian

The Acadian-Neoacadian orogeny (410-345 Ma) was a mountain building event which lasted from the Middle Devonian to the Late Devonian. Avalon, Caroline, periGondwanan superterranes, and possibly Gander collided directly with Laurentia and early Paleozoic terranes (Hatcher, 2010) (Figure 1.4). The folding caused the Laurentian-Taconian terranes to subduct further down. The folded, faulted, and highly metamorphosed rocks in the Appalachian mountain range are due to this event. Acadian plutons are abundant in New England due the final westward subduction emplacement of Avalon. Much of the Ordovician aged bedrock of the Mt. Cabot area was metamorphosed due to these events and the sedimentary and metasedimentary Devonian Terratine formation, found as xenoliths in the Mt. Cabot pluton, was formed.(Hatcher, 2010).

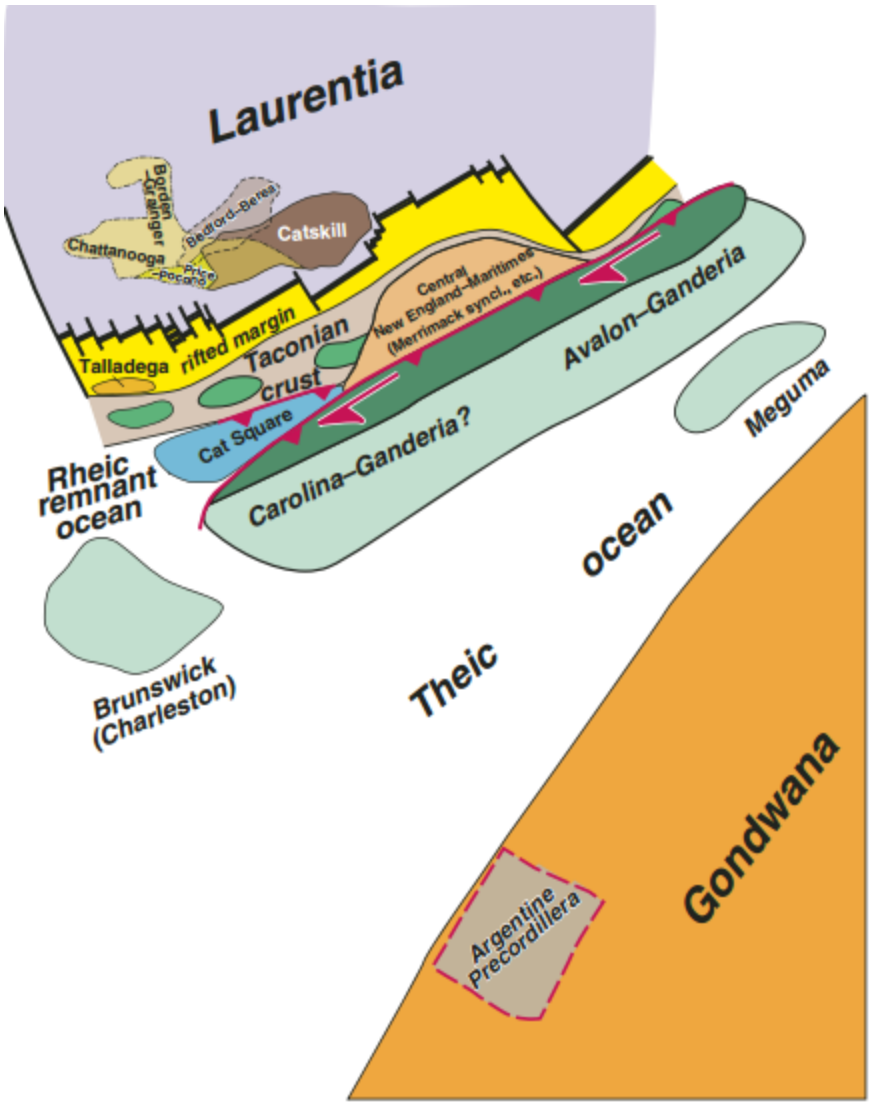

Figure 1.4: Map view of the Acadian-Neoacadian orogeny (Hatcher, 2010).

1.2.2 Alleghany

The Alleghanian orogenic event occurred from the early Carboniferous period to the late early Permian period (365-260 Mya). In short, Gondwana slammed into Laurentia to form the Alleghanian orogeny over multiple deformation events (Figure 1.5). The first deformation event in the late Early Carboniferous produced a sinistral fault in New England. This fault was immediately followed by dextral motion and pull-apart basins which shed clastic sediment on the continent. Then, southward rotation and movement of Gondwana caused even more sediment to disperse on Laurentia. Continued rotation of Gondwana closed the Theic-Rheic Ocean and caused more collisional event and thrust sheets in the Middle Late Carboniferous. Finally, Early Permian collisional events of Gondwana and Laurentia produced the Alleghanian fold-thrust fault and the Alleghanian suture. Again, much of the bedrock of the area from the Ordovician was further metamorphosed during these events (Hatcher, 2010).

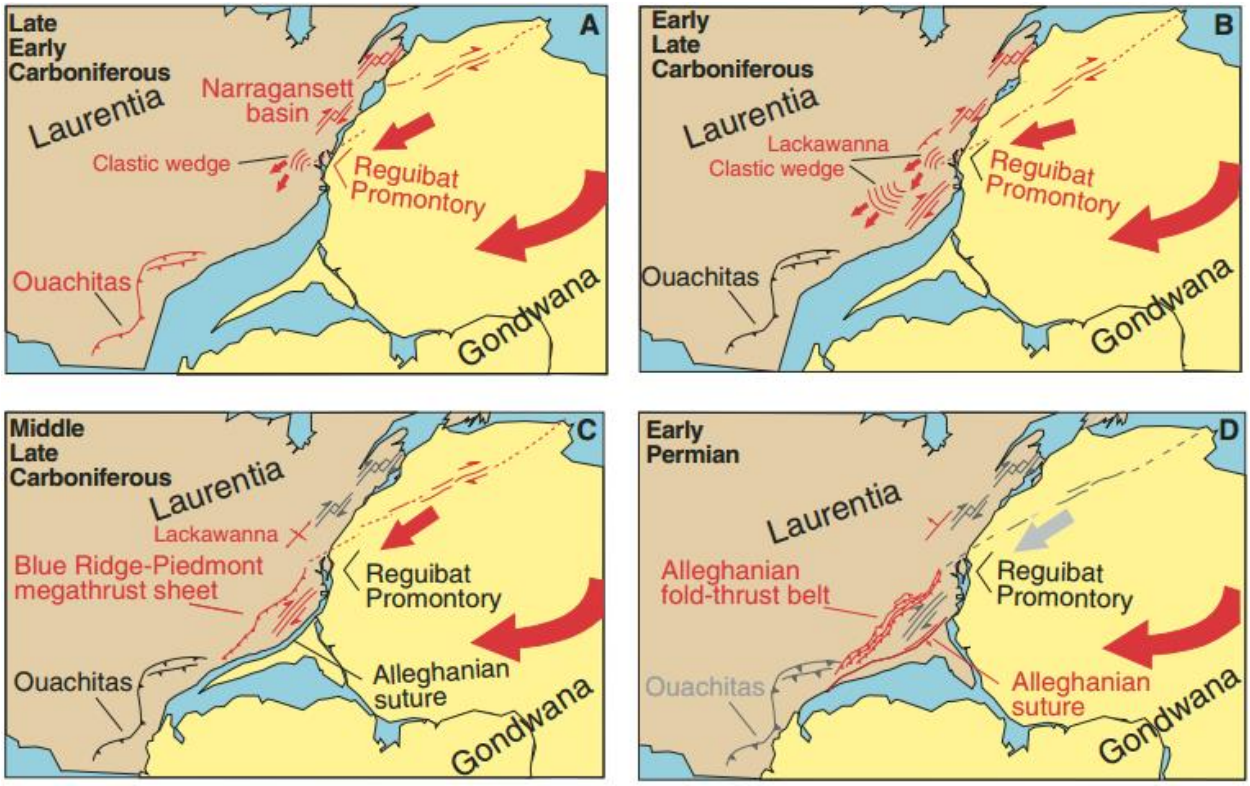

Figure 1.5: Map view of the Alleghanian orogenic events (Hatcher, 2010).

1.3 Ring Dike and Caldera Collapse

The bedrock and landscape of the Mt. Cabot region, specifically the Pliny Dike complex was partially controlled by the processes and consequences of ring dike formation and caldera collapse. Calderas are depressions in the terrain that are formed by the collapse of a drained magma reservoir (Corbi et al., 2015). Once the caldera collapses sill development takes place. Then, a propagation of lateral dikes in the bedrock occurs. Dikes eventually twist and bend due to stress of the area or eruptive fissures can occur and are limited by the outer rim of the caldera. These fissures are oriented radially or align with the regional tectonic stress field (Corbi et al., 2015). Magma emplaced creates sheet like dikes can be arranged centrally-inclined (cone sheets) or elliptical with a radial distribution (Figure 1.6). Ring dikes and collapsed calderas are common in the Pliny and Percy Region and partially dictate the distribution of igneous intrusive rocks in the area. These ring dikes are prevalent in New Hampshire and are the product of post orogeny magmatism from the opening of the now Atlantic ocean. The ring dikes and associated magmatism of the Pliny region is responsible for the Jurassic lithology of the Pliny ring dike complex and the Mt. Cabot pluton region (Figure 1.1) (Hatcher, 2010 and Eichelberger, 1971). Many of the xenoliths within the Mt. Cabot pluton form due to dropping into the granitic magma once the caldera collapsed (Hillenbrand, 2017). The Terratine formation, a Devonian sedimentary to weakly metasedimentary formation, previously had overlain the Jurassic granites. The formation eroded and during the caldera collapse integrated itself as a xenolith in the Mt. Cabot pluton (Hillenbrand, 2017 and Boucot, 1961).

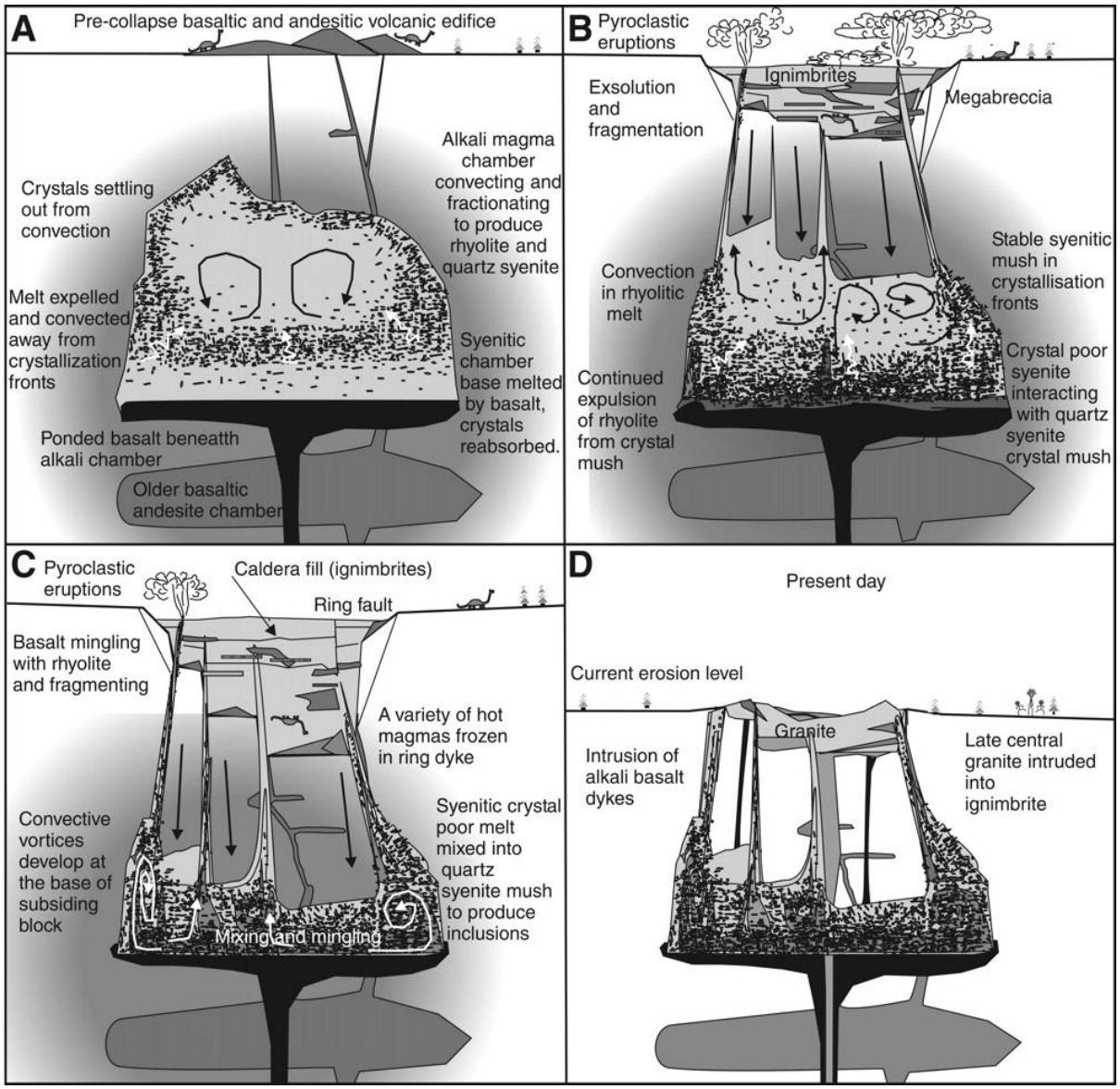

Figure 1.6: A cartoon of the major magmatic processes and the arrangement of stratification in the magma chamber: (A) before collapse; (B) early during caldera collapse; (C) during intrusion of the syenite; (D) after erosion (Kennedy and Stix, 2007).

1.4 Focus Area Geology

The Mount Cabot pluton is located within the Percy Region and the Pliny Region of both the Percy and Jefferson Quadrangles (Figure 1.7). It is part of the Triassic-Triassic (245-150 Ma) White Mountain igneous plutonic-volcanic series of plutons running N-S from the center to the north of New Hampshire (Figures 1.7 and 1.8). The pluton is surrounded by metasedimentary country bedrock and other Jurassic igneous intrusives. The plutonic stock contacts two ring dike complexes in the north in the south, the Percy ring dike complex and the Pliny ring dike complex. The part of the pluton in my study area mainly contacts a portion of the Pliny dike complex. The Mount Cabot pluton also contains an abundance of Conway granite, Albee formation, and Lost Nation xenoliths. This pluton is also surrounded by country rock of the late Ordovician Ammonoosuc volcanics and late Ordovician Lost Nation metasedimentary group. The Ammonoosuc volcanics is a formation with variably metamorphosed sedimentary and volcanic rocks of greenschist to granulite facies. The Lost Nation is mainly fine- to medium-grained dark intrusives consisting of highly metamorphosed quartz diorite and diorite. The Lost Nation group is part of the Highlandcroft Plutonic Suite. The Mt. Cabot pluton also contacts part of a quartz monzodiorite and diorite intrusive ring dike to the south which is part of the Pliny ring dike complex as described in Eichelberger (1971). The Albee formation, intermixed with the Ammonoosuc volcanics, is a late Ordovician fine-grained and pinstriped quartzite. Conway granite is composed mostly of pink K-feldspar, smoky quartz, and biotite, surrounds its northern and eastern extent (Figure 1.1) (Chapman 1935 and 1942).

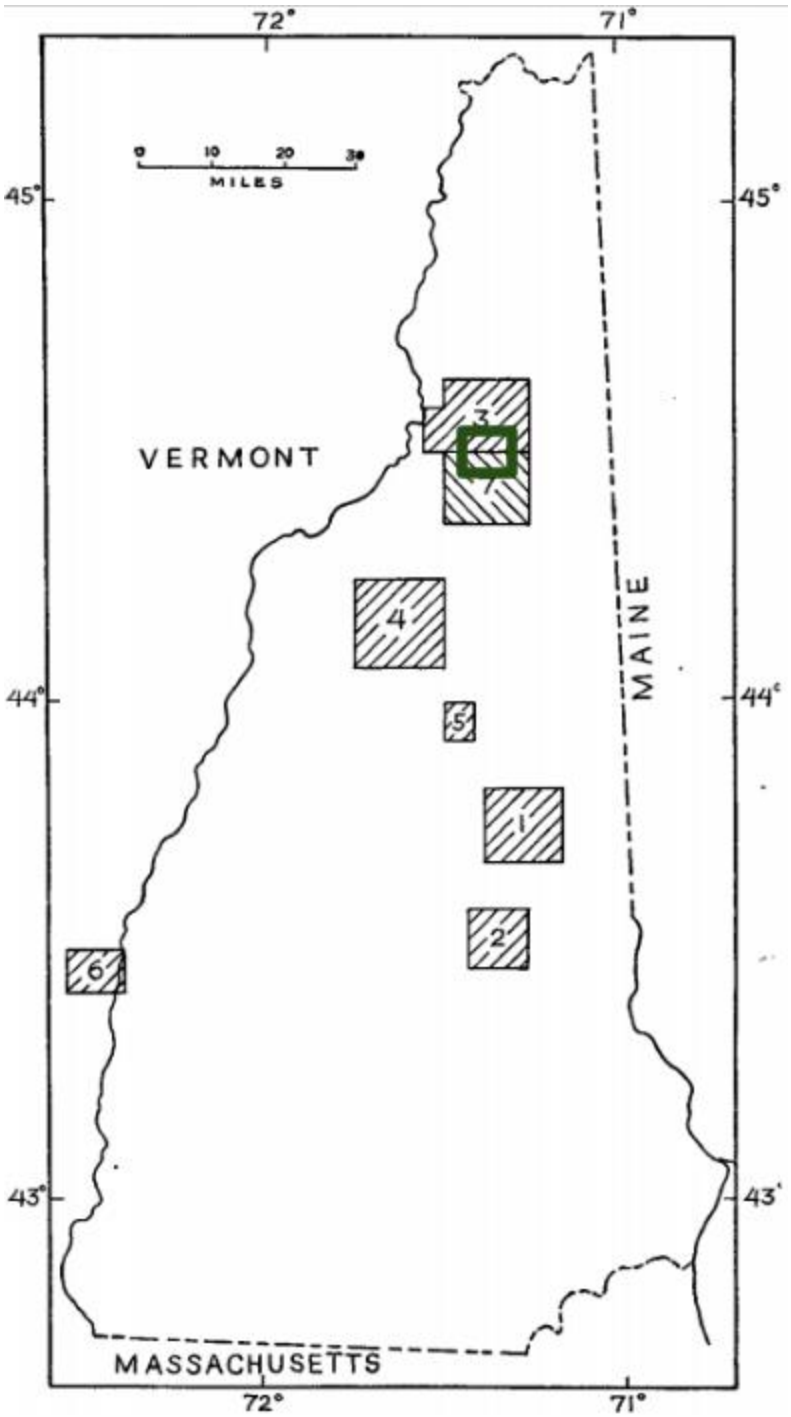

Figure 1.7: Map of the location of ring dike complexes in New Hampshire.
1: Ossipee mountains, 2: Belknap Mountains, 3: Percy Region, 4: Franconia Notch, 5: Mt. Tripyramid, 6: Ascutney Mountain, 7: Pliny Region. Area outlined in green is the Mount Cabot pluton (Chapman, 1942).

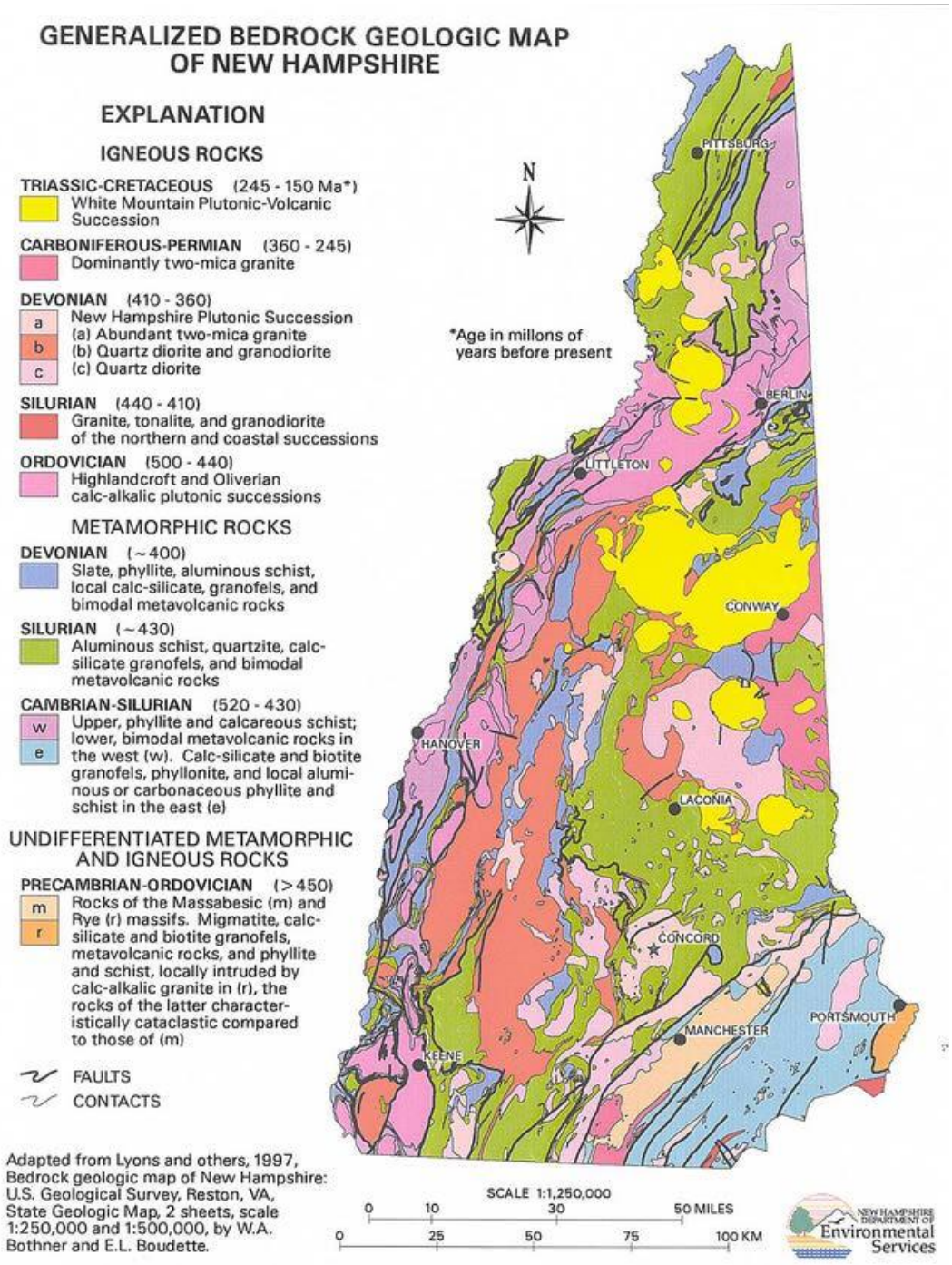

Figure 1.8: Modified New Hampshire State Bedrock Map (Lyons et al., 1997). Location of pluton is just west of Berlin and is the yellow White Mountain Plutonic-Volcanic Succession.

1.5 Previous Studies of the Hastingsite-riebeckite Mt. Cabot Pluton

1.5.1 Pliny Region

The Pliny region of the 15' Mt.Washington quadrangle, containing the southern half of the Mt. Cabot hastingsite-riebeckite granite, was first mapped by Chapman in 1942. The Pliny region is shown in Figure 1.1 and contains the Pliny region ring dike complex. The Mt. Cabot hastingsite-riebeckite granite is shown as a purple black stock. The ring dike complex is composed of the White Mountain magma series quartz monzodiorite and quartz monzonite, hastingsite-quartz syenite, hastingsite-riebeckite granite, hastingsite-biotite granite, granite porphyry, pink biotite granite, and Conway granite. These dikes are thought to be formed by cauldron subsidence or ring dike stoping, formed through magma chamber fracturing and collapse. Partial dikes will fill the fractured bedrock and intrude ring like sloping structures (Chapman, 1942).The country rock is similar to the Percy region and contains the Albee formation, Lost Nation group, and the Ammonoosuc volcanics. According to Chapman (1942) the relative ages of the dike complex units from oldest to youngest are: quartz monzodiorite and quartz monzonite, Hastingsite-quartz syenite, hastingsite-riebeckite granite, hastingsite-biotite granite, granite porphyry, pink biotite granite, and Conway granite. Like Chapman in 1935, the relative ages were determined through dike emplacement relationships. Chapman (1935) placed hastingsite-riebeckite granite younger in the Percy region than the Pliny region. Later studies by Chapman (1942 and 1948) of the Pliny region and the Percy region places the hastingsite-riebeckite as an intrusive igneous stock, rather than a thick ring dike. Exposures are found abundantly on the slopes of Mount Cabot and on the crest of Terrace Mountain. Chapman (1942)

also believes that the formation of the ring dikes was through fractionation and was derived from larger, more basic, parental lava.

Chapman (1942) describes the hastingsite-riebeckite pluton as an irregular plutonic mass along the northern part of the Pliny region an aerial extent of 6.5 miles. The pluton is made of three distinct amphiboles: hastingsite, riebeckite and hornblende. The hornblende, however, was not identified in any of the samples that he collected in the Pliny region, and was only found in the Percy region extension mapped by Chapman in 1935. It is a medium-grained rock containing principally feldspar, quartz, hastingsite, and riebeckite. Most of the hastingsite occurs irregular crystals that a devoid of inclusions and are 1-2 mm in size. Many of the specimens contain both riebeckite and hastingsite. Due to the difficulty and impartibility of defining distinct zones, he decided to lump the whole pluton into the term hastingsite-riebeckite granite (Chapman, 1942).

1.5.2 Percy Region

The northern half of the Mount Cabot region hastingsite-riebeckite granite was first mapped by Chapman in 1935. It is part of the southeast section of the Guildhall quadrangle. This part of the Mount Cabot granite is introduced as part of the Percy ring dike complex. The older rocks of the complex are metamorphic screens from the Albee formation, Ammonoosuc volcanics, and Lost Nation believed to be from the early and late Ordovician. The hastingsite-riebeckite granite and dikes are placed in context as being part of the ring dike complex. The ring dike complex is composed of dark syenite porphyry Cape Horn Ring Dike, coarse syenite Devil's Slide Ring Dike, syenite Pilot Complex, the Hastingsite-Riebeckite Granite Ring Dikes, and the Biotite Granite Ring dike. A geological map of this area can be found in Chapman (1948). The largest stocks of the area are biotite granites and the Mt. Cabot hastingsite-riebeckite granite (Chapman, 1935). Chapman believes the chronology of the intrusions from oldest to youngest is:

syenite porphyry, syenites, hastingsite-riebeckite granite, and biotite granite. He believes that the hastingsite-riebeckite ring dikes are younger than most the intrusions through analysis of relative proximity to each other and similar distribution around the syenite ring dikes. He believes igneous intrusions were derived from a basic parental magma and formed through differentiation and can be placed as being part of the White Mountain magma series based on the differences in mineral assemblages and changes in geochemical data. The hastingsite-riebeckite granites were described as small incomplete ring dike structures in the northern part of the region and a large complex in the Mount Cabot area. They can be categorized as hastingsite granites and riebeckite granites but are too genetically similar, due to their proximity one another, similar non-amphibole mineralogy, and presence of intermingling between hastingsite samples and riebeckite samples not to be placed as one unit (Chapman, 1935). Many of these granites were found with both hastingsite and riebeckite. The hand samples are medium-grained and coarse grained with a snow white to pinkish. The granites are composed of white to pink feldspar, colorless to smoky quartz, and blue to jet black amphibole (Chapman, 1935). Macroscopically and microscopically, these granites contain dominantly microperthite and quartz with riebeckite and hastingsite. Accessory minerals were astrophyllite, allanite, hornblende, and fluorite. It is uncommon to see riebeckite replacing hastingsite and radiating riebeckite minerals due to the hydrothermal reactions and late magmatic reactions that affected the pluton during crystallization. Although percentages of quartz and microperthite are slightly off compared to samples with only one of amphibole, the proximity of the duel amphiboles samples to the ones containing either riebeckite or hastingsite are similar, thus they are placed in the same lithology (Chapman, 1935). A similar description of the hastingsite-riebeckite granite in the Pliny region was given by Chapman in 1942.

The study by Chapman in 1948 is a more updated view on the Percy quadrangle and the Percy ring dike complex in the southwest portion of the quad. It provides an updated petrographical study of the Albee formation, Ammonoosuc volcanics, Lost Nation Group, Oliverian magma series, New Hampshire magma series, and White Mountain magma series with a similar petrographical description of the Mt. Cabot pluton. Although the study focuses on the portion of the Mt. Cabot pluton in the Pliny region, studies of both areas are similar and important in understanding the emplacement near ring dike complexes, geologic environment, and mineralogy of the pluton and the unit in the ring dike complexes.

1.6 The White Mountain Magma Series

Work done by Chapman in 1938, 1942, and 1948 on the Percy and Pliny regions shows that the Percy and Pliny Region igneous plutons are part of a larger intrusive igneous province called the White Mountain igneous province of New Hampshire. The White Mountain igneous province of New Hampshire is part of the larger New England-Quebec province, one of the Mesozoic igneous provinces described by McHone and Butler (1984). The New England province is represented by two periods of igneous activity. The first igneous activity occurred 200-155 Ma in the Jurassic and the younger series occurred between 130-100 Ma in the Cretaceous (Figure 1.9). The rocks of the Jurassic igneous activity are primarily composed of alkali syenite, quartz syenites, metaluminous and peralkaline granites (Eby, 1995).

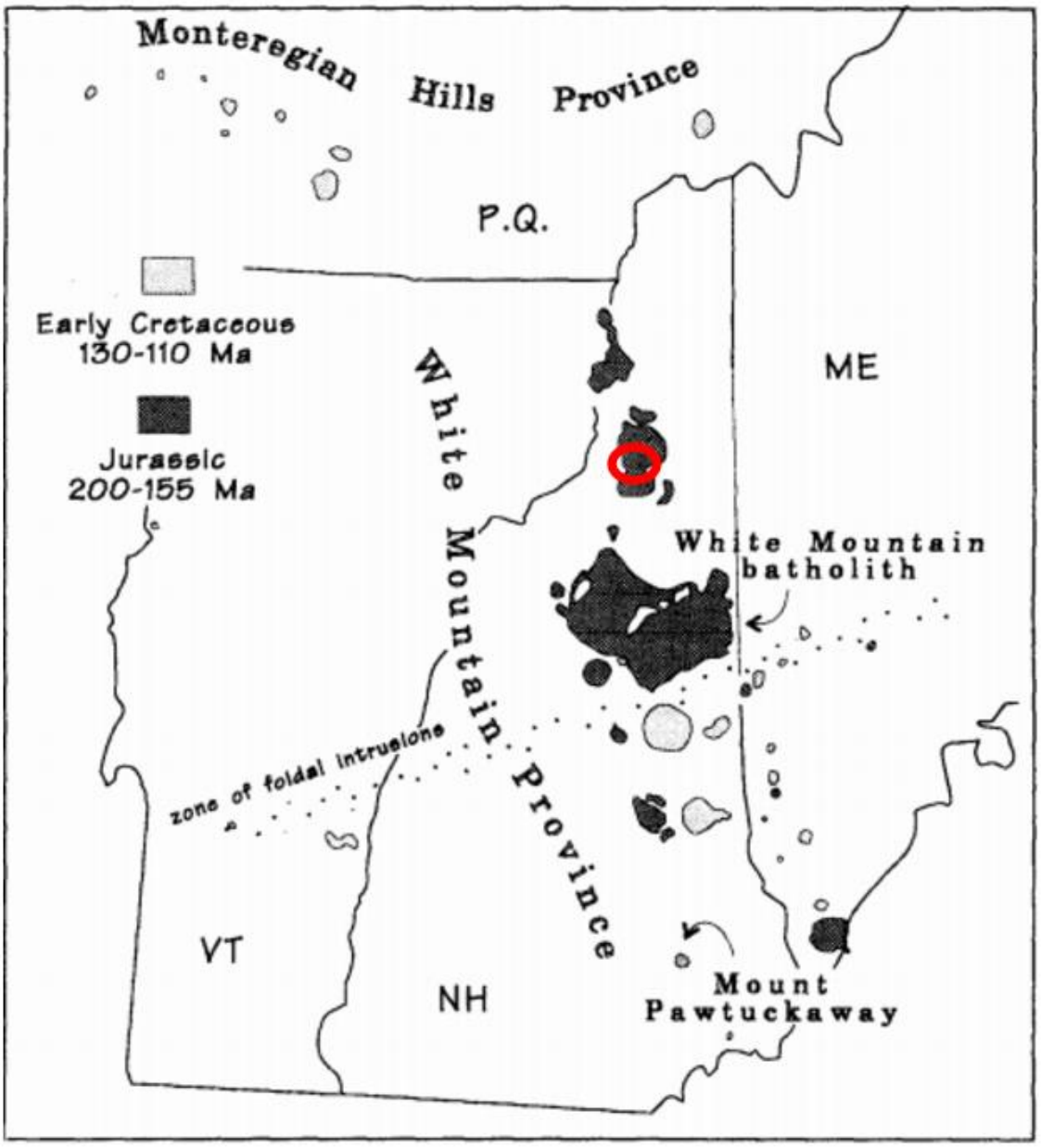

Figure 1.9: White Mountain igneous province. Red circle indicates area of study (Eby and Creasy, 1993).

The White Mountain igneous province and White Mountain Magma series represents one period of Mesozoic intraplate magmatism related to the opening of the Atlantic ocean from 240 Ma-95 Ma (McHone and Butler, 1984). The igneous provinces that formed due to the Mesozoic intraplate magmatism are the Coastal New England province (CNE), White Mountain magma series (WMMS) 200Ma-160Ma, Eastern North American Dolerite province (ENA) 200-165 Ma, and New England-Quebec province 135-95Ma (NEQ). The CNE is composed of alkali syenite and alkali dolerite from the first stages of igneous activity and are located within 60km of the eastern coast. The WMMS is broadly composed of syenite, granite, and monzonite and is located in a 75x100-km zone in northern New Hampshire. The ENA is composed of alkali dolerite and theolitic basalt located to the eastern side of the Appalachian anticlinorium. The NEQ is composed of gabbro, syenite, and lamprophyre located in most of Vermont, southern New Hampshire, and southern Quebec (McHone and Butler, 1984). The Mesozoic provinces in New England were formed from the Mesozoic rifting and spreading events of the North American plate and African plate to from the Atlantic Ocean (Figure 1.10). The CNE magmatic plutons were the first province to intrude and form due to the pre-rifting uplift in the Permian and Triassic. The ENA and the WMMS formed around the same time due to the separation of eastern North America from the northwestern Africa during the Jurassic period. The formation of the NEQ was due to the rifting and separation of the Newfoundland and Iberian Peninsula continental crust. Magmatism of the area ceased with the formation of the NEQ around 95 Ma (McHone and Butler, 1984).

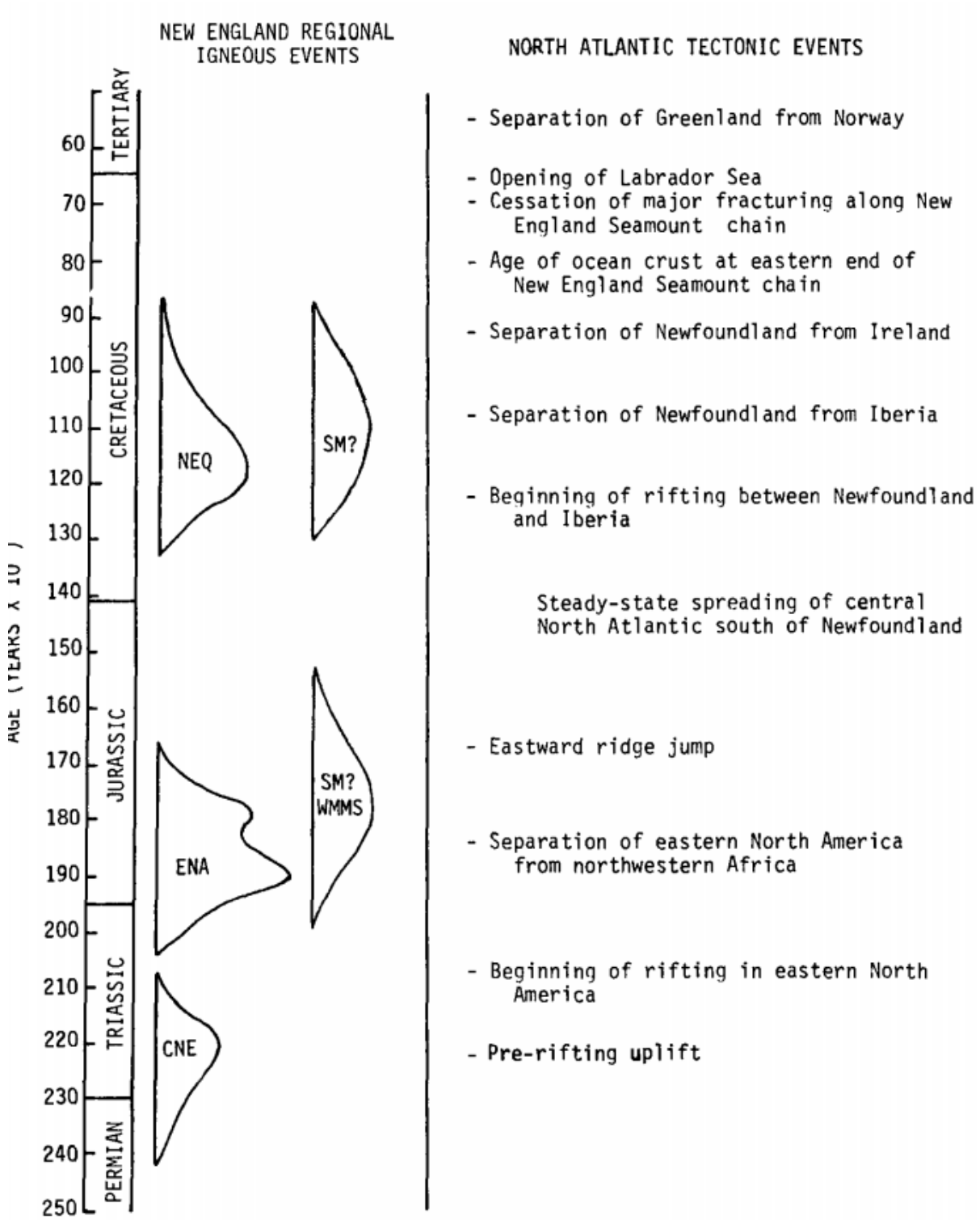

Figure 1.10: Correlation of magmatism with North Atlantic rifting and spreading during the Mesozoic era (McHone and Butler, 1984).

The largest pluton of the Jurassic White Mountain Magma series (WMMS) is the White Mountain batholith, located in central New Hampshire (Figure 1.11). The batholith is part of the north-south trend of igneous activity mapped in New Hampshire and it is south of the Pliny and Percy region mapped by Chapman (1935; 1942). This batholith is composed of many overlapping centers of felsic magmatism and has an areal extent of 1,000 km^3. The centers are composite ring dikes of porphyritic quartz syenite. The bulk of the White Mountain batholith ring dike complexes are composed of subalkaline to peralkaline silica-oversaturated amphibole granitoids (Eby, 1995). A simplified geologic map of the White Mountain batholith shows it being composed of nine different intrusive igneous rocks. The country rock consists of lower Paleozoic schists, gneisses, and granites. The Jurassic igneous intrusive plutons are the amphibole-bearing syenites to riebeckite granites of the Hart Ledge complex, granite porphyry, Mount Lafayette, Mount Garfield porphyritic quartz syenite, syenite porphyry Mount Carrigain complex, Albany porphyritic quartz, moat volcanics, various Jurassic syenites, Mt. Osceola granite, and Conway granite. The Mount Osceola granite, green and medium-grained amphibole granite, and the pink biotite Conway granite, compose 80% of the overall extent of the White Mountain batholith (Eby et al., 1992).

Genetically similar granites that compose 80% of the White Mountain batholith are the Mount Osceola granite and the peralkaline granite intrusions of the eastern center of the batholith. The Mount Osceola granite is medium- to course- grained hypersolvus granite that is dark green at fresh outcrops. It has small 3-10 mm anhedral and subhedral microperthite grains surrounding smoky quartz, interstitial ferrohastingsite and annite grains, and local sections of peralkaline rock containing ferrorichterite or riebeckite rimmed ferrohastingsite. The compositions of the amphiboles range from Al-poor ferrohastingsite→ ferrorichterite→

riebeckite. The appearance of several types of amphiboles in one hand sample shows variation in the degree of fractionation within local areas (Eby et al., 1992). Two amphiboles are present because of a continuous reaction series of the hastingsite group. As the temperature decreases in the melt, the amphibole composition turns from magnesium-rich to iron-rich to sodium-rich. Magnesiohastingsite is the magnesium-rich member, ferrohastingsite is the iron-rich member, and riebeckite is the sodium-rich endmember. Peralkaline dikes and small plutons cut through the Mt. Osceola and Conway granite. These dikes are spatially and genetically similar to the Mt. Osceola granite and are joined with gradual contact. The younger dike and plutons are composed of microperthite, clear quartz, blocky interstitial grains of riebeckite-afversonite, and aggregates of interstitial biotite (Eby et al., 1992). These two granitic bodies are similar in age and mineralogic composition as Chapman's (1935) description of the Mount Cabot granite.

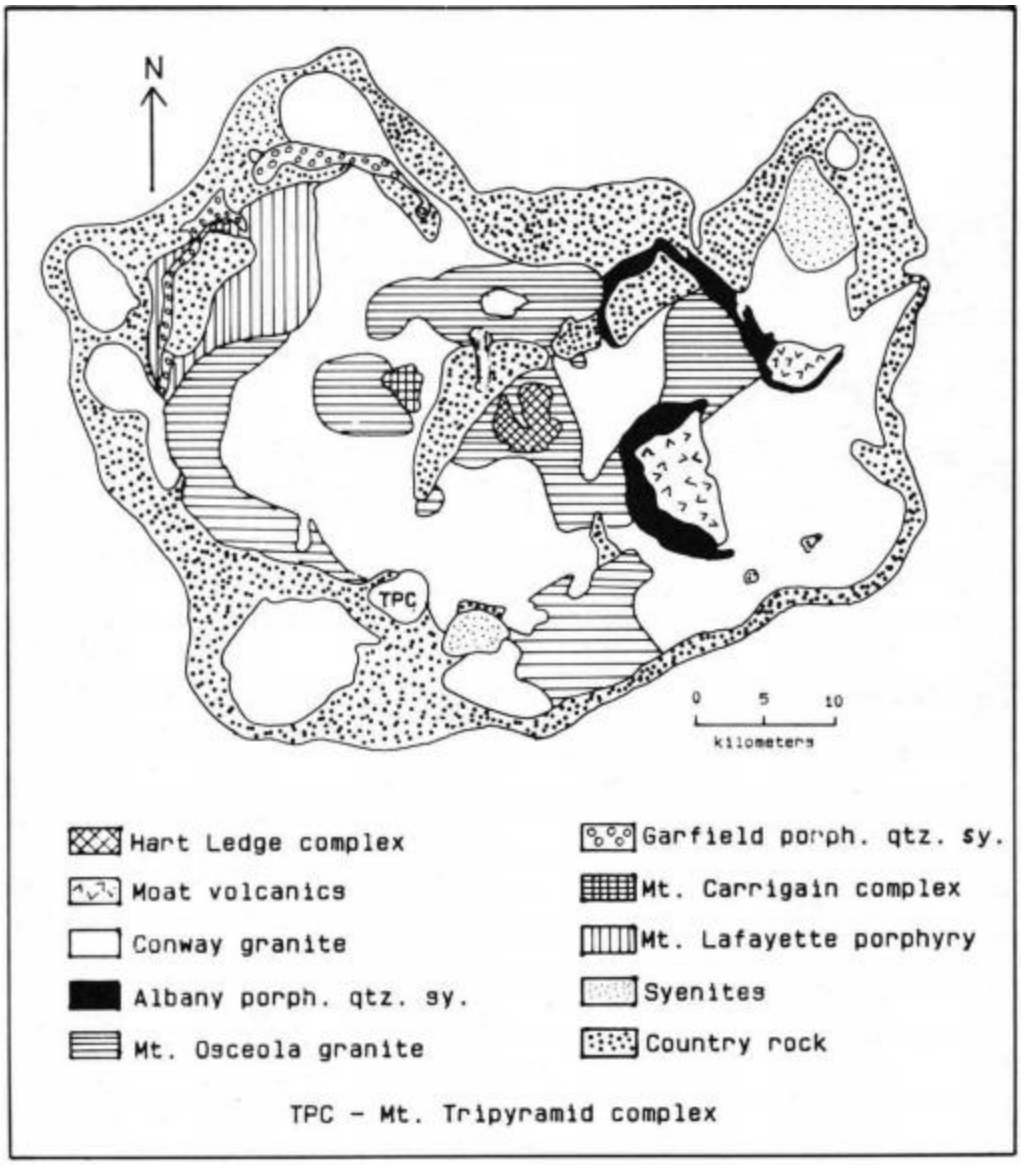

Figure 1.11: Simplified geology of the White Mountain batholith (Eby et al., 1992).

1.7 Similar Peralkaline Granites

1.7.1 A-Type Magmatism

The Mt. Cabot pluton and the WMMS can be classified as an A-type granite from the basis of the S-I-A-M classification system by Bruce Chappell and Allan White (1974). The classification system is based on geochemical information of the granite and the manner in which they were emplaced. S-type granites correspond to deep crustal melting of sedimentary rock. I-type granites are richer in Ca, Sr, Fe^{3+}/Fe^{2+}, and $^{143}Nd/^{144}Nd$ but lower in Cr, Ni, $\delta^{18}O$, and $^{87}Sr/^{86}Sr$ than S-type granites. The chemical signatures of I-type granites suggest genesis from partial melting mafic mantle-derived igneous rocks found at subducted-slab or older pluton sources. The M-type granitoid are derived from partial melting of subducted oceanic crust and form near continental margins. The final type is the A-type granites. A-type granites are commonly emplaced in intraplate anorogenic settings. Example settings are continental rifting and hot spots. These rocks usually precede tectonic events and are high in SiO_2, alkalis, Fe/Mg, and REEs. A-type granites are commonly alkaline, peralkaline, and have hornblende, biotite, aegirine, fayalite, riebeckite, and arfvedsonite as associated minerals. Rocks formed during rifting periods are usually associated with ring dikes and shallow intrusives (Winter, 2014 and Bonin, 2007).

1.7.2 A-type Magmatism Around the World

A-type magmatism can be found in many different parts of the world. Famous localities occur in Nigeria, Scotland, southwestern Alaska, Massachusetts, and Virginia. Characteristics of the magma include the appearance of microperthitic feldspar, quartz crystals, at least one amphibole, sometimes a pyroxene such as aegirine, and accessory minerals such as fluorite and

astrophyllite. Amphiboles that are common in these A-type granites include: riebeckite, arfvedsonite, and hastingsite. Although granites associated with A-type magmatism are not constrained to a certain time period in Earth's history, A-type magmatism was common in the late Proterozoic 1 Ga-541 Ma through a variety of post tectonic origins (Sherif et al, 2013; Tollo and Lowe, 1993; Lyons and Krueger, 1976; Abdel-Rahman and El-Kibbi, 2000; Khan et al, 2012; and Gross and Heinrich, 1966). Mesozoic A-type magma (Jiang et al, 2013; Eby et al, 1993; Thompson et al, 1982; and Chapman 1942 and 1948).

Late Proterozoic A-type plutons usually contain a suite of granites ranging from alkaline to peralkaline composition. A useful petrogenesis model by Sherif et al. (2013) shows an emplacement method of alkaline A-type granites and is similar to ring dike emplacement and caldera collapse shown in Figure 1.6 (Figure 1.12). First, basaltic rocks are formed from subduction zone melting. Alkaline magmas are produced through the partial melting of the continental crust. The partially melted crust creates horizontal silicic magma reservoir chambers. Due to the generation of large magma bodies, the upper portion of the crust begins to collapse. The magma flows up the fractures and joints to shallower depths during a rifting type environment. Fractional crystallization of the alkali granites during the transport of this magma to shallower depth creates riebeckite granites. A post collisional environment forms these alkali granites through fractional crystallization of the syenogranite melt. Granites in Egypt that are rich with riebeckite were most likely created through this pathway at the end of the Pan-African Orogeny (Sherif et al., 2013). Similar subalkalic to alkalic granites in Pakistan formed because of rift related intraplate magmatism, formed by an extensional post orogenic regime, contain riebeckite through similar but less evolved fractionalization crystallization of basaltic parental magma (Khan et al., 2012). The Amissville formation, in the Robertson River igneous suite in

Blue Ridge province of northern and central Virginia, is riebeckite-bearing peralkaline granite formed from an anorogenic rifting event that formed elongate dike-like plutonic bodies. The Amissville formation is synonymous with A-type anorogenic granites. Previous rhyolitic and conglomerate volcanics of the Robertson River formation represent waning volcanic activity while the peralkaline Battle Mountain and Amissville formation represent fractionated magma generation and crystallization as part of the plutonic-volcanic complex (Tollo and Lowe, 1993). The Mount El-Sibai granitic complex in Egypt is highly evolved and composed of hypersolvus feldspar, quartz, alkali amphibole, and accessory minerals. Amphibole chemistry indicates that the amphibole composition ranges from hastingsite to the arfedsonite end member. This granite complex was formed through fractional crystallization of magma created through cooling and fracturing of the newly formed Pan-African crust (Abdel-Rahman and El-Kibbi, 2000). Late Proterozoic A-type granite is usually of alkaline and/or peralkaline composition with characteristic perthite and formed from post orogenic fracturing and rifting events. These A-type granites formed in similar tectonic environments and have similar mineralogical makeup as the Mt. Cabot pluton.

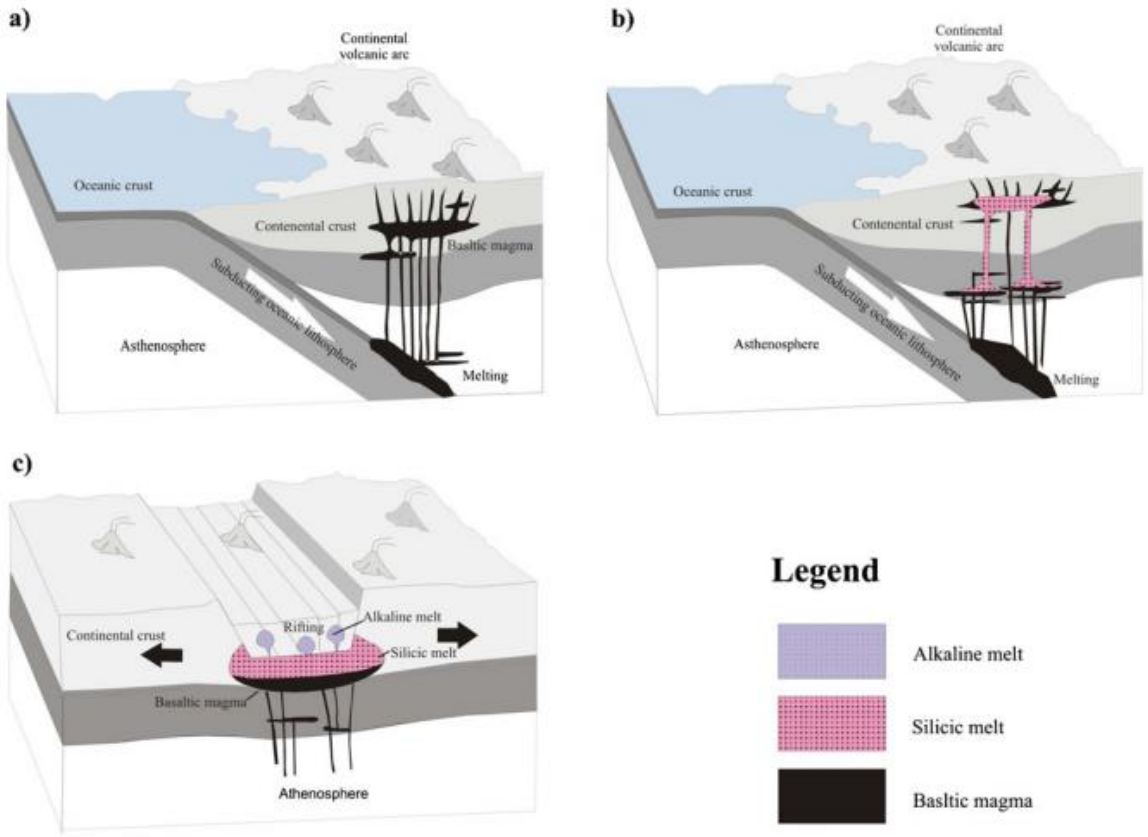

Figure 1.12: Evolutionary stages for granitic rocks at Sharm El-Sheikh area, Egypt (Sherif et al., 2013).

Late Proterozoic alkalic plutons in southern New England are close in chemical composition and proximity to the Mount Cabot pluton in northern New Hampshire (Figure 1.13). The Rattlesnake pluton in Sharon, Massachusetts is composed of coarse biotite and fine riebeckite granite. The Peabody granite is composed of entirely coarse-grained ferrohastingsite granite (Lyons and Krueger, 1976). The Quincy pluton has three closely related granites: medium grained riebeckite-aegirine granite (Quincy granite), mineralogically similar fine-grained granite, and riebeckite granite porphyry. The Cape Ann pluton has a ferrohastingsite unit, medium- grained riebeckite-aegirine granite, and ferrohastingsite syenite. The hypersolvus portions of the Rattlesnake pluton suggest crystallization at depth through blister collapse and cauldron subsidence. Temperatures closer to 660^{o}C represent the later stage granitic formation period while higher temperatures up to 925^{o}C represent early stage of volcanic rock creation. Declining water-vapor pressure triggers the change from coarse- to medium-grained texture to fine-grained. Variations and contamination of chemically different country rocks create differences in amphibole composition, from ferrohastingsite to riebeckite in spatially different areas (Lyons and Krueger, 1976).

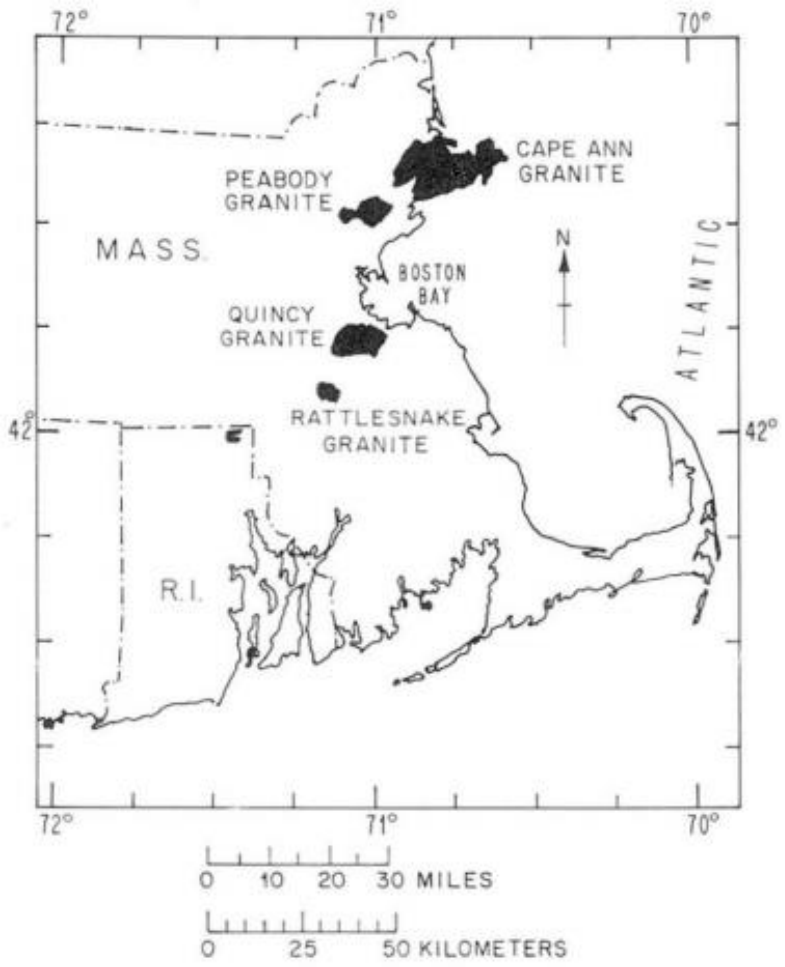

Figure 1.13: Distribution of alkalic plutons of southern New England (Lyons and Krueger, 1976).

A-type granites that occurred in the Mesozoic generally produced very silicic and alkaline magma in the end stages of intrusion. Ring-complexes in the younger granites of Nigeria are very similar to the ones found in WMMS of New Hampshire. The occurrence of rhyolites, biotite-granite, and riebeckite-granites are similar to Eby's studies (1992 and 1993) of the various intrusive pluton complexes of central and Northern New Hampshire and mirrors Chapman's studies (1935; 1942; and 1948) of Percy and Pliny ring dike complexes. The structure of the ring dikes is similar but the composition of the granites is more silicic and alkaline compared to previously studied granitic bodies. The appearance of riebeckite granite, late forming biotite-granite and early intermediate composition volcanics place are the key similarities between the two regions (Jacobson, 1958). A similar complex, Bokan Granite Complex, located in southeastern Alaska represents a more alkaline rich granitic environment with no biotite, subsolvus feldspar, and aegirine-riebeckite rich intrusions. However, this system represents a near orogenic and plate-edge environment with I-type and A-type characteristics. A complex set of intrusions show the appearance of both hypersolvus riebeckite granites at depth and subsolvus aegirine-riebeckite granites forming due to ring dike collapse. Subsequent magma crystallization represents a lower degree in oxidation and/or peralkalinity. The Bokan Granite Complex represents a highly diverse and complex alkaline ring dike complex formed high and lower pressure melting of magma controlled by fractional crystallization. Parental magma and crystallization environment help control the formation and chemical composition of A-type amphibole granites (Thompson et al., 1982). Riebeckite granophyre of the Da Hinggan Mts represent a period of A-type magmatism due to continental crust stretching in similar age to Eby and Kennedy's (2004) study of the younger WMMS Ossipee Ring dike complex. The Cretaceous 126 ± 2 Ma old riebeckite granophyres intrude into intermediate volcanics and granitic

intrusions. The granophyres are related to intraplate extensional rifting environment of the Mesozoic, an alkaline to peralkaline granite rich in REES, and underwent high differentiation in a magmatic-hydrothermal transition stage (Jianguo et al., 2012).

1.8 Amphiboles

The amphiboles in the amphibole super group are one of characteristic minerals that form in alkaline A-type granites. A standard amphibole has the general formula $A_{0-1}B_2C_5T_8O_{22}(OH,F,Cl)_2$ or $A(M4)_2\ \{[(M1)_2,M3\ ](M2)_2\}\ T_8O_{22}\ (OH,F)_2$ if the ordering sites are specified. The A site is Na,K, B slot is Na,Li,Ca,Mn,Fe^{2+}, C site is Mg,Fe^{2+}, Ti, and T site is Si, Al. The M4 site is Ca, Fe^{2+}, or Mg. The M1 site is Mg, Fe^{2+}, Fe^{3+}, Al, Cr, Mn^{2+}, Mn^{3+}, Ti (Verblen, 1981).The amphiboles are further divided into four subgroups based on the B group cation occupancy. The iron-magnesium-manganese group contains $(Ca+Na)_B$ <1.34. The calcic amphibole group has $(Ca+Na)_B \geq 1.34$ and Na_B <0.67. The sodi-calcic amphibole group is $(Ca+Na)_B \geq 1.34$ and $0.67 \leq Na_B$ <1.34. The final group, alkali amphibole group is $Na_B \geq 1.34$. Amphiboles can also be classified by the end-members of a solid solution. The key characteristic of the amphibole structure is the double chain of corner-linked tetrahedrals. The structure extends infinitely in one direction and has a general formula of $(T_4O_{11})_\infty$. The wide variety of cation coordinations in the amphiboles and the structural complexity of these minerals results in their chemical complexity (Verblen, 1981). The site occupancies and order-disorder relationships of cations in these amphiboles allows a better understanding of crystal chemistry and phase relations. Cations that can occur in different valence states in amphiboles are important for understanding their crystallization. The most important cation with different valence states is iron. Ferric iron is associated with the C-group cation. Ferric iron is strongly ordered on the M2 site but can be also attributed to the M1 and/or M3 site. The latter of the two could represent

equilibrium crystallization conditions or post-equilibration oxidation. Ferrous iron is usually associated with the B and C groups but the character of ordering patterns changes with amphibole group (Verblen, 1981). Since the hastingsite-riebeckite granite of Mount Cabot contains a calcic amphibole group member and an alkali group member, it is useful to understand the ordering of ferrous iron in those groups. The ordering of Fe^{2+} is extremely varied from mineral to mineral. The predominant ordering pattern is M1 ≥ M3 > M2 ≥ M4. However, Fe^{2+} ordering is highly dependent on the parental magma's bulk composition. The alkali amphibole group minerals show distribution preference of ferrous iron in metamorphic amphiboles such as riebeckite and glaucophane with M3 > M1. Igneous derived riebeckite mineral crystals, however, show irregularly high ordering rates with the M1 site (Verblen, 1981).

1.8.1 Hastingsite

The minerals hastingsite and riebeckite are endmembers in separate amphibole groups. Hastingsite is an endmember of the calcic amphibole group with a general formula of $NaCa_2(Fe^{2+}4Fe^{2+})Si_6Al_2O_{22}(OH)_2$ and is also part of the hornblende amphibole group. The major endmember in the hornblende group, ferrohastingsite, has a chemical composition of $NaCa_2Fe_4^{2+}(Al,Fe^{3+}[Si_6Al_2O_{22}](OH,F)_2$ (Deer et al, 1967). Hornblendes are characterized by their high Ca content and can be found in ultrabasic to acid and alkaline intrusives and rock of greenschist to lower granulite facies. Although the common hornblende is characteristic of intermediate to calc-alkalic granites, iron-rich ferrohastingsite is restricted to the more alkaline, syenite, and nepheline-syenites compositions (Deer et al, 1967). Generally, hornblende minerals can be considered as having three compositional series, with different aluminum content and ordering. First, the edenite-ferroedenite composition is $NaCa_2Mg_5(Si_7Al)O_{22}(OH)_2$ and can be

considered a derivation of tremolite. The second series, also derived from tremolite, involves replacement of Si by Al, Mg by Al, and a vacant A site. The end member of this series is $Ca_2(Mg_3Al_2)(Si_6Al_2)O_{22}(OH)_2$ (Deer et al, 1967). The combination of these series gives the iron and magnesium end members, pargasite and hastingsite, with a chemical composition of $NaCa_2(Mg,Fe^{2+})AlAl_2Si_6O_{22}(OH)_2$ (Deer at al, 1967).

Hornblendes are essential ferromagnesian minerals of diorites, intermediate, and alkaline rocks. Hornblendes are compositionally diverse in diorite type igneous rocks and do not typically have a compositional bias towards either ferrohastingsite or tschermakite compositions. In acidic and alkaline plutonic rocks however, hornblendes are usually restricted towards the hastingsite and ferrohastingsite compositions (Deer et al, 1967).

1.8.2 Riebeckite

Riebeckite is part of the alkali amphibole group and the glaucophane-riebeckite amphibole group with a general chemical formula of $Na_2(Mg_3Al_2)Si_8O_{22}(OH)_2$ for glaucophane and $Na_2(Fe^{2+}{}_3Fe^{3+}{}_2)Si_8O_{22}(OH)_2$ for riebeckite. Glaucophane usually forms in metamorphic rocks under P-T conditions of the glaucophane facies in glaucophane schists. While riebeckite can be found in metamorphic rocks, it is the only member of this alkali amphibole subgroup that has a igneous paragenesis. It is typically found in granites, quartz syenites, syenites, and nepheline syenites. Riebeckite is more common in quartz bearing igneous rocks. The presence of a large concentration of Al leads to crystallization of hastingsite and/or arfvedsonite rather than riebeckite (Deer et al, 1967).

1.8.3 Riebeckite and hastingsite in microperthite granites

Serious studies of the genesis of riebeckite and hastingsite in granites can be traced back to Murgoci (1905). Murgoci states that riebeckite is much more common in silica oversaturated rocks than previous literature concluded. He proposes that the most important factors that contribute to the formation of riebeckite are pressure, evolution of Si and alkali concentrations, and original composition of the magma. Fluctuations towards a higher partial pressure of oxygen allow riebeckite to crystallize. Also, riebeckite generally forms in silica rich magma. The silica rich magma is also rich in aluminum, sodium and potassium with large quantities of sodium and iron (Murgoci, 1905). Billings (1928) provides one of the earliest papers describing the formation of the hastingsite group minerals and riebeckite in granitic rocks. One of the most important conclusions of his paper is a definite evolution of the amphiboles in alkaline rocks based on decreasing temperature. He provides petrological significance and relationship between the members of the hastingsite groups (Figure 1.14). Ferrohastingsite crystallizes in granite at a relatively low temperature. Riebeckite forms in granites at an even lower temperature than ferrohastingsite. This final stage of differentiation of amphibole crystallization is due to the high silica and soda concentrations (Billings, 1928).

Lyons (1972) provides a more local study on the relationship and petrogenesis of spatially close riebeckite and hastingsite granites of eastern Massachusetts. Both hastingsite and riebeckite occur in perthite granites of Nigeria, New Hampshire, and eastern Massachusetts. Although they typically occur in separate plutons, some riebeckite granite and hastingsite granite is found in the same pluton. Mineralogical, chemical, and equilibria data are useful in understanding the amphiboles spatial relationship and petrogenesis and crystallization conditions. Lyons finds that the both the Quincy and Peabody granites in eastern Massachusetts

are microperthite granites that contain these amphiboles. The Quincy granite contains riebeckite and the Peabody granite contains the iron-rich endmember of hastingsite, ferrohastingsite.

Whole-rock geochemistry of the granites suggests the oxidation state of iron is key in the formation of either riebeckite or ferrohastingsite. Iron content is the same but the Quincy granite is rich in ferric iron and the Peabody granite is rich in ferrous iron. The alkali feldspar chemistry and amphibole phase equilibria data show that the Quincy and Peabody magmas crystallized at around 650-750°C. The composition of the amphiboles in each granite sample was controlled by the parent magma and oxygen fugacity. Higher oxygen fugacity in the Quincy granite favored ferric-rich riebeckite and lower oxygen fugacity favored ferrohastingsite amphibole in Peabody. Although the factors that led to the higher oxidation conditions are speculative, an external factor or mechanism, such as ones elaborated in Eugster and Wones (1962) could be telling.

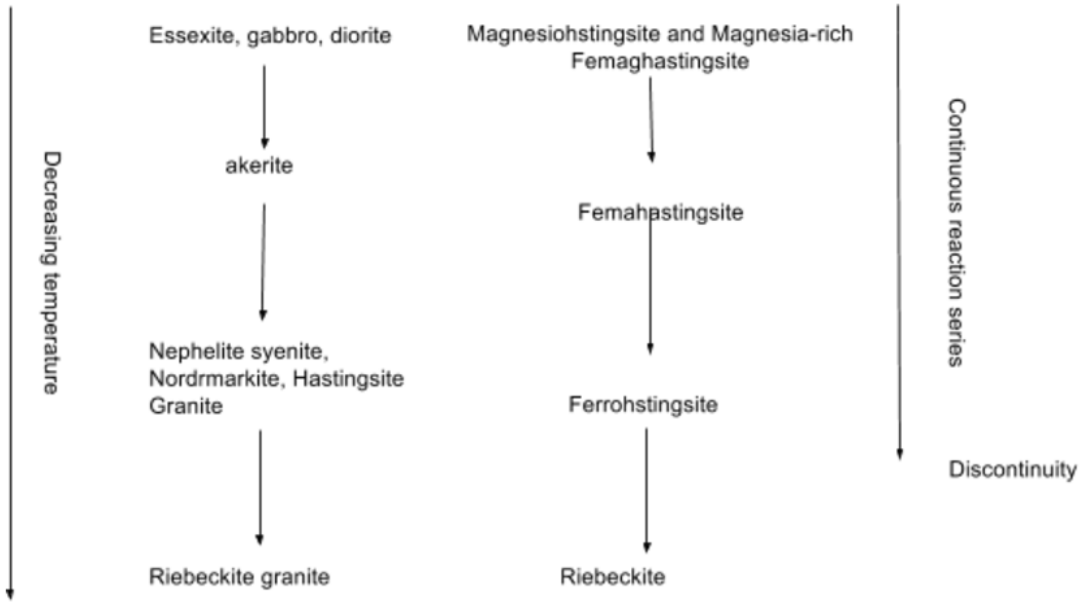

Figure 1.14: Genesis of the Hastingsite group and riebeckite amhpbioles with decreasing temperature. Adapted from Billings (1928).

1.9 Purpose

The ultimate goal of this study is to understand the textures, mineral chemical composition, and geochemistry of the Mount Cabot hastingsite-riebeckite granite located in the northern part of the northern half of the 7.5' Jefferson quadrangle shown in Figure 1.1. The study intends to produce a detailed mineralogical and petrological analysis of the granite through the analysis of thin section, geochemical data, and textural mapping of the granite with the production of a map using GIS. The hastingsite-riebeckite relationship was studied and analyzed in the context of the evolution of parental magma melt and plotted in zones based on mineralogy. Whole-rock and trace element geochemistry will provide adequate data to compare this pluton to the A-type magmatic plutons in New England and around the world and understand its parental magma. In-depth textural data of the hastingsite-riebeckite will be used to understand the petrogenesis and mode of emplacement of the magma. This study will build upon previous studies of the Mount Cabot granite from Chapman (1938 and 1942) and intends to complement Lyons (1972) analysis of similar hastingsite and riebeckite granites of New England. It will aim to answer the following questions: What is do the amphiboles hastingsite and riebeckite tell us about the parental composition of the magma? What conditions control the albitization? Why are there distinct zones of mineralogy? Is this pluton chemically similar to other New Hampshire intrusives? What are the general crystallization conditions from emplacement to final stage crystallization? Is the crystallization conditions possibly controlled by the structural elements of the nearby ring dike complexes? All these questions deal with the petrogenesis and crystallization of the hastingsite-riebeckite granite of Mt. Cabot, New Hampshire.

Methods

2.1 Field Methods

2.1.1 Traverse Planning

Fieldwork was completed over the course of 4 weeks in July of 2016 with Professor Eusden and Ian Hillenbrand. Traverses were planned out to make the best usage of our time and to cover as much ground as possible in the 7.5' Northern Jefferson Quadrangle. The Mt. Cabot area focused on traverses where LiDAR and the topographic map showed the largest change of elevation. Consultation with private landowners helped in finding obscure bedrock locations and with traverse planning. Most of the bedrock was located on stream traverses and on the steep slopes of mountains. Outcrop was particularly abundant on the peaks of the highest slopes and in the southeastern portion of the Pliny range. Generally, there was more bedrock on the peaks of mountains rather than the stream traverses. We collected data from 60 locations in the Mt. Cabot region and 173 overall in the Northern Jefferson 7.5' quadrangle.

2.1.2 Data Collection

We recorded strike, dip, rock type, and sketches at each outcrop. Mineralogical and textural observations and structural data were recorded in the field notebook and Juno Trimble GPS. A standard Brunton Compass was used for all strike and dip measurements. The two Juno Trimble GPS systems were used for GPS locations, preloaded topographic map, preloaded LiDAR map, and preloaded topographic maps. Google Maps was also used for data collection and mapping.

2.1.3 Sample Collection

Rock samples were collected with a standard rock hammer. They were collected to help in identification, record textural differences within the pluton, and to provide material for petrographic and geochemical analysis. Rocks were collected from the western topographical low, central and eastern topographical high, and eastern topographical low of Mt. Cabot (Figure 1.1). Freshness, texture, and location were the factors in deciding where to take samples. Rocks were collected if they were part of an outcrop, not float rock. Xenoliths of metamorphic rocks within the pluton were also measured for strike and dip of the veins and foliations.

2.2 Laboratory Methods

2.2.1 Thin Section Preperation

Four rock samples of the hastingsite-riebeckite granite were chosen for thin sectioning. These samples were chosen based on freshness, texture variety, and ease of preparation. A Diamond Pacific TR-18 slab saw was used to prepare rock sections for trimming. A Lortone, Inc. Lapidary Trim Saw FS8 was then used to trim and cut down the sample down to an appropriate size to send them out to Spectrum Petrographics Inc. in Vancouver, WA. All of the samples were ordered to be 30μm thickness and 27x46mm with a microprobe polished surface. Two samples were K-feldspar stained on 75% of the surface of the slide.

2.2.2 Hastingsite-riebeckite Textural Maps

Using a modified version of Hillenbrand (2016) Northern Jefferson 7.5” quadrangle GIS map a textural mapping of the hastingsite-riebeckite granite in the Mt. Cabot region was created.

GIS and a digital elevation models were used to create a 2D and 3D version of the map. Textures were described from hand sample analysis and petrographic microscope analysis. Colors and map markings were used to differentiate between the different textural types. Boundaries in areas with little coverage by hand sample or thin section analysis were placed based on elevation changes, location near lenses of other bedrock, and relation to other bedrock units.

2.3 Analytical Methods

2.3.1 Hand Sample Analysis

Hand sample analysis was performed on rocks of the three distinct textures and samples that provided areal extent of the Mt. Cabot pluton. Mineral identification and modal analyses were performed. Grain sizes for each sample were measured with a ruler. Basic mineral identification was done first without a microscope and with a simple light microscope. Preliminary descriptions of textures were also performed.

2.3.2 Thin Section Analysis

Four thin sections were analyzed using an Olympus BH-2 model BHSP polarizing microscope at Bates College. An in-depth petrographical analysis was performed on each thin section. Both qualitative and quantitative petrographical analyses were performed. A plane polarized and cross polarized image was collected for each point at 2X magnification. Modal analysis was performed by scanning and collecting the number of each mineral in each thin section.

2.3.3 X-ray Fluorescence Analysis

The X-ray fluorescence spectrometer (XRF) is a destructive technique used to measure the chemical composition of rock samples. The XRF, similar to the non-destructive techniques such as the EDS, detects X-rays emitted from a solid sample (Nesse et al, 2012). The characteristic X-rays measured by the detector are produced by bombarding the sample with a continuous spectrum of X-rays produced by an X-ray tube instead of an electron beam. The continuous X-rays produced by the machine dislodge inner K shell electrons. Outer shell electrons then take the vacant inner electron space and produce characteristic X-rays based on the type of element (Nesse et al, 2012). These characteristic X-rays hit a diffracting crystal and eventually hit the X-ray detector (Figure 2.1). The continuous X-rays produced by the X-ray tube cannot be guided like the electron beam for EDS techniques. Finely grinding the sample into powder allows the XRF have a larger, more uniform, surface area to hit. Unlike the EDS, spot chemical analyses are not possible with an XRF and they instead yield a bulk average analysis of the sample with a minimized background noise and accuracy up to 1 ppm (0.0001 wt %) (Nesse et al, 2012). Generally, the XRF can only analyze elements that are the atomic weight of sodium or higher (Nesse et al, 2012).

X-ray fluorescence (XRF) analysis was performed at Dave Gibson's XRF laboratory at the University of Maine at Farmington. Sample preparation and analysis are based on Takahashi (2015). The pressed powder method was used for sample preparation on Jhrg-52. The sample was first crushed up into fine powder to a grain size of about 300-400 mesh using the Spex ShatterBox at Bates College. The powder was then pressed using a 300-500kN maximum load press machine. Due to changes in X-ray intensity with differing pelletization pressure, it was important to select the right pressure and to release pressure several times before target pressure

was reached to avoid sample breakage. The sample was then placed into the machine and an analyzed for major, trace element and rare earth element geochemistry.

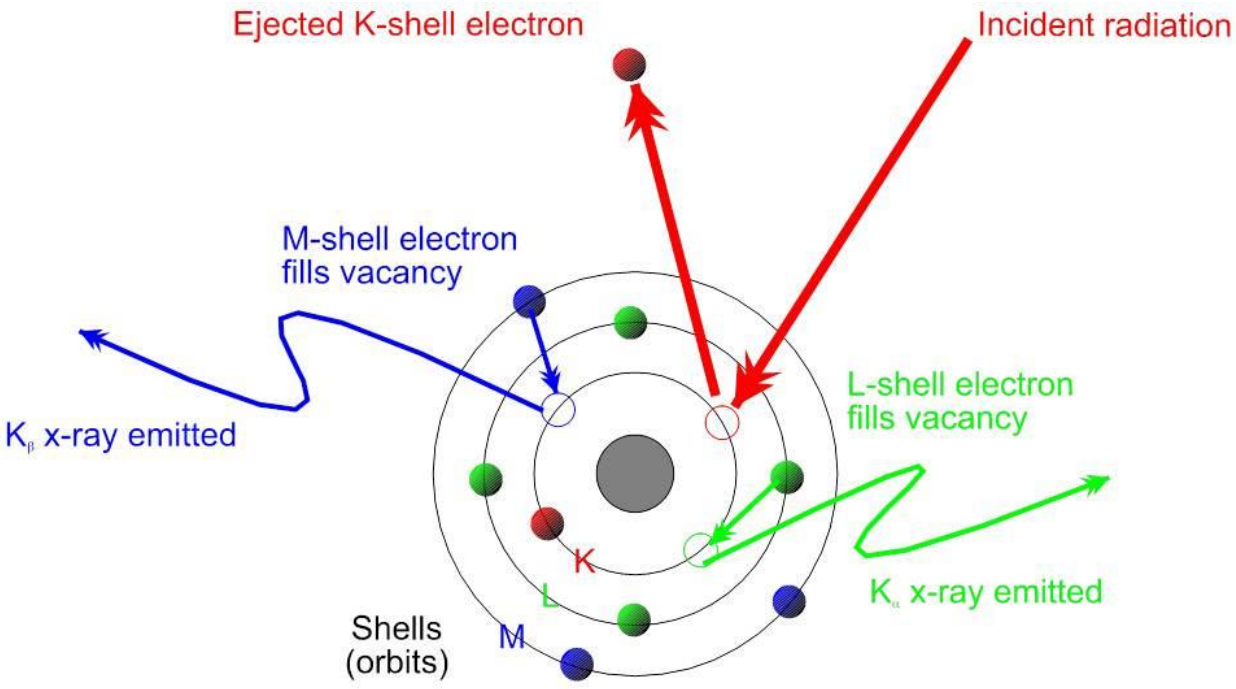

Figure 2.1: XRF process of creating X-ray fluorescence (Bruker, 2016).

Results

3.1 Mt. Cabot Granite Lithology Descriptions

3.1.1 Riebeckite Syenogranite Sample 52

The riebeckite syenogranite sample is medium grained (1-5mm), cream white rock with the largest phenocrysts of creamy white alkali feldpsar and dark black amphibole. The salt and pepper texture consists of bluish to black riebeckite, smoky gray quartz and off-white mineral grains (Figure 3.1). The smallest grains (1-3 mm) in the rock are dark blue to black riebeckite crystals that have a vitreous luster. The grains of riebeckite clump up around creamy white feldspars and smoky quartz grains and rarely appear as a lone grain. These riebeckite grains make up roughly 15% of the rock. The colorless to smoky gray quartz grains (1-4 mm) make up around 20% of the rock and are vitreous in luster. The quartz grains are located both inside clumps of dark black riebeckite and as lone grains dispersed in the rock sample. The off cream feldspar grains (1-5mm) make up most of the rock, around 65%. A very small amount of plagioclase rimming the alkali feldspar makes up around 10% of the rock. Classification and percentages of minerals can be seen in Figure 3.2 and Table 3.1.

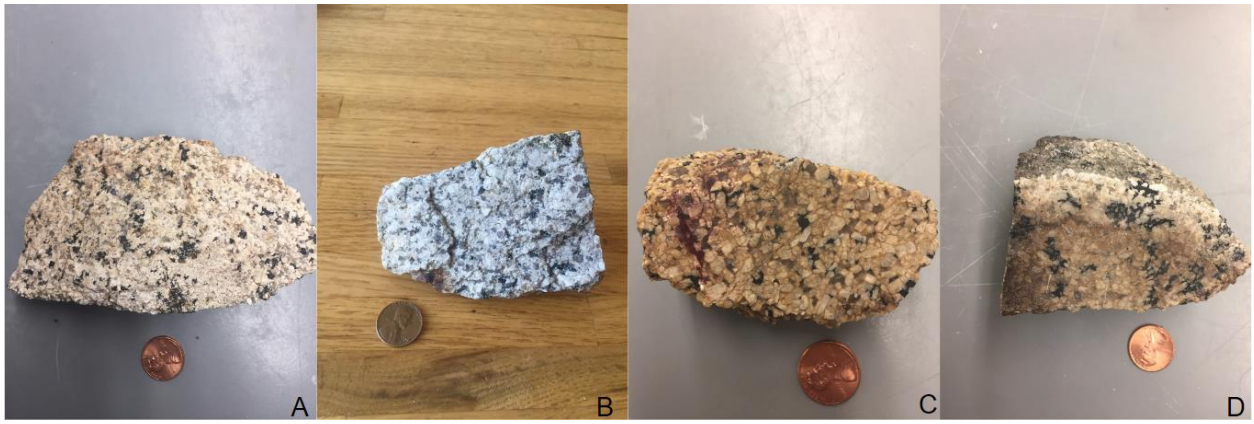

Figure 3.1: (A) riebeckite syenogranite sample 52 (B) hastingsite syenogranite sample 61 (b) riebeckite quartz syenite sample 104 (c) riebeckite quartz syenite sample 165.

Sample	Amphibole	Quartz	Alkali Feldspar	Plagioclase
52	15%	25%	65%	10%
61	10%	30%	60%	10%
104	15%	15%	70%	15%
165	15%	18%	70%	12%

Table 3.1: The APQ and amphibole percentages of each sample shown. The amphibole percentage represents the amount of amphibole in the sample. Alkali feldspar, quartz, and plagioclase percentages were normalized to 100% without taking into consideration the percentage of amphibole in each slide.

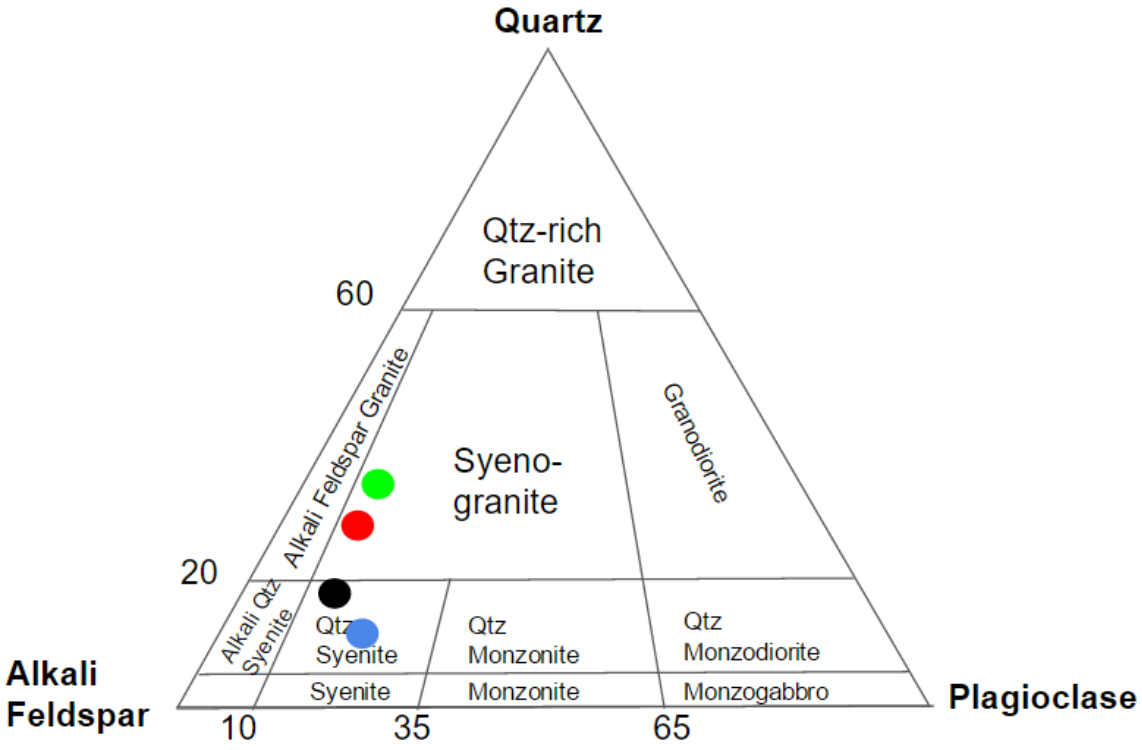

Figure 3.2: APQ classification of thin sections plotted. Red is sample 52, green is sample 61, black is sample 165, and blue is sample 104.

The sample is made up of three primary minerals: perthitic feldspar, quartz, and riebeckite. The perthitic feldspar makes up around 65% of the thin section (Figure 3.3). The perthite grains are subhedral, 1-3 mm in size and often contain small quartz grain intrusions and are rimmed by plagioclase. The ratio of the K-rich endmember to the sodium rich endmember in each individual crystal is about 60/40. In plane polarized light the K-rich endmember of the pertthite has a medium a cloudy and turbid appearance (Figure 3.3). Staining causes the color to change from cloudy grey to gold/brown. The K-rich endmember of perthite usually occurs as an irregular tabular crystal that exhibits carlsbad twinning. The sodium rich endmember makes up around 40% of each perthite crystal and occurs as lamellae and irregular blobs within the perthite. The staining does not affect the transparent colorless nature of the sodium rich endmember in either plane or cross polarized light. In plane polarized light the endmember shows very low relief. The second most abundant mineral, quartz, makes up around 35% of the sample with irregular shaped crystals grains ranging from <1 mm to 3 mm (Figure 3.3). Riebeckite makes up around 15% of the sample. It occurs as <1 mm to 3 mm anhedral amorphous grains interstitially forming near perthite and quartz grains (Figure 3.3). Another major mineral in this sample is plagioclase. The plagioclase occur as anhedral and irregular strands of multiple small <1 mm thick rims that form around perthite crystals (Figure 3.4). They primarily rim or penetrate perthite grains (Figure 3.5). Limonite, a secondary mineral in thin section, occurs as a replacement and alteration of about 10% of the riebeckite grains (Figure 3.5). It occurs as very small <1 mm to 1 mm alteration grains. It appears ass orange to dark orange as anhedral irregular alterations within or around the riebeckite grains. In some cases the limonite chemical alteration has completely replaced a riebeckite grain (Figure 3.6).

This sample is holocrystalline and phaneritic hypidiomorphic rock. Individual quartz grain inclusions and plagioclase rim grains are fine-grained (<1 mm). The majority of the quartz, perthite, and riebeckite crystals are medium-grained (1-5 mm). Although some quartz grains look coarse-grained, the large crystals can be identified in cross polarized light as made up of much more smaller grains. Perthite occurs as primarily subhedral, with some euhedral, mineral grains. Quartz occurs as subhedral grains. Riebeckite occur as anhedral grains that develop interstitially between the perthite grains (Figures 3.5 and 3.7).

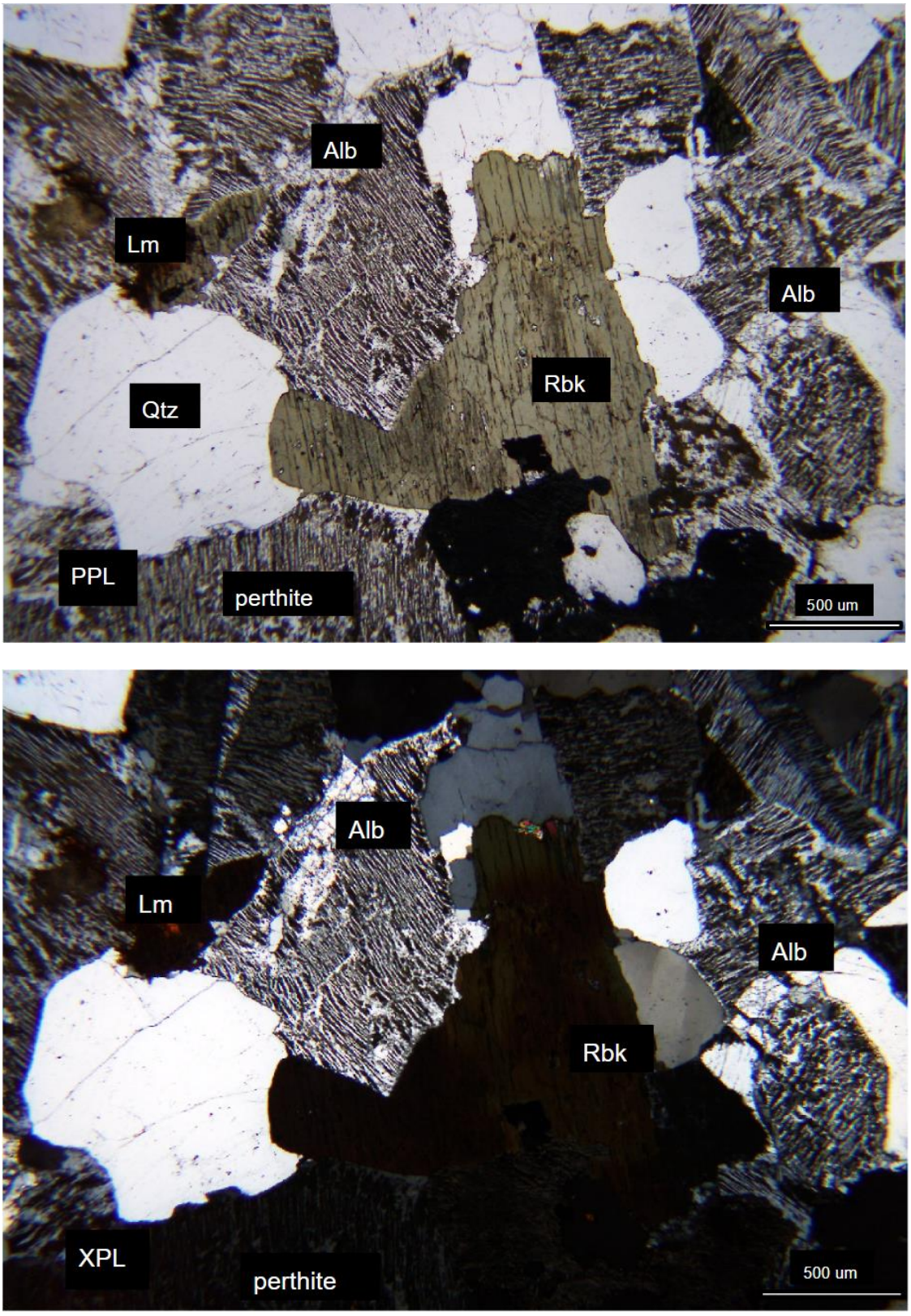

Figure 3.3: Riebeckite grains are either unaltered or chemically weathered with limonite. There is also albite replacement within and around the subhedral perthite grains.

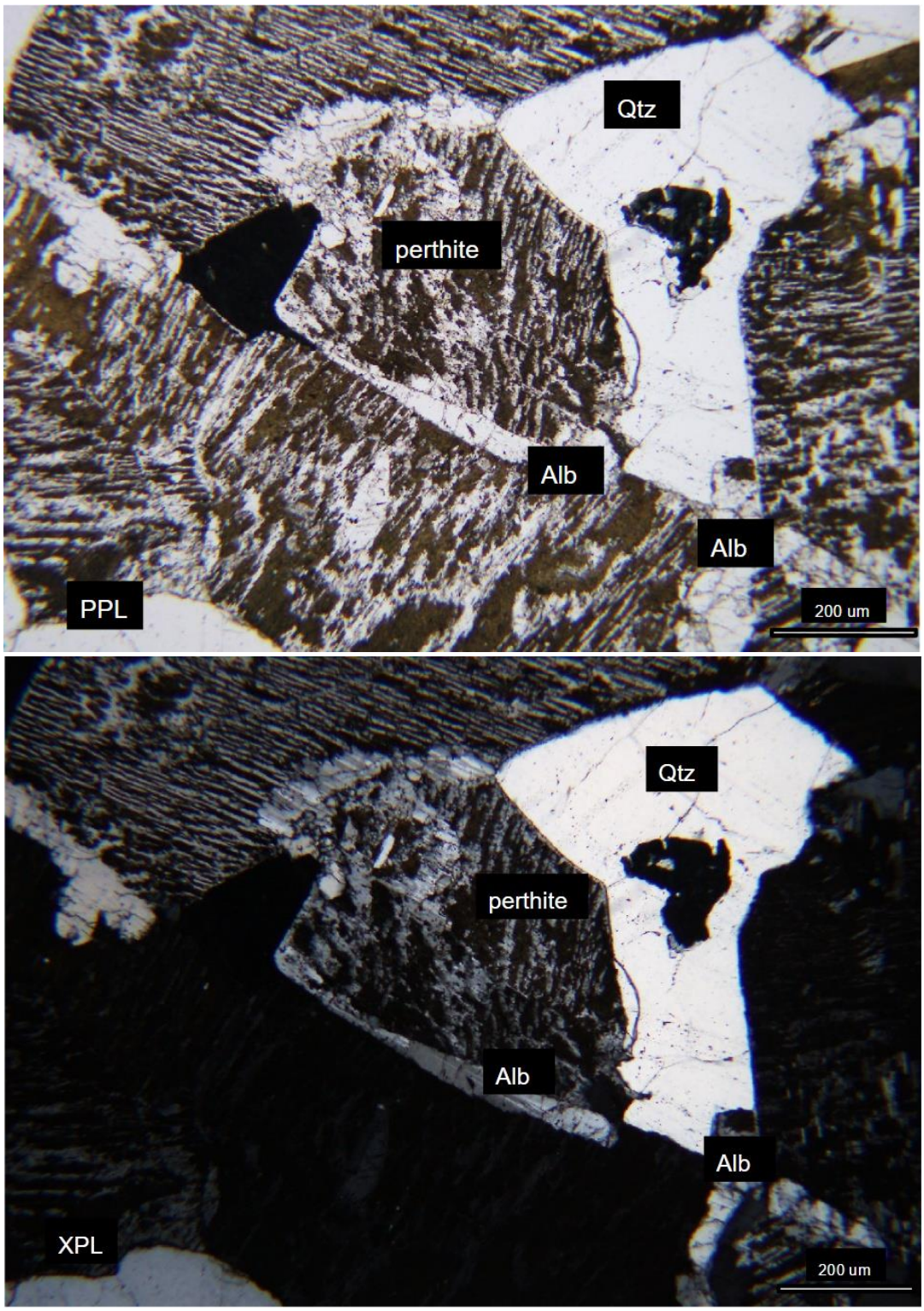

Figure 3.4: Typical albite rimming of a sample. Albite is not along the boundaries between quartz and perthite, just perthite-perthite boundaries. The opaque grain is an iron rich mineral.

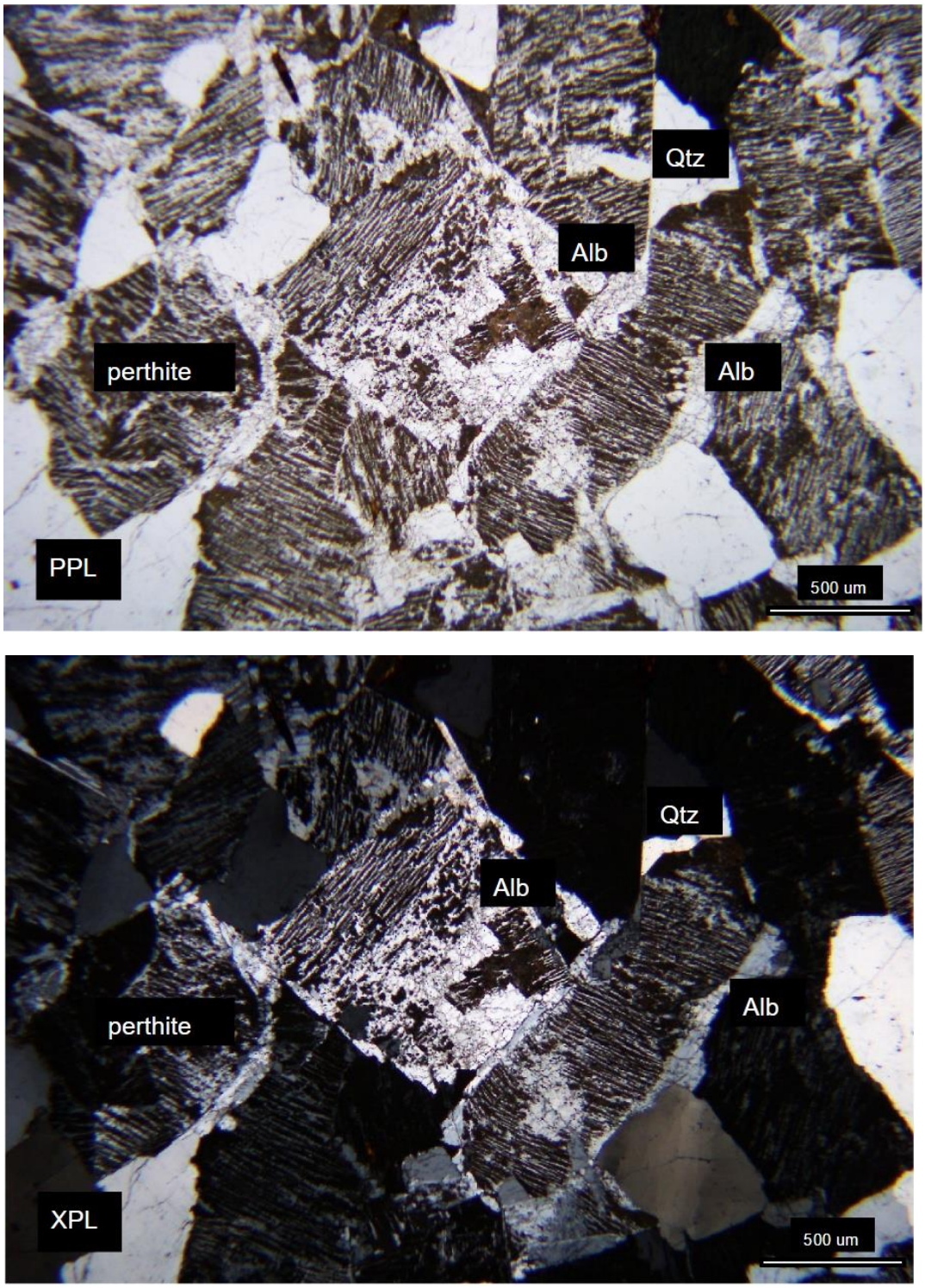

Figure 3.5: Notice the undalose extinction in quartz. There is albite rimming and penetration within the perthite grains. The penetrating albite comes in contact with perthite and quartz.

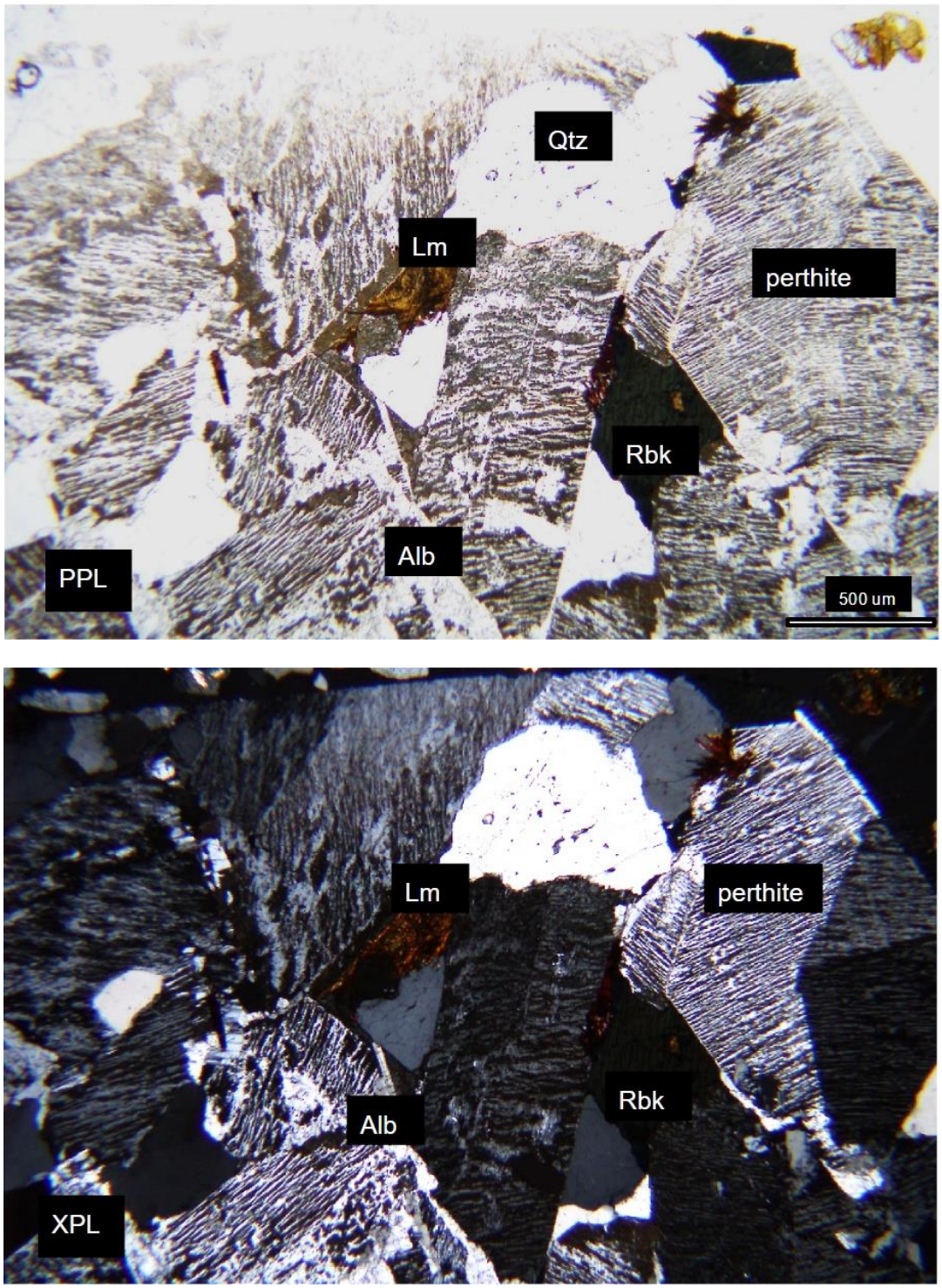

Figure 3.6: Unaltered and altered riebeckite. Riebeckite is interstitial to the perthite. Orange limonite replaces the altered riebeckite. There is prevalent intermingling of subhedral perthite and quartz grains. It shows the extent and coverage of albite penetration and replacement.

3.1.2 Hastingsite Syenogranite Sample 61

The sample is a fine-medium phaneritic rock with crystals averaging <1-5 mm in size. Some large crystals of perthite are euhedral. It is a primarily white rock from the alkali feldspar with a salt and pepper texture containing smoky quartz and dark black amphibole (Figure 3.1). The rock is holocrystalline and does not contain any glass crystals. It is made up primarily of minerals perthite, quartz, and hastingsite. The bulk of the mineral grains are fine to medium grained (<1 mm -3 mm) and are subhedral in form (Figure 3.7). Perthite makes up roughly 65% of the sample. The main phase of the perthite, around 50-60% of each grain, is a potassium rich member of alkali feldspar. The potassium member forms nice even lamellae in each mineral grain. The sodium rich end-member makes up around 40% of each perthite grain. There is no zoning within the perthites. In most of the perthite grains the sodium rich end member makes simple lamellae. Some perthite grains, however, contain a much larger percentage (70%+) of irregular blobs, lamellae, or patches of sodium rich endmember inside the perthite grain. Subhedral perthite grains are medium grained 1-2 mm grains while anhedral grains usually form <1 mm broken up grains (Figure 3.7). Quartz is the second most abundant mineral (30%) and forms fine to medium subhedral grains (<1 mm- 2 mm) (Figure 3.8). The grains are irregular, unaltered, and appear inside perthite grains or next to perthite grains. Primarily, medium-large grains of quartz form next to perthite grains with clear boundaries. Finer quartz grains (<1 mm) form as perthite grain inclusions. The main amphibole, hastingsite, is around 10% of the sample (Figure 3.8). Each grain is round <1 mm to 2mm and is typically anhedral. Grains are typically broken up and develop interstitially between quartz and perthite. Hastingsite grains also appear as separate grains near perthite and quartz grains. The next most abundant mineral at <10% is plagioclase feldspar (Figure 3.9). Classification and percentages of

minerals in the sample can be seen in Figure 3.2 and Table 3.1. The plagioclase feldspar in this sample forms thin rims on perthite grains and typically forms a reaction rim corona similar to rapakivi texture, without ovoid alkali feldspars. This reaction rim occurs around the immediate rim of perthite and often breaks up irregular perthite crystals. The rims are around 10 um in thickness and typically form around the perthite grains but can envelop small <1 mm quartz grains. The smoky grey appearance is due to the small grain size and rectangular laths (Figure 3.7). In one section, the plagioclase forms a large grain (3mm) that has partially been altered to sericite (Figure 3.10).

Unlike the riebekite syenogranite sample 52, there are several accessory minerals. The main accessory mineral is replacement anhedral shaped limonite. Limonite appears as a replacement mineral to the amphibole hastingsite (Figure 3.7). Hornblende makes up <1% of the slide and is found in one small portion of the slide (Figure 3.10). The hornblende is fine-grained (<1 mm) and the only whole cluster is surrounded and intermingled with perthite and plagioclase (Figure 3.11).

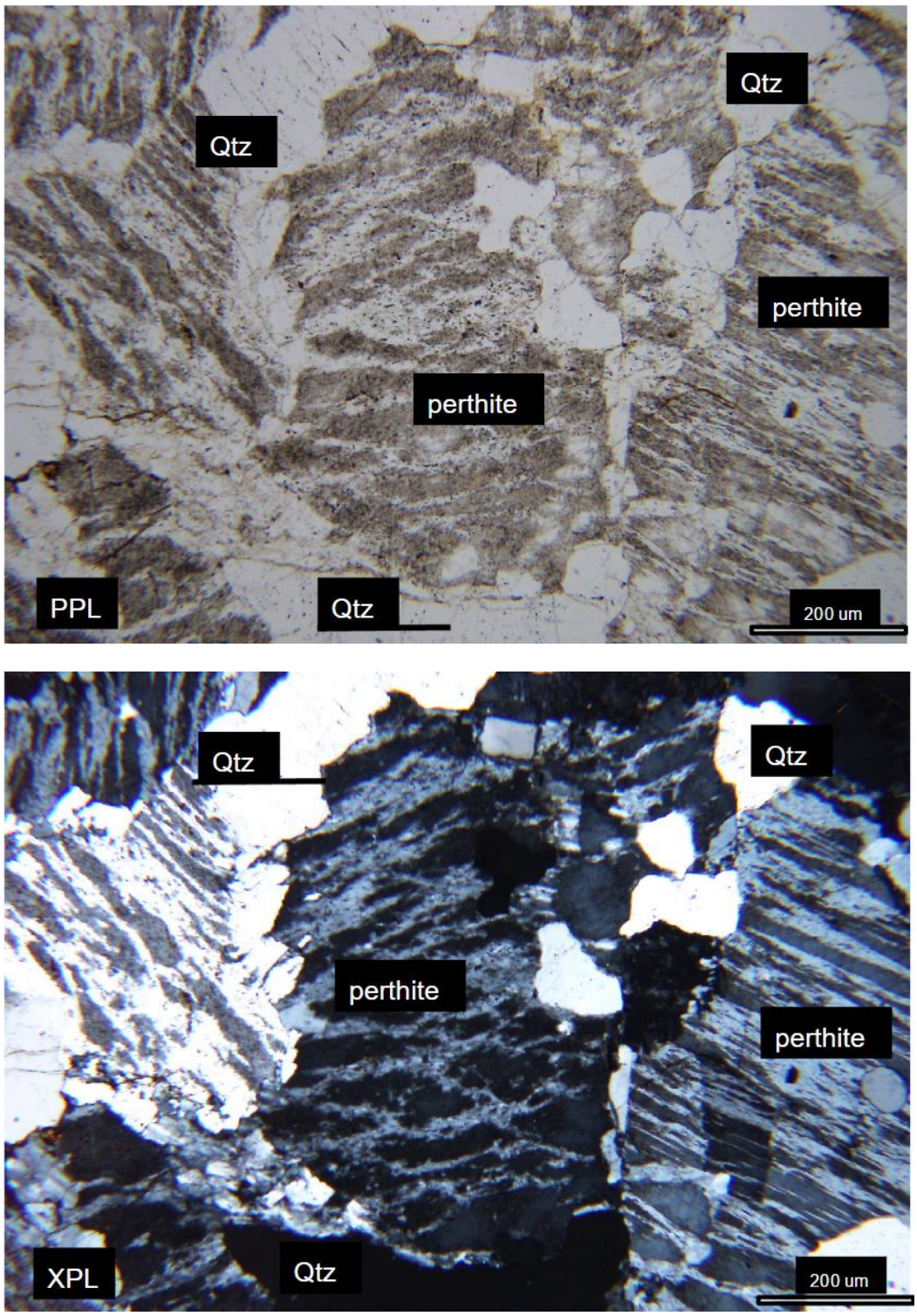

Figure 3.7: Subhedral perthite and quartz grains. Inclusions of quartz are prevalent in perthite grains.

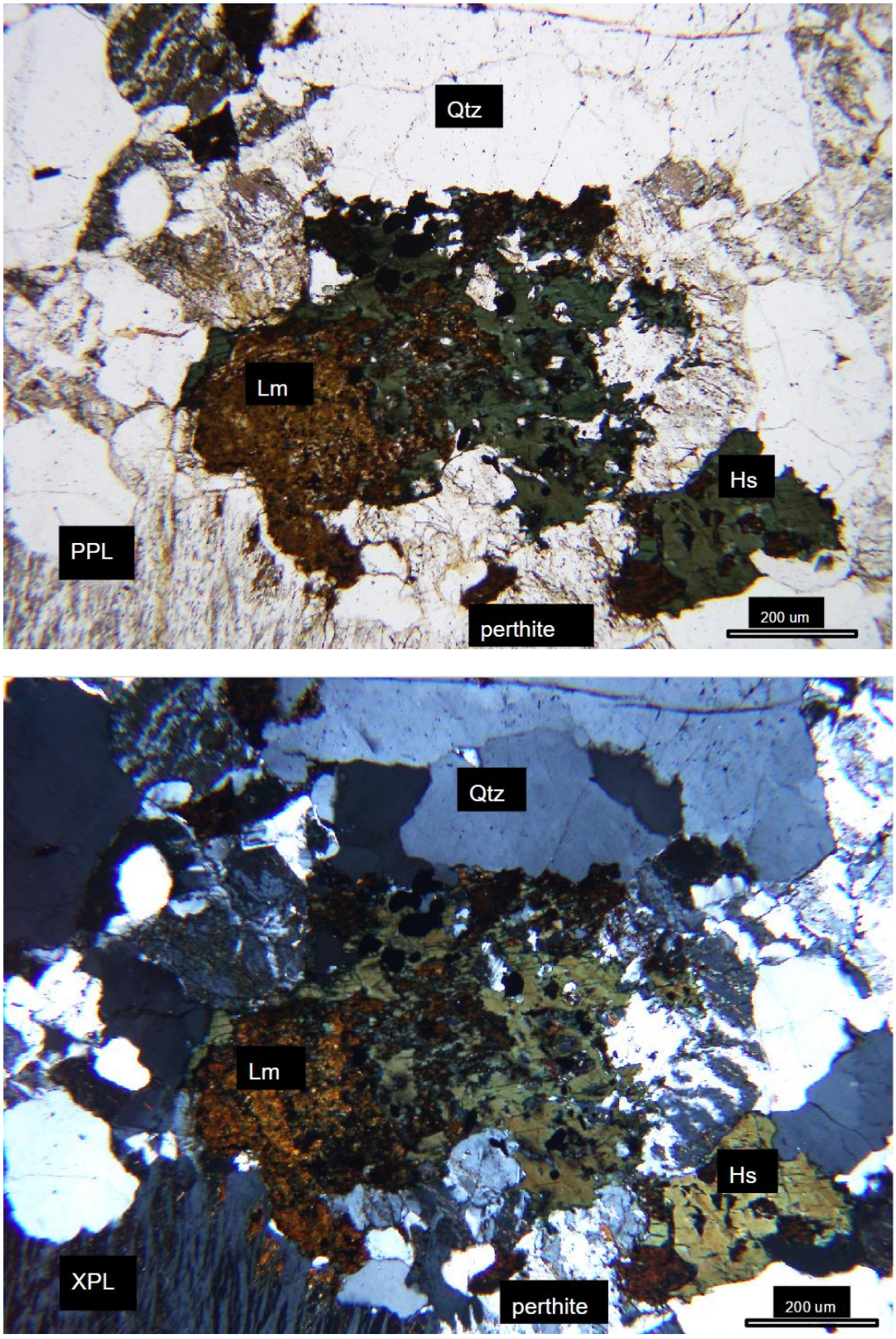

Figure 3.8: Hastingsite light green and green pleochroic nature. Limonite and opaque mineral weathering is prevalent.

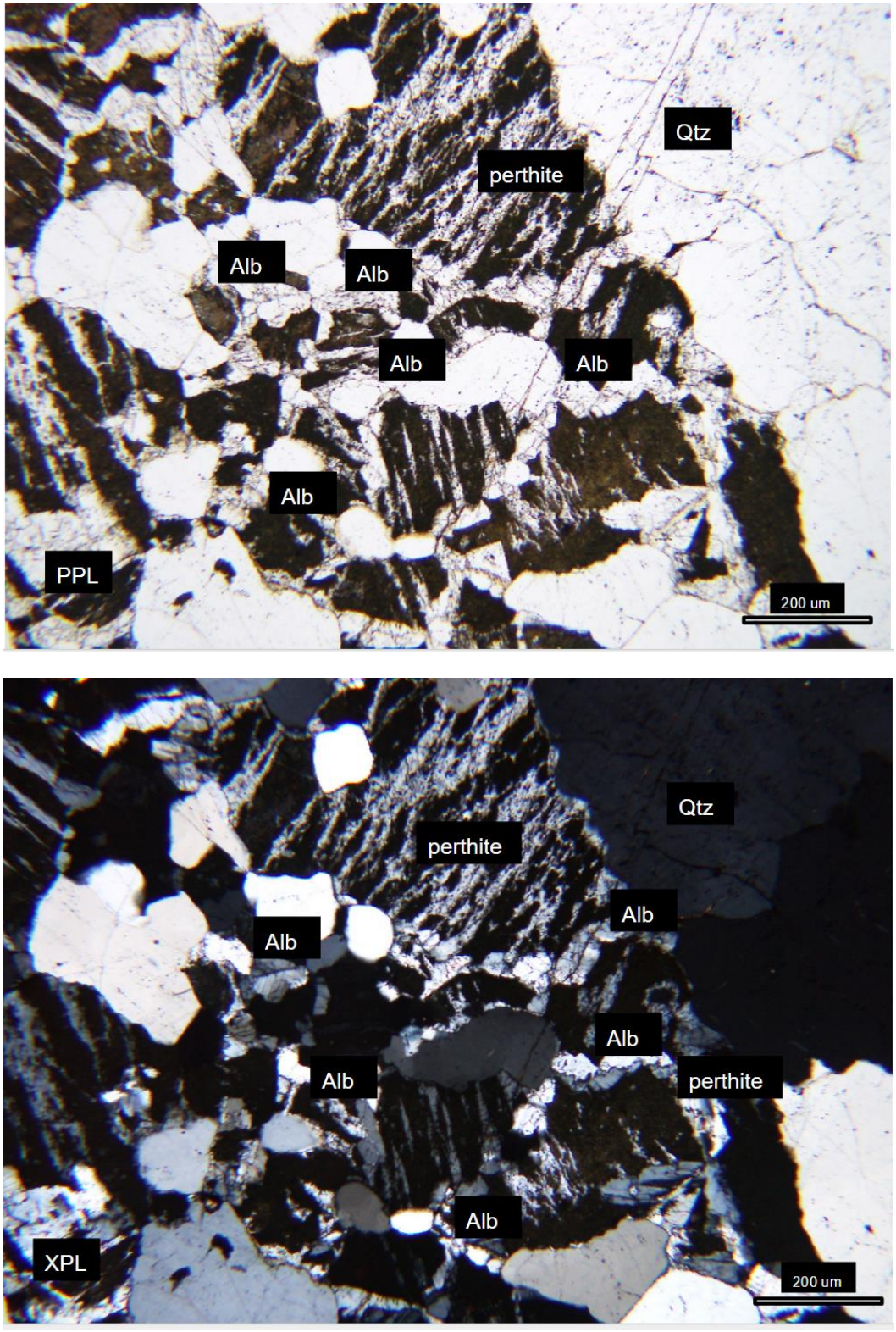

Figure 3.9: Intergranular albite penetrating the anhedral perthite grains. Albite does not penetrate quartz, nor does it share boundaries between quartz and perthite.

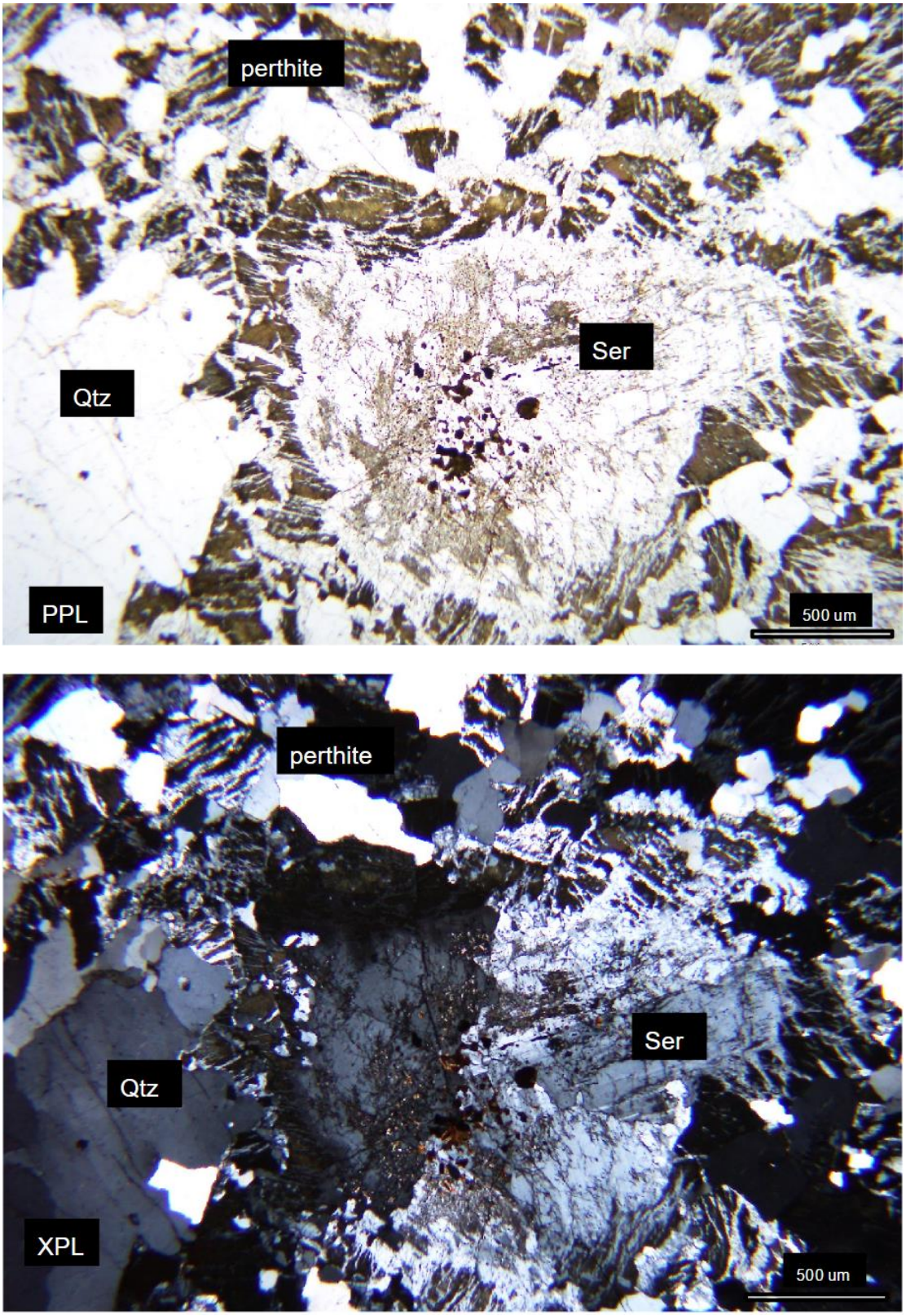

Figure 3.10: Sericitization of the plagioclase feldspars with larger quartz crystals and broken up anhedral perthite grains.

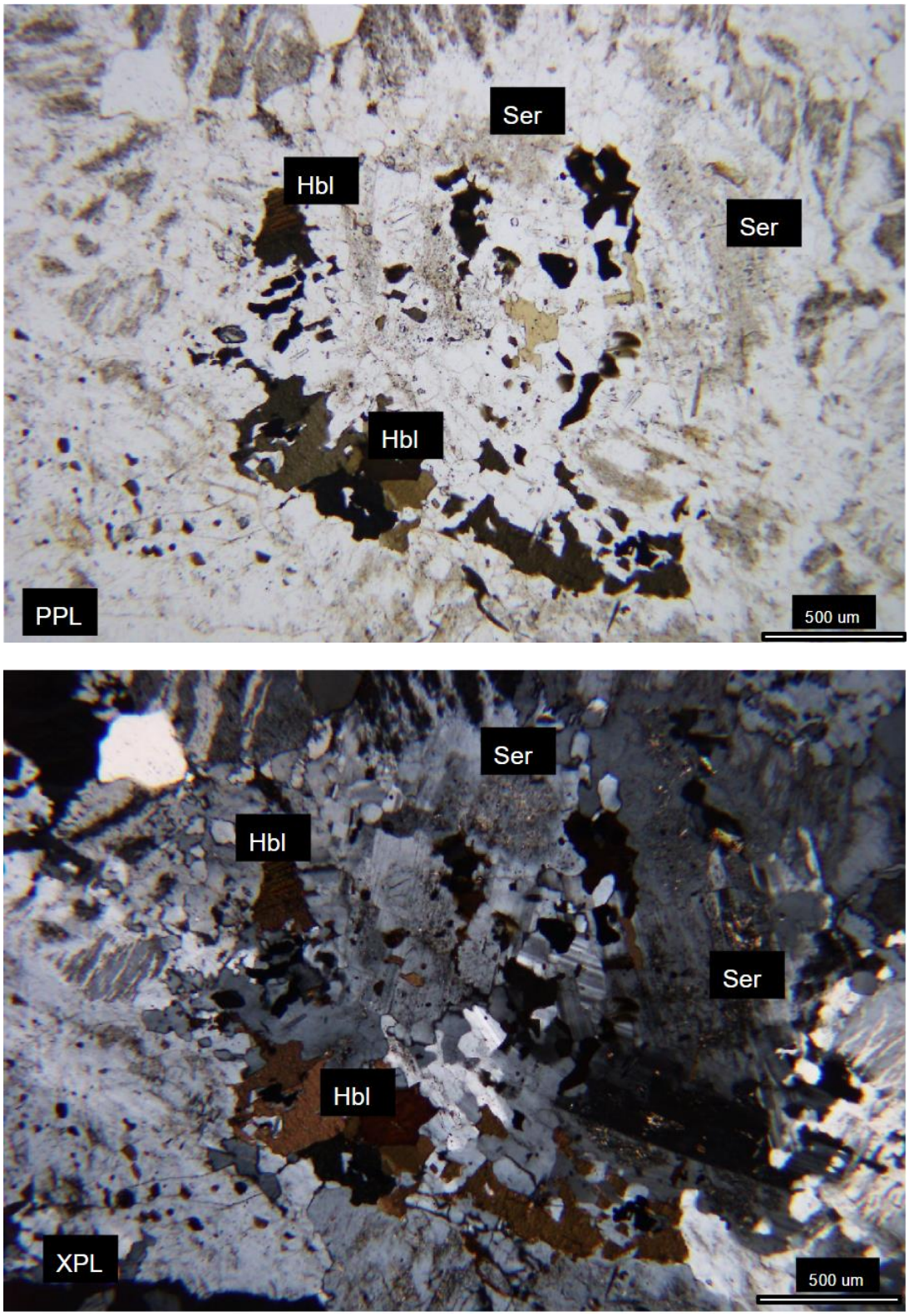

Figure 3.11: Only instance of hornblende in all the samples. Sericitization of the plagioclase feldspar is prevalent.

3.1.3 Riebeckite Quartz Syenite Sample 104

This sample is a medium to coarse grained with large creamy white feldspar grains and a smattering of black amphibole (Figure 3.1). The largest phenocrysts are creamy to beige alkali-feldspars. The rock contains creamy brown to beige weathered feldspar, smoky gray quartz grains, and riebeckite clumps. The riebeckite (1-5mm) makes up roughly 15% of the rock and normally encircles quartz and feldspar grains in clumps. The smoky quartz grains (1-5mm) appear within riebeckite clumps make up around 15% of the rock. The feldspar (1-6mm) makes up around 65% or more of the rock and is the main mineral constituent. Plagioclase rims surrounding alkali feldspar grains make up around 15% of the rock. Classification and mineral percentages can be seen in Table 3.1 and Figure 3.2. The quartz and riebeckite grains seem suspended in the mass of feldspar crystals. The alkali-feldspar grains have very well developed crystal faces and seem to crowd the riebeckite and quartz grains. In some areas, lighter plagioclase feldspar acts as a matrix around alkali-feldspar crystals. Half of the alkali-feldspar grains are elongate and euhedral. The other alkali-feldspar grains are poorly developed subhedral crystals. Quartz grains are generally large and well developed while the riebeckite are irregular crystals and shows no cleavage. The sample is prone to breaking and crumbling when handling (Figure 3.1).

The sample is primarily made up of perthite, quartz, and riebeckite. The bulk of the grains are medium-grained (1-5 mm). Perthite makes up the largest portion of the sample and is primarily euhedral. Similar to the other samples, the perthite is made up of a potassium rich alkali feldspar endmember and a sodium rich endmember. The potassium rich endmember is cloudy grey and the sodium rich endmember of perthite is colorless. Unlike samples 52 and 61,

the perthite exhibits a more uniform and euhedral shape (Figure 3.12). The perthite is typically not broken up but the borders of around 50% of the perthite grains are partially surrounded by either subpoikilitic riebeckite or plagioclase rims (Figure 3.12). Quartz grains are the second most dominant mineral, but 10-15% lower than samples 52 and 61. Quartz grains are irregular and form clear boundaries next to perthite and riebeckite grains. Unlike the quartz grains in samples 52 and 61, the quartz grains are 1-3 mm and are not found as inclusions in any of the feldspar grains. Riebeckite grains occur solely as interstitial subpoikilitic grains (Figure 3.14). The subpoikilitic to poikilitic riebeckite occur in around 15% of the slide mostly in clumps around euhedral perthite grains (Figures 3.12 and 3.13).

The general rock textures in this sample are similar to samples of 52 and 61. The rock is holocrystalline, medium phaneritic, and hypidiomorphic (Figures 3.12 to 3.15). Like the perthite crystals in samples 52 and 61, there are reaction rims/coronas of plagioclase feldspar around a significant amount of the perthite grains. The reaction rims are twice as thick, in some cases 20 µm, and twice as abundant. In some cases, the perthite grains have a plagioclase outer corona and they combine for a thicker more easily defined crystal boundary. Smaller portions of perthite grains are surrounded by partial coronas that do not completely surround each crystal grain. Perthite lamellae is also more consistently with small thin lamellae of sodium rich alkali feldspar striping the perthite (Figures 3.14 and 3.15).

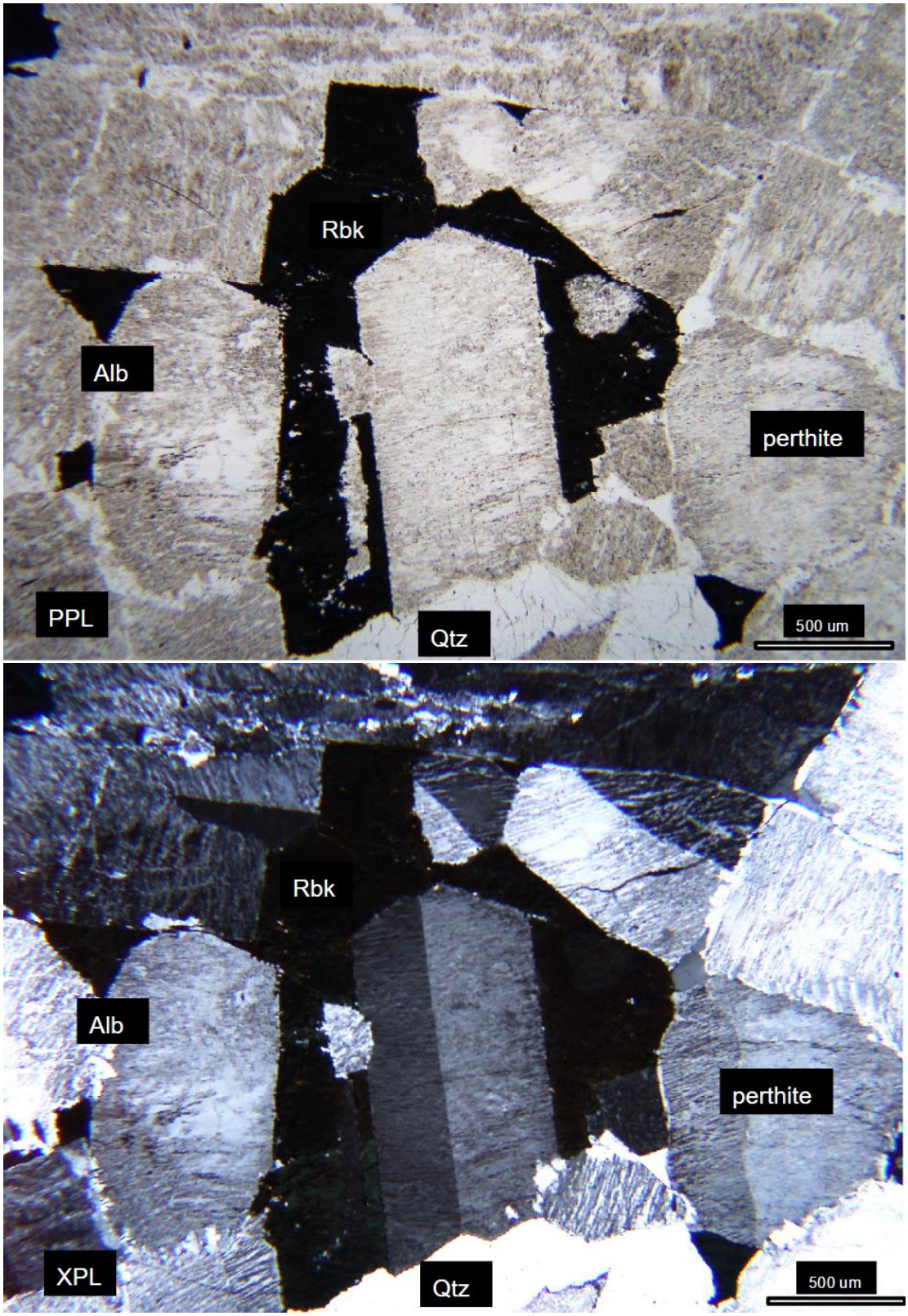

Figure 3.12: Subpoikilitic riebeckite engulfing a large euhedral perthite grain. The subhedral perthite grains have albite rims.

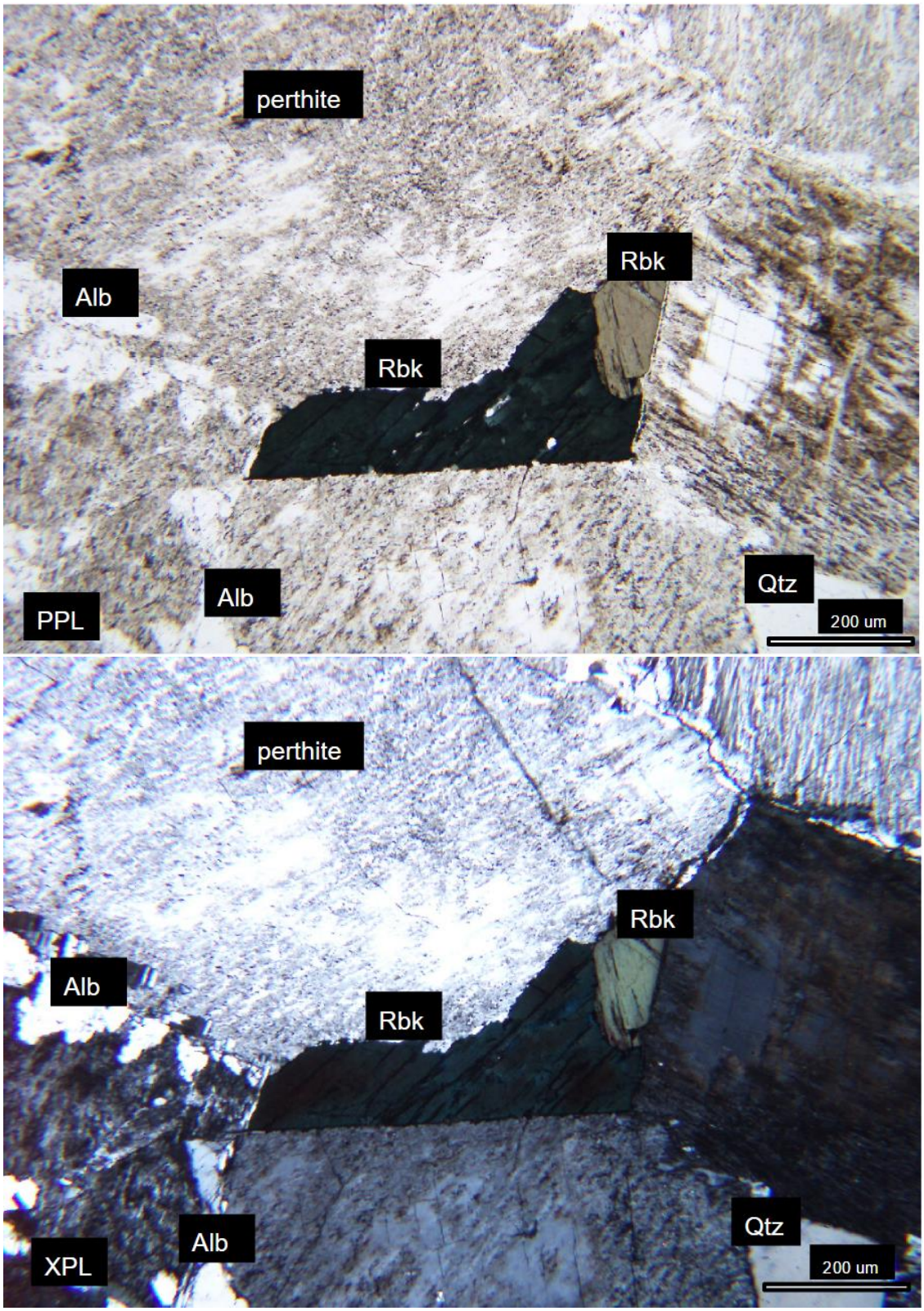

Figure 3.13: Two differently oriented riebeckite crystals with light clean to dark blue pleochroism. Riebeckite grain is anhedral, not poiklitic. Albite is rimming subhedral perthite.

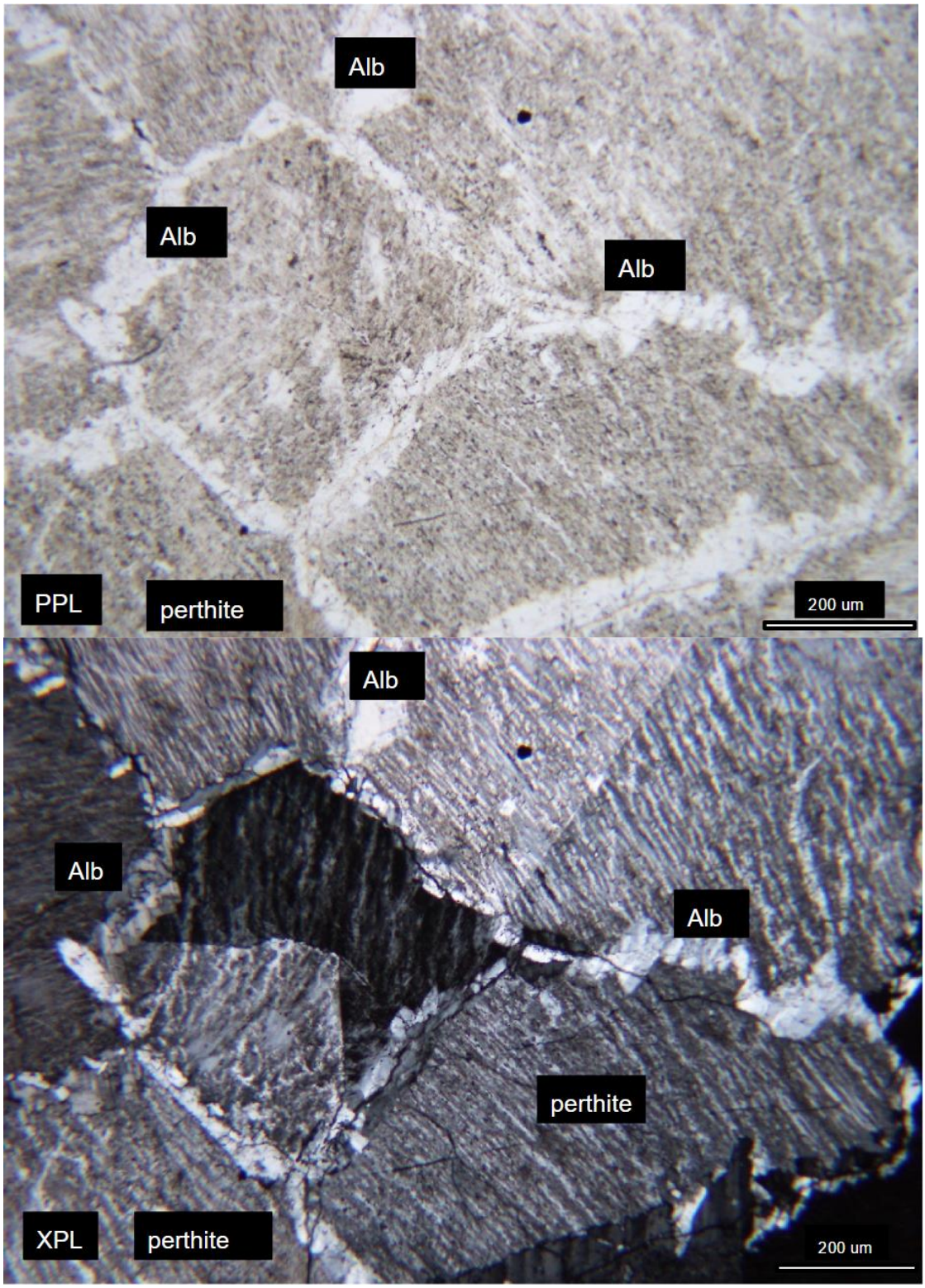

Figure 3.14: Close-up of albite rims on subhedral perthite grains. Notice they both rim and penetrate grain boundaries.

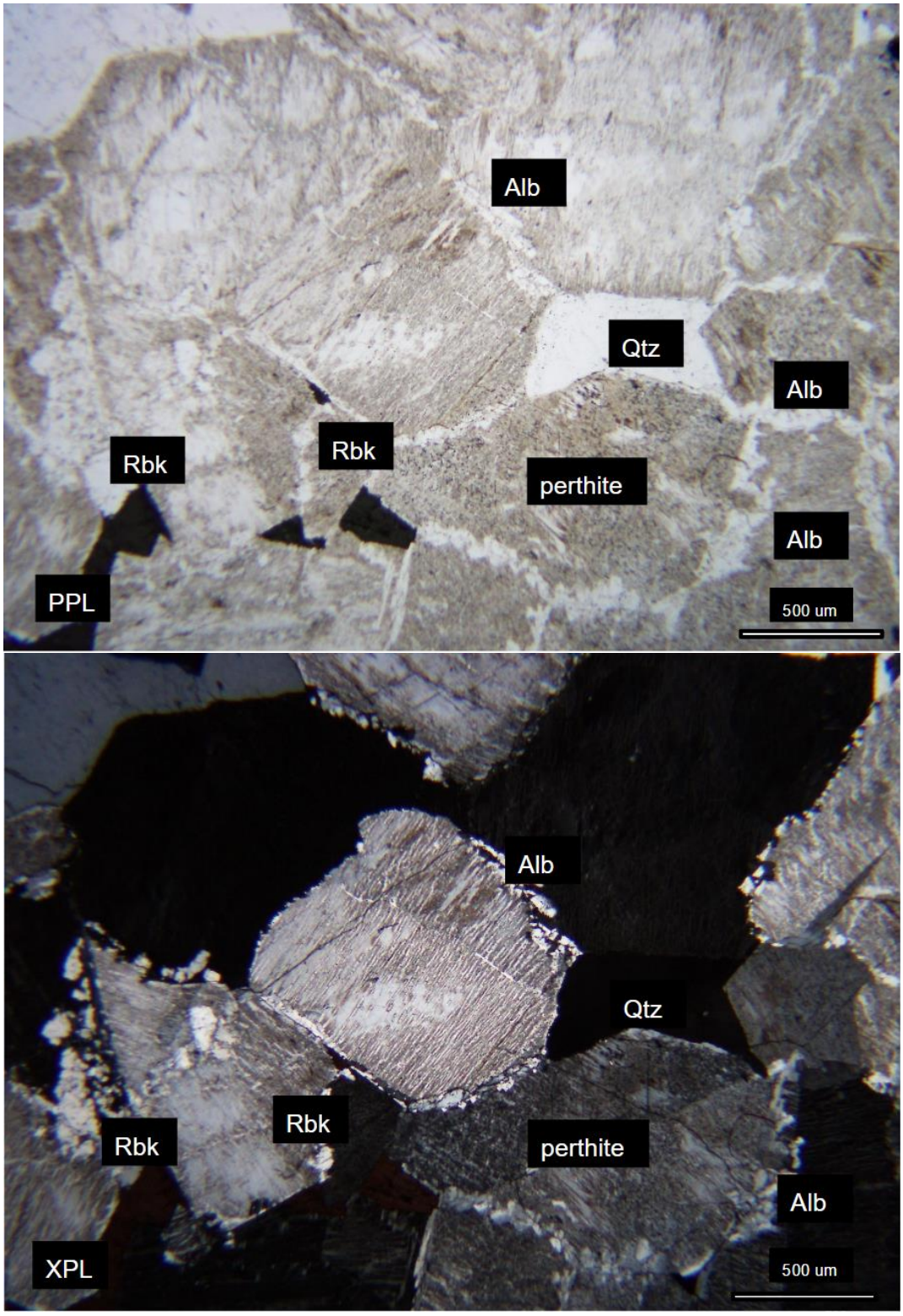

Figure 3.15: Zoomed out example of albite rims and minor albite penetration within perthite grains. Thicker albite rims are prevalent on broken boundaries.

3.2. Riebeckite Quartz Syenite Sample 165

Sample 165 is a medium grained and creamy white colored rock. The rock primarily contains off white alkali-feldspar, smoky quartz, and dark blue riebeckite amphibole (Figure 3.1). Once cut, the rock shows a plagioclase and/or quartz matrix around the feldspar, quartz, and riebeckite grains. The largest grains (>3mm) are amorphous semi-poikilitic riebeckite grains that enclose alkali feldspar grains and are around 15% of the rock. These riebeckite grains rarely form single small crystals and instead form in clumps. The medium grains (1-5mm) are alkali-feldspar and quartz grains. The alkali-feldspar, 65% of the rock form medium subhedral grains, not as well developed as the alkali-feldspar grains in sample 104. Quartz crystals are also small but mostly are located near riebeckite clumps. Quartz makes up 18% of the rock, less prevalent than hand samples 52 and 61. Although primarily seen if the rock is cut, plagioclase rims on the feldpsar make up around 12% of the rock Classification and mineral percentages can be seen in Figure 3.2 and Table 3.1.

Sample 165 is primarily made up of perthitic feldspar, quartz, and riebeckite (Figure 3.16). The most abundant mineral is alkali feldspar perthite with a potassium rich endmember and a sodium rich endmember. Perthite grains are usually 1-3 mm in size and subhedral to anhedral in grain shape. Some perthite are broken up by plagioclase intergrowth or interstitial growth (Figure 3.15) The potassium end member of the alkali feldspar is the dominate phase and makes up 50-70% of the perthite grains with a smudged to smoky appearance (Figures 3.16 and 3.17). Quartz is the next most abundant minerals and crystal sizes range from <1 - 3 mm in size. They are irregular subhedral crystals that typically form as large fractured crystals or small inclusions in perthite grains (Figure 3.16). Riebeckite grains are the next most abundant mineral

and make up around 15% of the thin section. These riebeckite grains are not altered. They commonly occur as medium to large grained subpoiklitic-poikilitic complexes that formed interstitially between quartz and perthite crystals (Figures 3.16 and 3.17). Typical inclusions in riebeckite are dark iron-rich opaque minerals and quartz and (Figure 3.17). Like samples 52, 61, and 104 the next abundant mineral is plagioclase feldspar. Primarily occurring as small <1 mm irregular crystals, plagioclase forms around perthite crystals and penetrates subhedral perthite grains, subsequently breaking them up. Rims of plagioclase are usually 10 μm laths of plagioclase are around 50 to 100 μm in width. Unlike sample 104, plagioclase appears both as small crystals with typical feldspar twinning and plagioclase rims (Figure 3.16).

This sample is holocrystalline and a medium phaneritic rock (Figures 3.16-3.18). The perthitic feldspars are subhedral to anhedral with very little plagioclase replacement affecting their general mineral grain shape. Generally the rock is hypidiomorphic. An interesting and rare texture is that on one grain of perthite there are wormy intergrowths of quartz, typically called myrmekite (Figure 3.18). This sample is very similar with sample 104 in terms of riebeckite growth, perthite crystal shape, plagioclase rims, and similar amount of perthite, quartz, and feldspar.

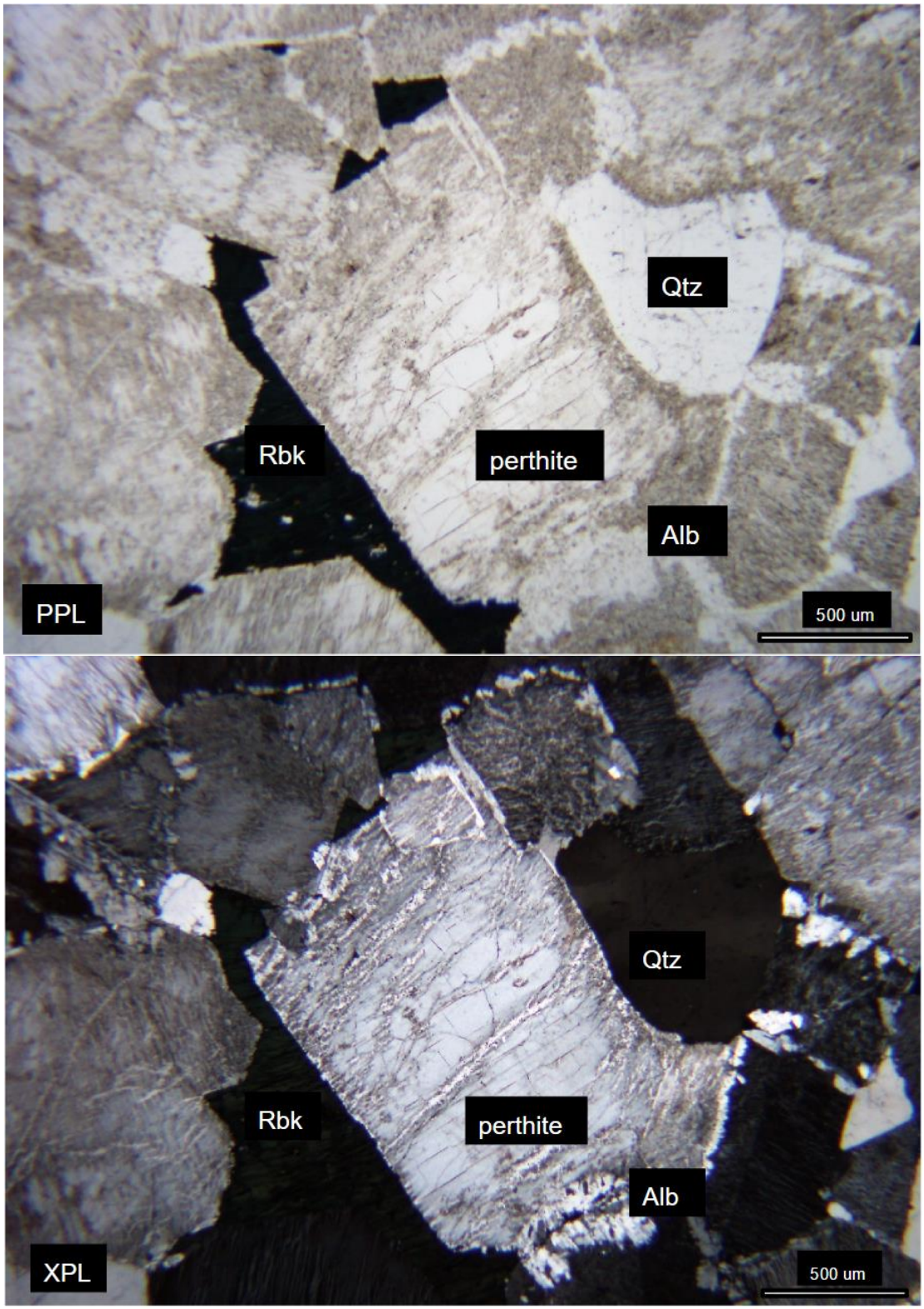

Figure 3.16: Prevalent albite riming between perthite-perthite boundaries.

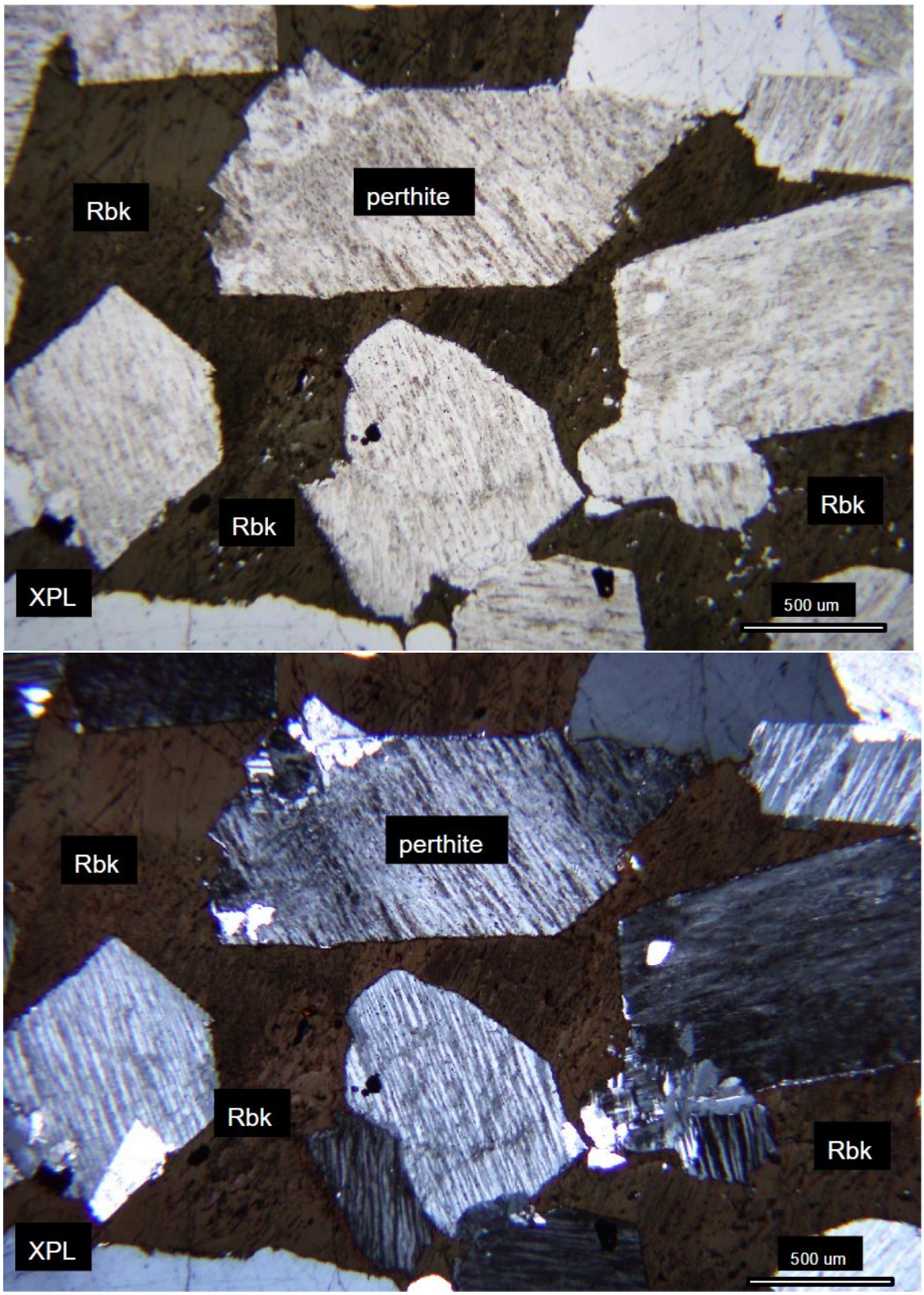

Figure 3.17: Large poikilitic grain of riebeckite. No albite rimming or penetration around perthite inclusions.

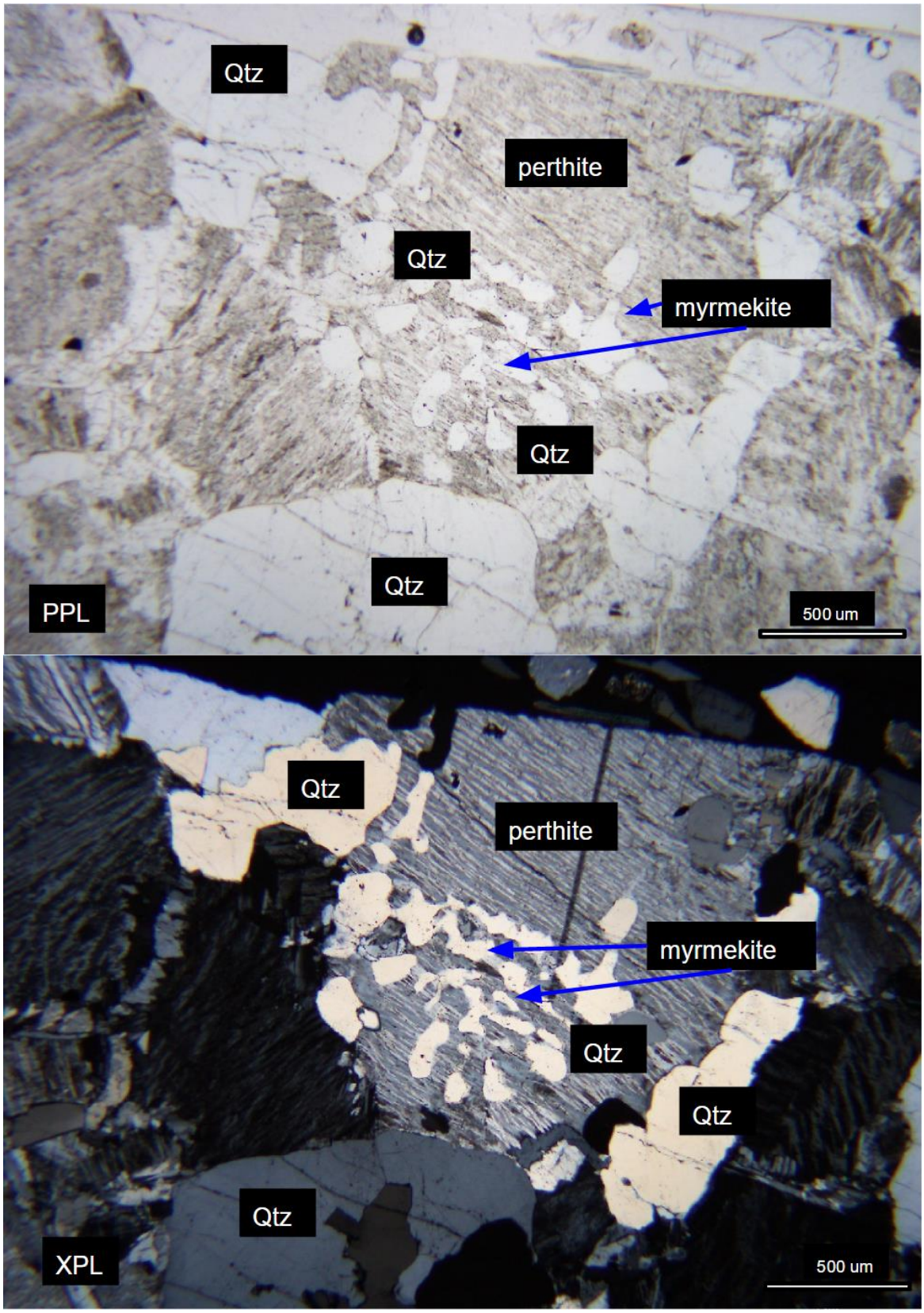

Figure 3.18: Only example of visible myrmekite texture in all of the rock samples.

3.4 Sample 52 Geochemistry

The riebeckite syenogranite sample 52 geochemical data is presented in Table 3.2. The data has bulk-rock and trace element geochemical data. Highest amount of bulk rock elements in the rock, from highest percentage to lowest according to the modal analysis, are SiO_2, Al_2O_3, Na_2O, Fe_2O3, and K_2O. Notable bulk rock elements that constitute a very small percentage of the sample are CaO, MnO, and TiO_2. The sample is relatively high in trace element concentrations (PPM) of Cr, Zn, Zr, Rb, Nb, and Ba. The sample has low concentrations (PPM) of Sr and Y (Table 3.2). The CIPW norm calculation is shown in Table 3.3. The sample is particularly high in albite, orthoclase, and quartz. Other notable minerals predicted to make up the composition include hematite, magnetite, ilmenite, and apatite (Table 3.3). The CIPW data shows a large percentage of the rock is albite, orthoclase, and quartz. Much of the percentage of albite is interpreted as being the exsolved sodium rich endmember of perthite. Geochemistry data does match up correctly with the modal analysis results for riebeckite syenogranite sample 52.

Sample		Bates-52	Bates-52	Bates-52	Bates-52	Average	Standard deviation	Weight Percent (%)
Al_2O_3 (%)		13.46	13.48	13.50	13.59	13.51	0.06	14.07
CaO (%)		0.430	0.430	0.430	0.420	0.430	0.01	0.445
Fe_2O_3 (%)		3.57	3.6	3.59	3.59	3.59	0.01	3.70
K_2O (%)		4.92	4.94	4.95	4.96	4.94	0.02	5.10
MgO (%)		0.05	0.05	0.04	0.04	0.05	0.01	0.00
MnO (%)		0.085	0.085	0.086	0.085	0.085	0.0005	0.10
Na_2O (%)		5.36	5.37	5.34	5.38	5.36	0.02	5.60
P_2O_5 (%)		0.021	0.02	0.02	0.021	0.021	0.001	0.00
SiO_2 (%)		67.6	67.8	67.9	68.0	67.8	0.16	70.6
TiO_2 (%)		0.127	0.126	0.128	0.131	0.128	0.002	0.10
Ba (PPM)		72	47	55.5	47	55.5	11.8	0.00
Cr (PPM)		88	82	98	87	88.8	6.7	0.00
Zn (PPM)		108	100	97	102	101.8	4.6	0.00
Sr (PPM)		7.0	7.0	7.0	7.0	7.0	0.0	0.00
Y (PPM)		21	23	20	21	21.3	1.3	0.00
Zr (PPM)		241	240	232	233	237	5.0	0.00
Rb (PPM)		110	112	111	110	111	1.0	0.00
Nb (PPM)		68	68	67	67	67.5	0.6	0.00
Sum (%)		95.68	95.96	96.02	96.25	95.98	0.23	100.0

Table 3.2: Geochemical data for riebeckite syenogranite sample 52. Sample 52 was analyzed four times in the XRF.

Minerals	Weight Norm %	Volume Norm %
Quartz	19.15	19.30
Zircon	0.00	0.00
K2SiO3	0.00	0.00
Anorthite	0.00	0.00
Na2SiO3	0.00	0.00
Acmite	2.87	2.13
Diopside	0.00	0.00
Sphene	0.00	0.00
Hypersthene	0.00	0.00
Albite	44.13	44.99
Orthoclase	30.14	31.45
Wollastonite	0.20	0.19
Olivine	0.00	0.00
Perovskite	0.00	0.00
Nepheline	0.00	0.00
Leucite	0.00	0.00
Larnite	0.00	0.00
Kalsilite	0.00	0.00
Apatite	0.53	0.44
Halite	0.00	0.00
Fluorite	0.00	0.00
Anhydrite	0.00	0.00
Thenardite	0.00	0.00
Pyrite	0.00	0.00
Magnesiochromite	0.00	0.00
Chromite	0.00	0.00
Ilmenite	0.19	0.11
Calcite	0.00	0.00
Na2CO3	0.00	0.00
Corundum	0.00	0.00
Rutile	0.00	0.00
Magnetite	0.04	0.02
Hematite	2.68	1.37
Total	99.94	100

Table 3.3: CIPW normal calculation for riebeckite syenogranite sample 52. Excel software created by Hollocher (2017).

Discussion

4.1General Crystallization Order of Plutonic Minerals

The order of crystallization is typical of a granitic system described first by Bowen (1956) and can also be interpreted from results of Martin and Bonin (1976), Lyons (1972), Best (2003), and Griet et al. (1980). The specific minerals can be broken up into primary and secondary mineral crystallizations. Essential primary minerals, which make up most of the rock, are microperthite, consisting of sodium-rich and potassium-rich alkali feldspar as perthite and quartz, and albite. Distinguishing primary minerals are hastingsite and riebeckite. A major accessory mineral is hornblende. Secondary and post crystallization minerals include albite, sericite, limonite, and iron rich opaque minerals. Medium to large-grained euhedral grains of perthitic feldspar were consistently the first to start crystallizing. Quartz crystallization was concurrent with euhedral perthite grains. A single alkali feldspar phase, consisting of a solid solution between the potassium and sodium rich endmembers, was the first to crystallize in early high temperature conditions. Once temperatures began to fall, the K-feldspar and albite endmembers started to separate from each other. The main host is the K-feldspar and the albite endmember is the exsolved lamellae. In most cases, subhedral perthite grains and irregular shaped quartz grains started to form and crystallize at the same time as each other. The last main forming mineral are the amphiboles, hastingsite and riebeckite. The chemistry of the melt would dictate which amphibole crystallized (Griet et al., 1980). Plagioclase albite either forms as early to middle phase unmixing from the sodium rich alkali-feldspar or as late stage intergranular replacement of perthite grains (Best, 2003 and Martin and Bonin, 1976). The limonite and sericite and most of the opaque iron rich minerals are indicative of late stage post magmatic alteration and replacement. To recap, early phase high temperature crystallization is from the alkali-feldspar and quartz grains, middle stage amphibole crystallization, microperthite unmixing

and albite rim propagation, and late stage, possibly hydrothermal, post magmatic mineral replacement and alteration (Figure 4.1).

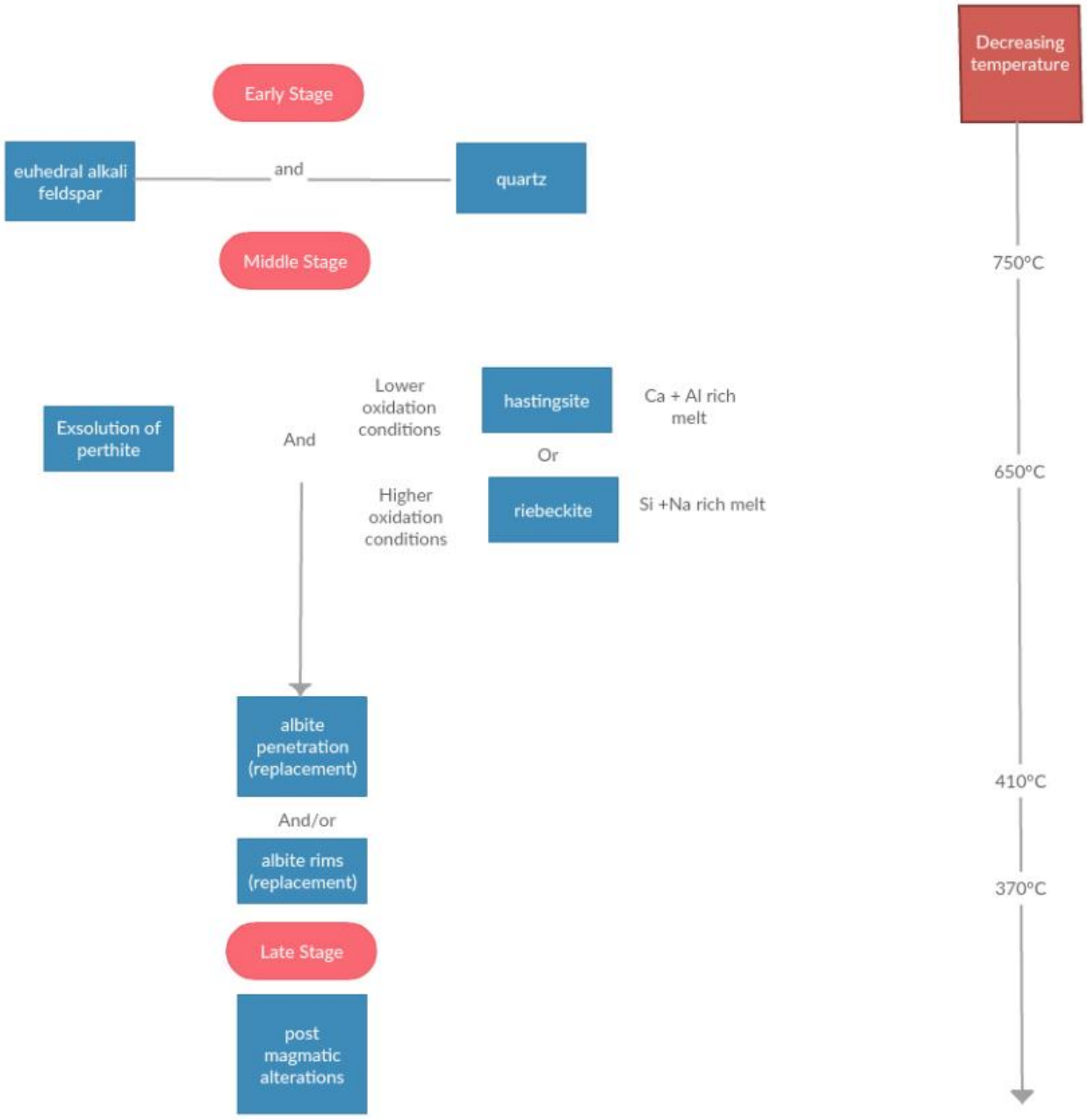

Figure 4.1: Crystallization timeline with some key conditions for amphibole formation.

4.2 Conditions for Perthite Formation

Microperthite textures are indicative of low depth and low pressure magma emplacement environment during crystallization of the granitic pluton. The dominance of microperthite feldspar in the hastingsite-riebeckite granitic pluton is very important in constraining the pressure, depth, and crystallization conditions of the pluton (Winter, 2014). The Mt. Cabot pluton and other similar Jurassic plutonic granites formed, at most, ~5.3 - 7.6 km in depth with pressures hovering around 1.5 - 2.1 kbar (Doherty and Lyons, 1979). Unsurprisingly, the whole pluton contains perthite as its only phase of feldspar, barring late stage hydrothermal alteration processes. Early emplacement conditions crystallized an alkali feldspar solid solution series. The grains were not exsolved and contained a solid solution composition from around 750-650℃ (Figure 4.2). During the middle period of crystallization, ~650℃, the sodic phase of early, more euhedral alkali feldspar, started to unmix from the perthite grain created a two composition feldspar inside of single grain as other minerals were crystalizing. This first stage of sodic endmember would have started to unmix at the later period of hastingsite or riebeckite crystallization as described later and elaborated on by Lyons (1972). Sodic feldspar would have exsolved earlier than any secondary stage replacement albite and crystallized before 410℃. Any plagioclase or albite derivatives would have been due to hydrothermal or late magmatic residual liquids (Lee and Parsons. 1972; Peng, 1970; and Martin and Bonin, 1976).

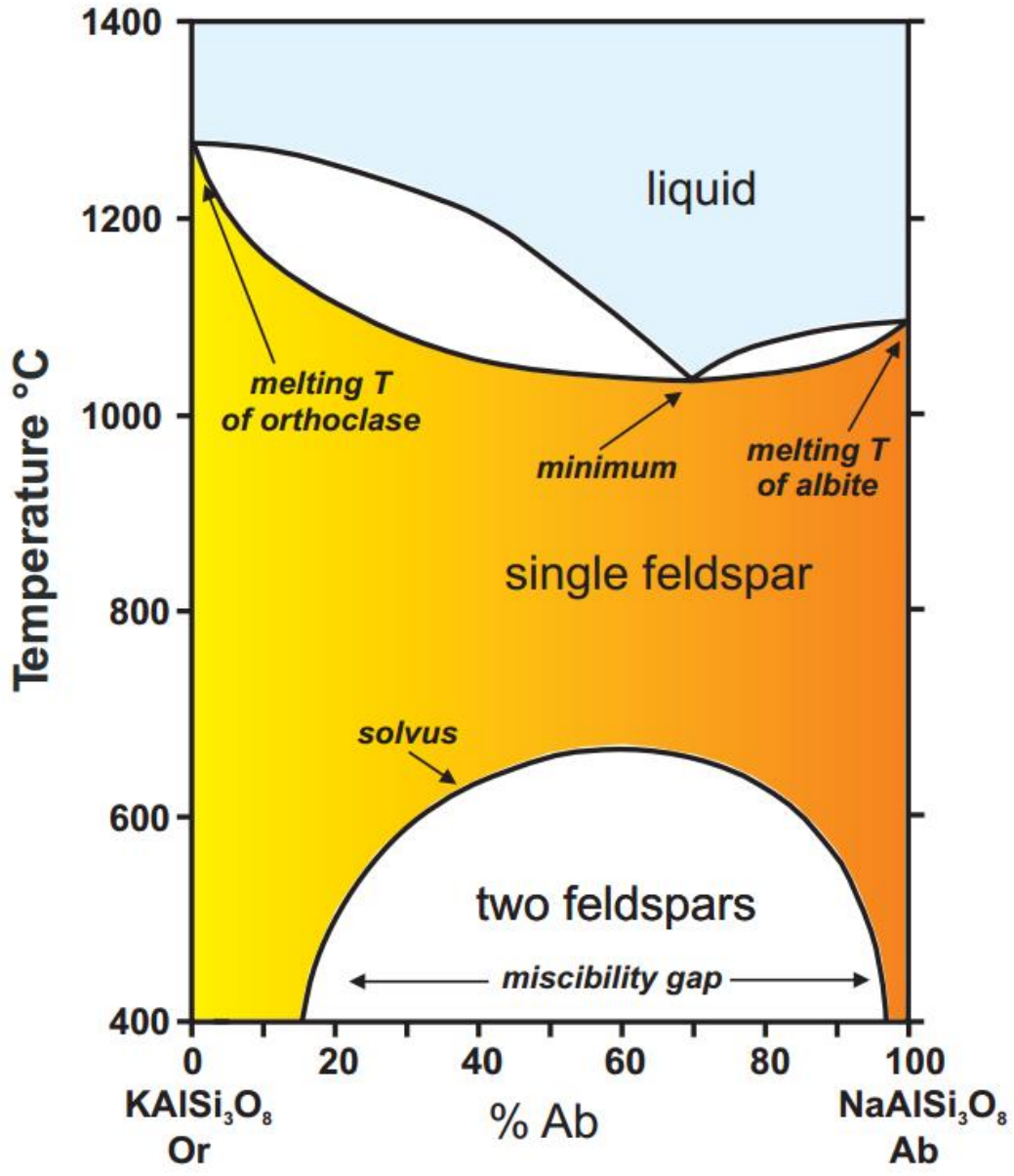

Figure 4.2: Typical KAlSiO -NaAlSiO System phase diagram for feldspars forming in hypersolvus granite under 5 kbar of pressure (Perkins and Brady, 2017).

4.3 Indicators for Parental Magma Composition

Plutonic samples from the Mt. Cabot pluton contain either riebeckite or hastingsite as the main amphibole (Figure 4.3). The distinct zonation in amphibole composition within Mt. Cabot pluton is a possible indication for composition changes or fluctuations of parental magma composition and redox reactions during crystallization of the amphibole phase. The genesis of the hastingsite group of amphibole minerals was first observed by Billings (1928) and can be applied to the Mt. Cabot pluton. A key observation by Billings (1928) was that there was a clear continuous series of the Ca-rich amphibole group from the magnesium rich hastingsite endmember to the iron rich ferrohastingsite endmember (Figure 4.4). Generally, riebeckite was not included in the granites the Billings (1928) studied that contained hastingsite but could occur in a small band of equilibrium, either due to temperature or a favorable ratio of sodium and calcium. Considering that there were no samples that included both amphiboles in the Mt. Cabot granite, equilibrium conditions were not present in the pluton. Lyons (1971) suggests that temperature changes do not account for the appearance of either of the amphiboles. Instead, riebeckite and hastingsite conditions are dependent on the partial pressures of oxygen and the composition of the magma and form at similar, near magmatic, temperature. Although the study of oxygen fugacity was above this particular study of the Mt. Cabot pluton, magma chemistry can be inferred by models of amphibole stability. A calcium-iron-aluminum rich composition favored the iron-rich calcium bearing mineral hastingsite, $NaCa_2Fe^{2+}{}_4Fe^{3+}(Si_6Al_2O_{22})(OH)_2$. The western side of the pluton, the hastingsite syenogranite zone, would have been Ca-Fe-Al rich. Parental magma depleted in calcium and aluminum favored the sodium-iron rich amphibole of riebeckite, $Na_2Fe^{2+}{}_3Fe^{3+}{}_2(Si_8O_{22})(OH)_2$ as seen by the two distinct types of riebeckite samples. A

fluid pressure of over 700 bars favors the crystallization of the iron rich riebeckite amphibole instead of hastingsite. Griet et al. (1980) also suggest that magma chemistry is one of the most critical factors controlling compositions of amphiboles in Si-oversaturated rocks originating from alkaline ring-complex environments (Figure 4.5). They suggest a gap separating the (Ca + Al)-rich, (Si + Na + K)-poor group of amphiboles from the (Ca + Al)-poor and (Si + Na + K)-poor. Early stage amphibole crystallization of silica poor amphiboles is possibly contemporaneous with alkali feldspars. Riebeckite in the Mt. Cabot pluton would have developed later than the alkali feldspars in more sodium rich and silica rich conditions during the later magmatic conditions or changes in redox reactions. Two solid-solution series, silica-poor for hastingsite and silica-rich for riebeckite, are thus postulated in an addition to changes in fugacity levels during the crystallization of the Mt. Cabot pluton. Earlier crystallization of Ca-rich and Si-poor amphiboles allows an introduction of Si into the magma melt, permitting more silica-rich differentiated liquids Griet et al. (1980). The appearance and/or lack of each amphibole in each sample of the Mt. Cabot pluton is indicative to the concentration of elements in the magma and redox conditions during crystallization and does not necessarily constrain the temperature of middle stage crystallization of the pluton (Lyons, 1971). These amphiboles help us understand the evolution of the chemistry and composition of the magma throughout its crystallization.

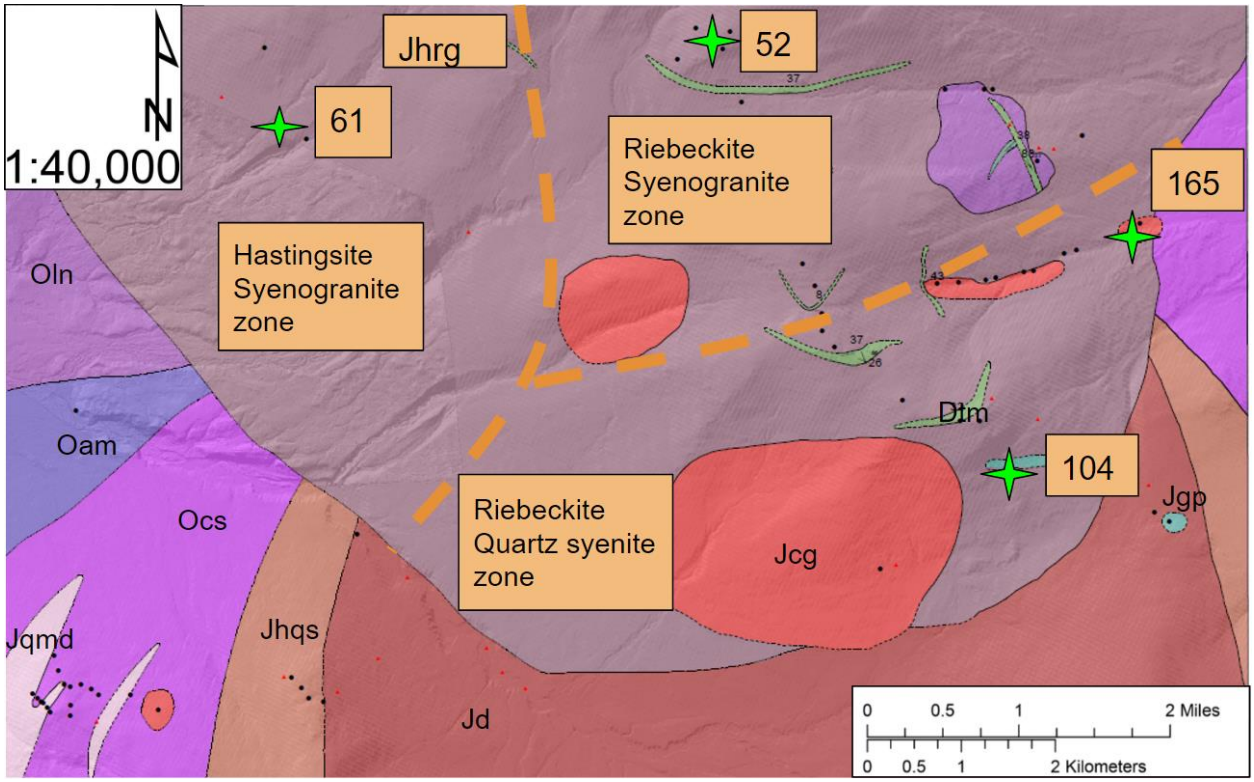

Figure 4.3: Mineralogical map of hastingsite-riebeckite pluton. This map is based on amphibole and APQ classifications. Modified from Figure 1.1 and Hillenbrand (2017). Orange zone lines are approximate boundaries between zones.

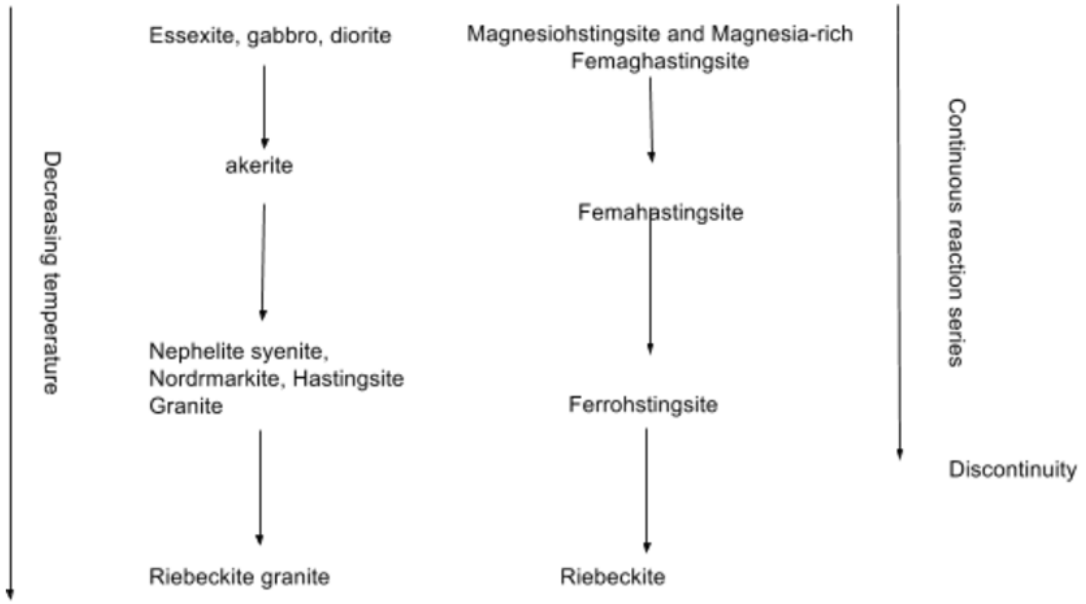

Figure 4.4: Diagram showing the possible evolution of the hastingsite group and riebeckite due to temperature of crystallization and associated granitic type. Adapted from Billings (1928).

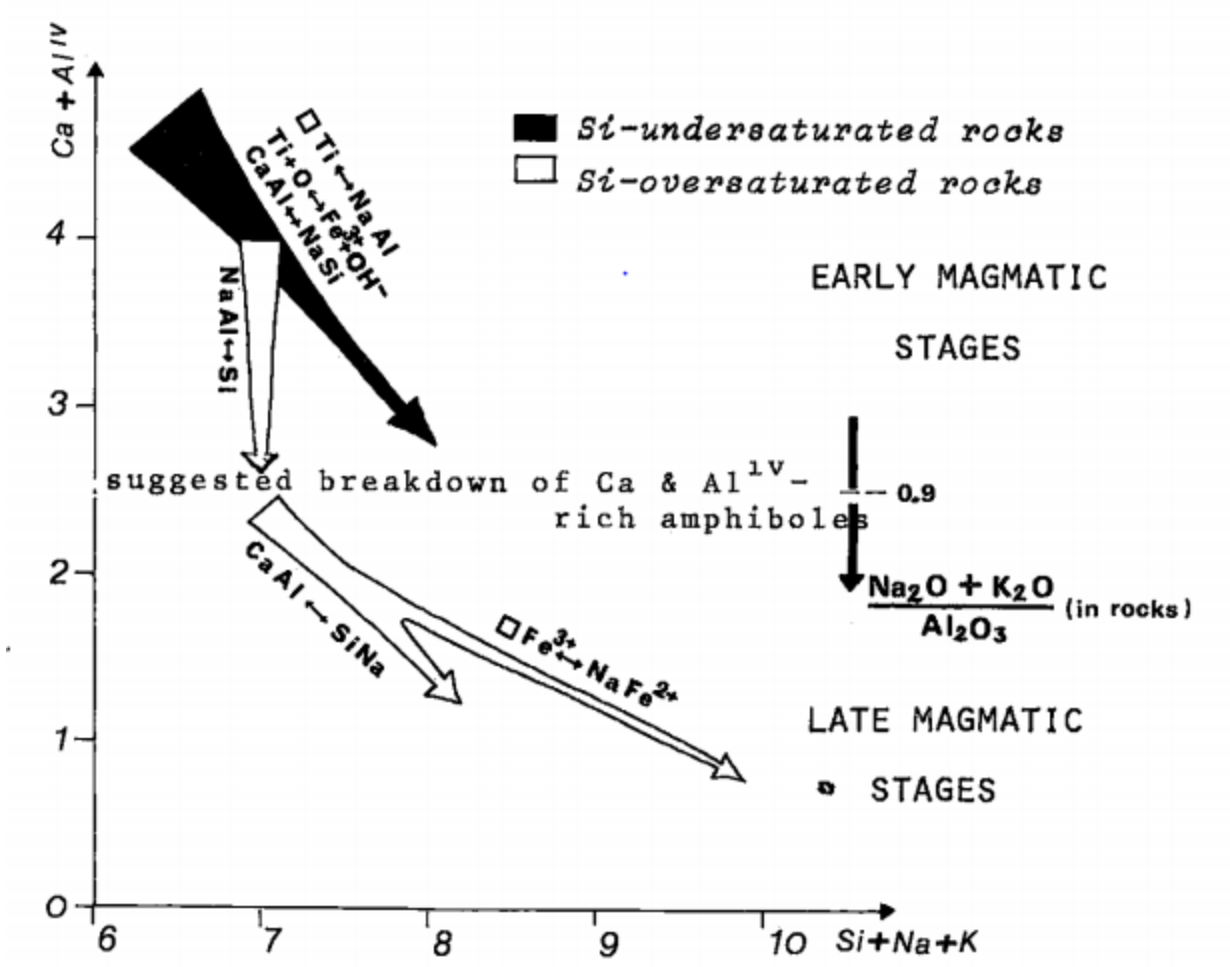

Figure 4.5: Magmatic evolution of the composition of magma melt and associated amphibole formation (Griet et al., 1980).

4.4 Origins of Intergranular Albite and Hydrothermal Alterations

The presence of two types of albite replacement, penetration albite and albite rims, found in the Mt. Cabot samples is helpful in understanding crystallization conditions of the pluton. Found in every sample collected from the Mt. Cabot pluton, the two forms that are equally important in understanding the crystallization conditions of albite plagioclase and possible near or post magmatic processes that occur at different stages of crystallization. The two types of middle to late stage albite crystallization, intergranular albite found in granitic portions of the pluton and rimming albite found in both granite and syenite samples of the pluton, are interpreted as being of replacement origin. According to the study by Lee and Parsons (1997) all albite replacement would have occurred after the exsolution of the sodic and potassic phases of the perthite grains. Two phases of replacement and albite alteration were found in the samples and would have occurred after unmixing of the perthite. The first phase of albite replacement involves albite crosscutting exsolution microtextures throughout the grain interiors, occurring in the hastingsite-riebeckite syenogranite sample. Due to the similarity of Lee and Parsons (1971) study, I hypothesize a replacement of perthite grains by albite through interaction with magmatic fluids at around 410°C. Samples in the Mt. Cabot pluton with anhedral perthite and the albite penetration would have been in direct contact with an influx of magmatic fluids and residual melt around this temperature. The second phase, found in all samples of the Mt. Cabot pluton, consisted of later generation rimmed albite replacing edge dislocations on highly elastically strained feldspars. This second generation of albite replacement could have been produced by pluton wide interactions with magmatic-hydrothermal fluids at around 370°C (Lee and Parsons 1997). Similar conclusions have been postulated by Peng (1970) on granite and syenite samples

in Hong Kong. Intergranular albite, in the samples collected at Mt. Cabot, form as small platelet like grains that have replaced and directly cut into anhedral to subhedral perthite grains. Strong cases of replacement for albite films and edges, rather than unmixing, go towards the small films unevenly cutting the sodium and potassium portions of the perthite crystals. Peng (1970), suggests a similar origin of both types of albite replacement. He suggests that they both were the product of pure contact with late magmatic residual melt. Differing from Lee and Parsons (1997), however, Peng (1970) does not indicate different stages of melting and does not hint at a late magmatic hydrothermal reaction causing replacive albite. Due to the presence of other post magmatic alterations, I suggest the two part replacement system derived by Lee and Parsons (1997). Accompanying the precipitation and replacement properties of albite are a host of textures indicating similar widespread hydrothermal conditions. Precipitation of albite, altered grains of both orthoclase and sericitized plagioclase, small pockets of myrmekite, and chemical alteration and replacement of amphiboles all reflect data collected by Martin and Bonin (1976) for their Cape Ann plutonic series and best fit the textures found at Mt. Cabot

4.5 Relation to Other New Hampshire Igneous Intrusions

Geochemical data from one section of the Mt. Cabot pluton suggests a similar chemical makeup between alkalic and riebeckite granites of the White Mountain Batholith (Figure 4.6). Although there is not enough data to compare the significances between the contents of rare earth elements between, the bulk-rock geochemistry is consistent with similar the alkalic granites provided in the Eby et al. (1992). Specifically, it is very similar to the Osceola granite and Hart ledge syenites, quartz syenites, and riebeckite granites. The Mt. Cabot granite, at least the riebeckite portion, has a similar chemical signature and it can be inferred that they would have

similar petrogenesis models and a comparison of these models is possible. This data shows that there are chemical similarities between the different Jurassic igneous intrusive plutons.

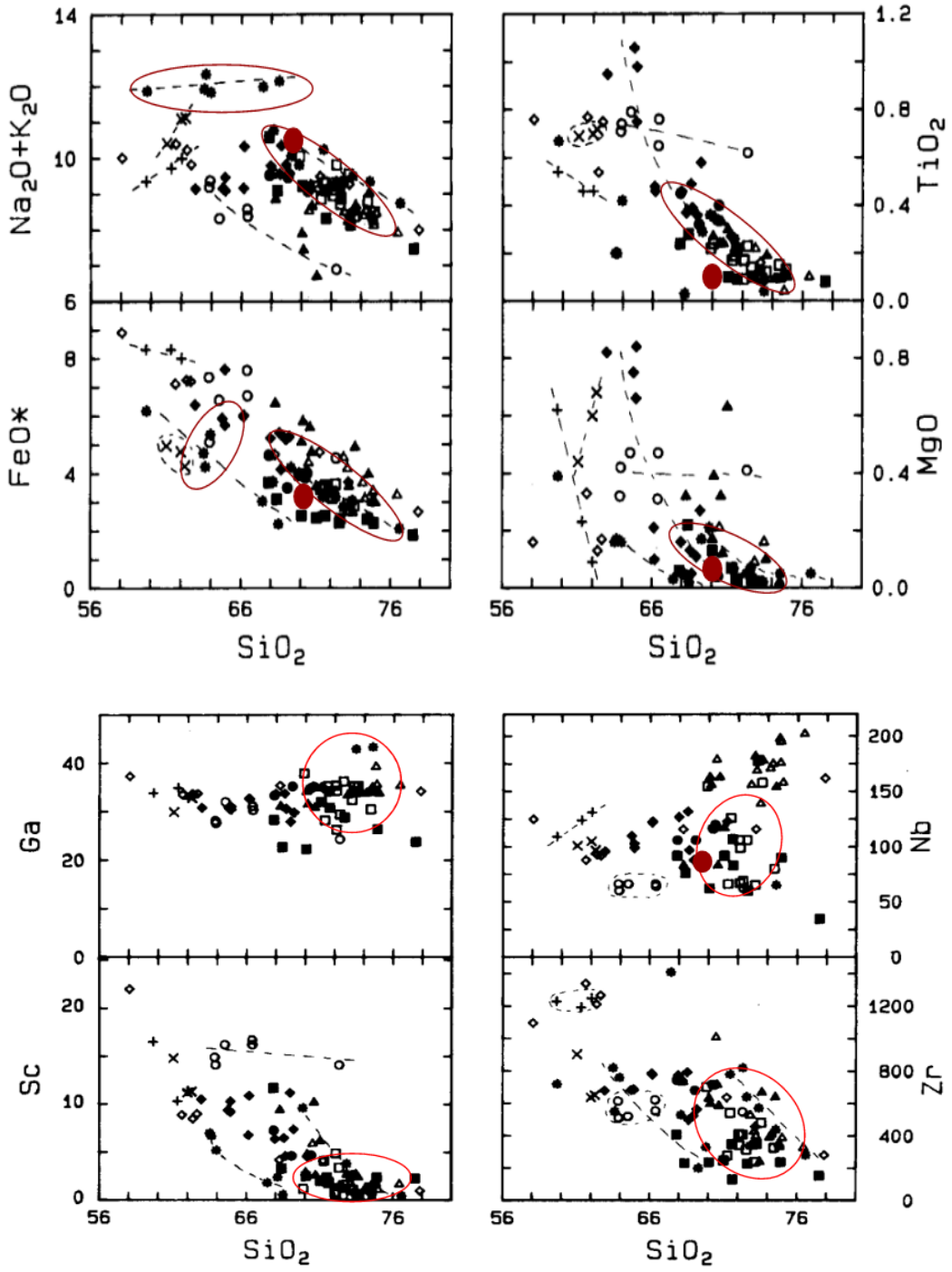

Figure 4.6: Geochemical data from Eby et al. (1992) and sample 52 from the Mt. Cabot region. The red circles indicate ranges of values from Eby et al. (1992) and the red dot represents sample 52.

4.6 Proposed Petrogenic Model of Pluton and Conclusions

According to Chapman (1938; 1942; and 1948), Eby et al. (1992), Eby and Creasy (1993), Hatcher (2010), Van Staal et al. (2009), and Corbi et al. (2015) the Mt. Cabot pluton has the typical emplacement as other White Magma Mountain series granites. Due to the presence of a single type of feldspar, perthitic feldspar, and chemical and mineralogical similarity to the White Mountain Batholith, the depth and pressure of emplacement are ~5.3 - 7.6 km in depth with pressures hovering around 1.5 - 2.1 Kbar (Best, 2003 and Creasy and Eby, 1993; and Doherty and Lyons, 1971). Crystallization conditions were relatively dry and allowed unimpeded crystallization of alkali feldspar, quartz, hastingsite, and riebeckite. Parental magma and redox conditions were not consistent throughout the magma. The hastingsite zone magma had a composition that was higher in Ca and Al but low in Si and Na. Possible breakdown of early crystallized hastingsite amphiboles, the propagation of silica rich residual melt, or a combination of higher oxygen fugacity and silica rich magma in the riebeckite zones allowed for the riebeckite to form and crystallize. The interstitial and poikilitic nature of the riebeckite suggests that it formed slightly later than the hastingsite in its respective portions of the pluton while the crystal nature of hastingsite suggests crystallization during earlier feldspar formation. If pressure and temperature did not control the formation of either amphibole then it could be assumed that it did not affect amphibole composition at different depths in the pluton, which could have been up to 2-3 km thick according to the height current height of Mt. Cabot (1,271 m) and estimates of the White Mountain batholith being 1.5 km thick unexposed versions (Creasy and Eby, 1993). Consequently, the hastingsite and riebeckite zones would not change from top to bottom and current mineralogical patterns are remaining constant with depth. Once the amphiboles

crystallized at temperatures around 650-750 ℃ the magma cooled to around 500 ℃ and the sodic alkali feldspar endmember began to exsolve and unmix into fine lamellae. At slightly lower temperatures, ~410℃, residual magmatic liquid interacted with the eastern, central, and northeast portion of the pluton to form perthite penetrating albite. At lower temperatures, ~370℃, a second introduction of hydrothermal water helped produce replacive albite rims on subhedral to euhedral perthite grains (Lee and Parsons, 1971). Meteoric water, derived from precipitation and the water table, continued to produce metasomatic changes in the beginning the pluton's post magmatic life. The earlier stage of penetrative albitization, at ~410℃, was present only in the riebeckite syenogranite zone and the hastingsite syenogranite zone. The later stage albitization, occurring around 370℃, happened throughout the whole pluton. Hydrothermal alteration is inferred by textures including: sericitization, alteration of amphiboles, and possible precipitation of more albite from perthite grains. Post magmatic conditions are similar to Martin and Bonin's (1976) description of a hypersolvus and subsolvus environment because of the introduction of water at the late stages of the pluton's crystallization. Sericitization of feldspars, myrmekite, and limonite weathering of amphiboles all could represent the last stages of magmatic crystallization and a presence of meteoric water (Martin and Bonin, 1976).

The coexistence of both quartz syenite and syenogranites and the introduction of magmatic liquids and hydrothermal water in the Mt. Cabot pluton could be explained by the structural controls on pluton emplacement. According to Chapman (1976) syenites and granites are commonly associated with each other in intrusive plutons of the White Mountain Magma Series due to magma mixing. This could have happened in the Mt. Cabot pluton through early crystallized silicic rock dropping into a syenite magma body or fractures tapping the magma chamber at multiple levels to inhibit both liquid phases to mix at all levels (Chapman, 1976).

Fracturing could relate to both the influx of magmatic and/or hydrothermal fluid and associated alterations and albitization, a distinct pocket of syenite within the pluton, and the influxes of magma and melting conditions conducive to the crystallization of two different amphiboles. However, to fully support this hypothesis would require a study of the other intrusive plutons in the area, thin section creation other samples in the Mt. Cabot pluton to provide better geographic coverage, and geochemical data for the samples for whole-rock, REE, and trace element geochemistry. Geochemical data for multiple samples could help pinpoint fluxes of hydrothermal or magmatic liquids due to their richness in rare elements (Martin and Bonin, 1976). More thin sections in previously under covered areas of the pluton would help create a more accurate map and the possibility of finding a sample or zone with both amphiboles. Study of more plutons in the area, including the northern half of the hastingsite-riebeckite granite in the Percy region, would help determine if there is homogeneity in the types of reactions found in this section of the pluton.

References

Abdel-Rahman, A. and El-Kibbi, M., 2001, Anorogenic magmatism: chemical evolution of the Mount El-Sibai A-type complex (Egypt), and implications for the origin of within-plate felsic magmas: Geological Magazine, v. 138, p. 67-85, doi: 10.1017/s0016756801005052.

Best, M., 2003, Igneous and Metamorphic Petrology: Hobokan, Blackwell Science Ltd. p. 122-241.

Billings, M., 1928, The Chemistry, Optics, and Genesis of the Hastingsite Group of Amphiboles: Mineralogical Society of America, p. 287-296.

Bonin, B., 2007, A-type granites and related rocks: Evolution of a concept, problems and prospects, Lithos, Volume 97, Issues 1–2 , p. 1-29, http://dx.doi.org/10.1016/j.lithos.2006.12.007.

Boucot, A., 1961, Stratigraphy of the Moose River synclinorium, Maine: USGS Bulletin Series, p. 153-188.

Bruker, 2016, How Does XRF Work? https://www.bruker.com/products/x-ray-diffraction-and-elemental-analysis/handheld-xrf/how-xrf-works.html (accessed December 2016)

Chapman, C., 1976, Structural Evolution of the White Mountain Magma Series: Geological Society of America Memoir, v.146, p. 281-300.

Chapman, R., 1935, Percy ring dike complex: American Journal of Science, v. s5-30, p. 401-431, doi: 10.2475/ajs.s5-30.179.401.

Chapman, R., 1942, Ring structures of the Pliny Region, New Hampshire: Geological Society of America Bulletin, v. 53, p. 1533-1568, doi: 10.1130/gsab-53-1533.

Chapman, R., 1948, Petrology And Structure Of The Percy Quadrangle, New Hampshire: Geol Soc America Bull, v. 59, p. 1059, doi: 10.1130/0016-7606(1948)59[1059:pasotp]2.0.co;2.

Chappell B. W. & White A. J. R. 1974. Two Contrasting Granite Types. Pacific Geology 8, 173–174.

Corbi, F., Rivalta, E., Pinel, V., Maccaferri, F., Bagnardi, M., and Acocella, V., 2015, How caldera collapse shapes the shallow emplacement and transfer of magma in active volcanoes: Earth and Planetary Science Letters, v. 69, no. 1, p. 1-26.

Creasy, J. W. and Eby, G. N.. 1993, Ring dikes and plutons: A deeper view of calderas as illustrated by the White Mountain igneous province, New Hampshire. In Cheney, J. T. and Hepburn, J. C. (eds.) Field Trip Guidebook for the Northeastern United States: 1993 Boston GSA, Vol. 1. Contribution No. 67, Department of Geology and Geography, University of Massachusetts, Amherst, MA, pp. N1-N25.

Deer, W., Howie, R., and Zussman, J., 1963, Rock-forming minerals: Volume Two: London, Geological Society, p. 183-199.

Devoe, M., 2015, Deformation Post-Doming: New mapping of the Oliverian Jefferson Dome, Mt. Dartmouth 7.5’ Quadrangle, New Hampshire.

Doherty, J., and Lyons, J., 1980, Mesozoic erosion rates in northern New England: Geological Society of America Bulletin, v. 91, p. 16, doi: 10.1130/0016-7606(1980)91<16:merinn>2.0.co;2.

Earth and Planetary Science Letters, v. 431, p. 287-293.

Eby, G. N. and Kennedy, B. (2004). The Ossipee ring complex, New Hampshire. In Hanson. L. (ed) Guidebook to Field Trips from Boston, MA to Saco Bay, ME. New England Intercollegiate Geological Conference, Salem, MA, p. 61-72.

Eby, G. N., 1995,.White Mountain magma series. Third Hutton Symposium on Granites and Related Rocks, Pre-Conference Field Trip Guide, Part 1, University of Massachusetts, Lowell, MA, p. 27.

Eby, G. N., Krueger, H. W., and Creasy, J. W. (1992) Geology, geochronology, and geochemistry of the White Mountain batholith, New Hampshire. In Puffer, J. H. and Ragland, P. (eds.) Mesozoic Magmatism in Eastern North America, Geological Society of America Special Paper 268, p. 379-397.

EUGSTER, H., and WONES, D., 1962, Stability Relations of the Ferruginous Biotite, Annite: Journal of Petrology, v. 3, p. 82-125, doi: 10.1093/petrology/3.1.82.

Gross, E. and Heinrich, E., 1966, Petrology and Mineralogy of the Mount Rosa Area, El Paso and Teller Counties, Colorado. II Pegmatites: The American Mineralogist, v. 54, p. 299-323.

Harrison, R. and Brook, M., 1987, Geology, petrology and geochemistry of Ailsa Craig, Ayrshire: London, H.M.S.O.

Hatcher, R. D., 2010, The Appalachian orogen: A brief summary, Volume 206, p. 1-19.

Hillenbrand, I., 2017, Newly Discovered Albee Formation in the Northern Half of the Jefferson, NH 7.5' Quadrangle: Detrital Zircons, Structure, and Tectonics [B.S Honors Thesis]: Lewiston, Bates College, np.

Hollocher, K., 2017, Calculating of a CIPW norm from a bulk chemical analysis: Kurt Hollocher,.

Jacobson, R.R., Black, R., Macleod, W.N., 1958, Ring Complexes in the Younger Granite Province of Northern Nigeria, Geological Society, London, Memoirs, v. 1, p. 5-71, doi: 10.1144/gsl.mem.1958.001.01.01.

Jianguo, W., Zhonghua, H., Lin, C., Qing, W., and Ling, J., 2013, Petrogenesis of Early Cretaceous riebeckite granophyres in southern Da Hinggan Mts.: Global Geology, v. 16, p. 26-34.

Kennedy, B., and Stix, J., 2007, Magmatic processes associated with caldera collapse at Ossipee ring dyke, New Hampshire: Geological Society of America Bulletin, v. 119, p. 3-17, doi: 10.1130/b25980.1.

Khan, T., Murata, M., Rehman, H., Zafar, M., and Ozawa, H., 2012, Nagarparker granites showing Rodinia remnants in the southeastern part of Pakistan: Journal of Asian Earth Sciences, v. 59, p. 39-51, doi: 10.1016/j.jseaes.2012.05.028.

Lee, M. and Parsons, I., 1997, Dislocation formation and albitization in alkali feldspars from the Shap Granite: American Mineralogist, v. 82, p. 557-570, doi: 10.2138/am-1997-5-616.

Loiselle, M. C., Wones, D. R., 1979. Characteristics and origin of anorogenic granites. Geological Society of America Abstracts with Programs 11, no. 7, 468.

Lyons, J.B., Bothner, W.A., Moench, R.H., Thompson, J.B., Jr., 1997, Bedrock Geologic Map of New Hampshire: U.S. Geological Survey, Denver, CO, 2 sheets, 1:125,000 scale bedrock and 1:50,000 scale derivative maps.

Lyons, P., 1972, Significance Of Riebeckite And Ferrohastingsite In Microperthite Granites: American Mineralogist, v. 57, p. 1404-1412.

Lyons, P.C. and Krueger, H.W., 1976. Petrology, chemistry, and age of the Rattlesnake pluton and implications for other alkalic granite plutons of southern New England. *Geological Society of America Memoirs, 146*, pp.71-102.

Martin, R. and Bonin, B., 1976, Water and Magma Genesis: The Association Hypersolvus Granite--Subsolvus Granite: Canadian Mineralogist, v. 14, p. 228-237.

McHone, J.G. and Butler, J.R., 1984, Mesozoic igneous provinces of New England and the opening of the North Atlantic Ocean: Geological Society of America Bulletin, v. 95, p. 757-765.

Murgoci, G., 1905, On the genesis of riebeckite and riebeckite rocks: American Journal of Science, v. s4-20, p. 133-145, doi: 10.2475/ajs.s4-20.116.133.

Nesse, W., 2012, Introduction to mineralogy: New York, Oxford University Press.

Peng, C., 1970, Intergranular Albite in Some Granites and Syenites of Hong Kong: The American Mineralogist, v. 55, p. 270-282.

Perkins, D., and Brady, J., 2017, Binary Phase Diagrams: Teaching Phase Equilibria,.

Phemister, J., 1950, The Riebeckite-Bearing Dikes of Shetland: Mineralogical Magazine, v. 29, p. 359-373, doi: 10.1180/minmag.1950.029.211.12.

Sherif, M., Ghoneim, M., Heikal, M., and El Dosuky, B., 2013, Petrogenesis of granites, Sharm El-Sheikh area, South Sinai, Egypt: petrological constrains and tectonic evolution: Mineralogy and Petrology, v. 107, p. 765-783, doi: 10.1007/s00710-013-0267-5.

Takahashi, G., 2015, Sample preparation for X-ray fluorescence analysis: Rigaku Journal, v. 31, p. 26-30.

Thompson, T., Pierson, J., and Lyttle, T., 1982, Petrology and petrogenesis of the Bokan Granite Complex, southeastern Alaska: Geol Soc America Bull, v. 93, p. 898, doi: 10.1130/0016-7606(1982)93<898:papotb>2.0.co;2.

Tollo, R. and Lowe, T., 2016, Geologic Map of the Robertson River Igneous Suite, Blue Ridge Province, Northern and Central Virginia: U.S Geological Survey, p. 1-15.

Van Staal, C. R., Whalen, J. B., Valverde-Vaquero, P., Zagorevski, A., and Rogers, N., 2009,Pre-Carboniferous, episodic accretion-related, orogenesis along the Laurentian margin of the northern Appalachians: Geological Society Special Publication, v. 327, p. 271-316.

Veblen, D., 1981, Amphiboles and other hydrous pyriboles: Washington, D.C., Mineralogical Society of America.

Warren, C. and Palache, C., 1911, The Pegmatites of the Riebeckite-Aegirite Granite of Quincy, Mass., U. S. A.; Their Structure, Minerals, and Origin: Proceedings of the American Academy of Arts and Sciences, v. 47, p. 125, doi: 10.2307/20022716.

Winter, J., 2014, An introduction to igneous and metamorphic petrology: Upper Saddle River, NJ, Prentice Hall, p. 334-362.